Wavelet Transforms

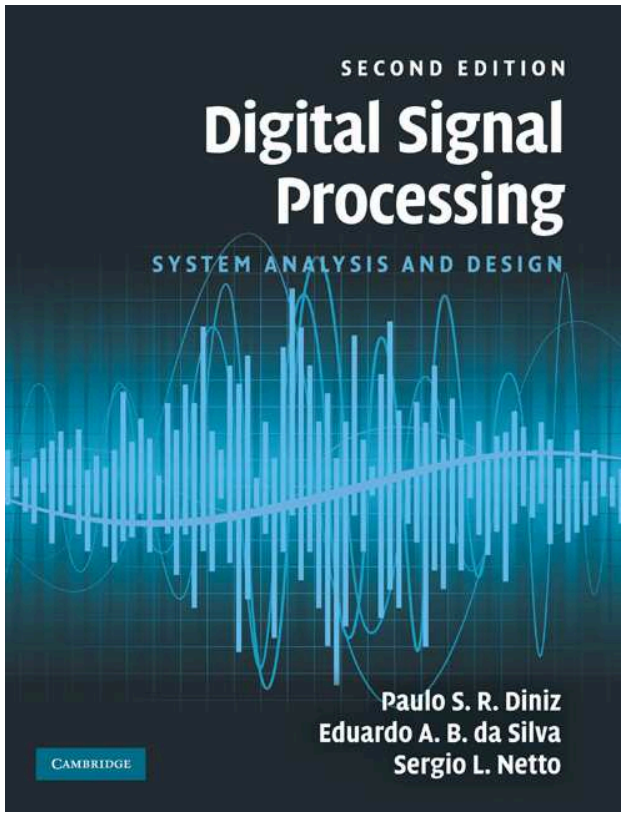

Paulo S. R. Diniz

Eduardo A. B. da Silva

Sergio L. Netto

diniz,eduardo,sergioln@lps.ufrj.br

September 2010

Contents

- Wavelet transforms
- Wavelet transforms and time-frequency analysis
- Multiresolution representation
- Wavelet transforms and filter banks
- Regularity
- Wavelet transforms of images
- Wavelet transforms of finite-length signals
- Do-it-yourself: Wavelet transforms

Wavelet transforms

- Wavelet transforms are a relatively recent development in functional analysis that have attracted a great deal of attention from the signal processing community. The wavelet transform of a function belonging to $\mathcal{L}^2\{\mathbb{R}\}$, the space of the square integrable functions, is its decomposition in a base formed by expansions, compressions, and translations of a single mother function $\psi(t)$, called a wavelet.
- The applications of wavelet transforms range from quantum physics to signal coding.
- It can be shown that for digital signals the wavelet transform is a special case of critically decimated filter banks.
- In fact, its numerical implementation relies heavily on that approach.

Hierarchical filter banks

- The cascading of 2-band filter banks can produce many different kinds of critically decimated decompositions.
- For example, one can make a 2^k-band uniform decomposition, as depicted in Figure 1a, for $k = 3$.
- Another common type of hierarchical decomposition is the octave-band decomposition, in which only the lowpass band is further decomposed.
- In Figure 1b, one can see a 3-stage octave-band decomposition.
- In these figures, the synthesis bank is not drawn, because it is entirely analogous to the analysis bank.

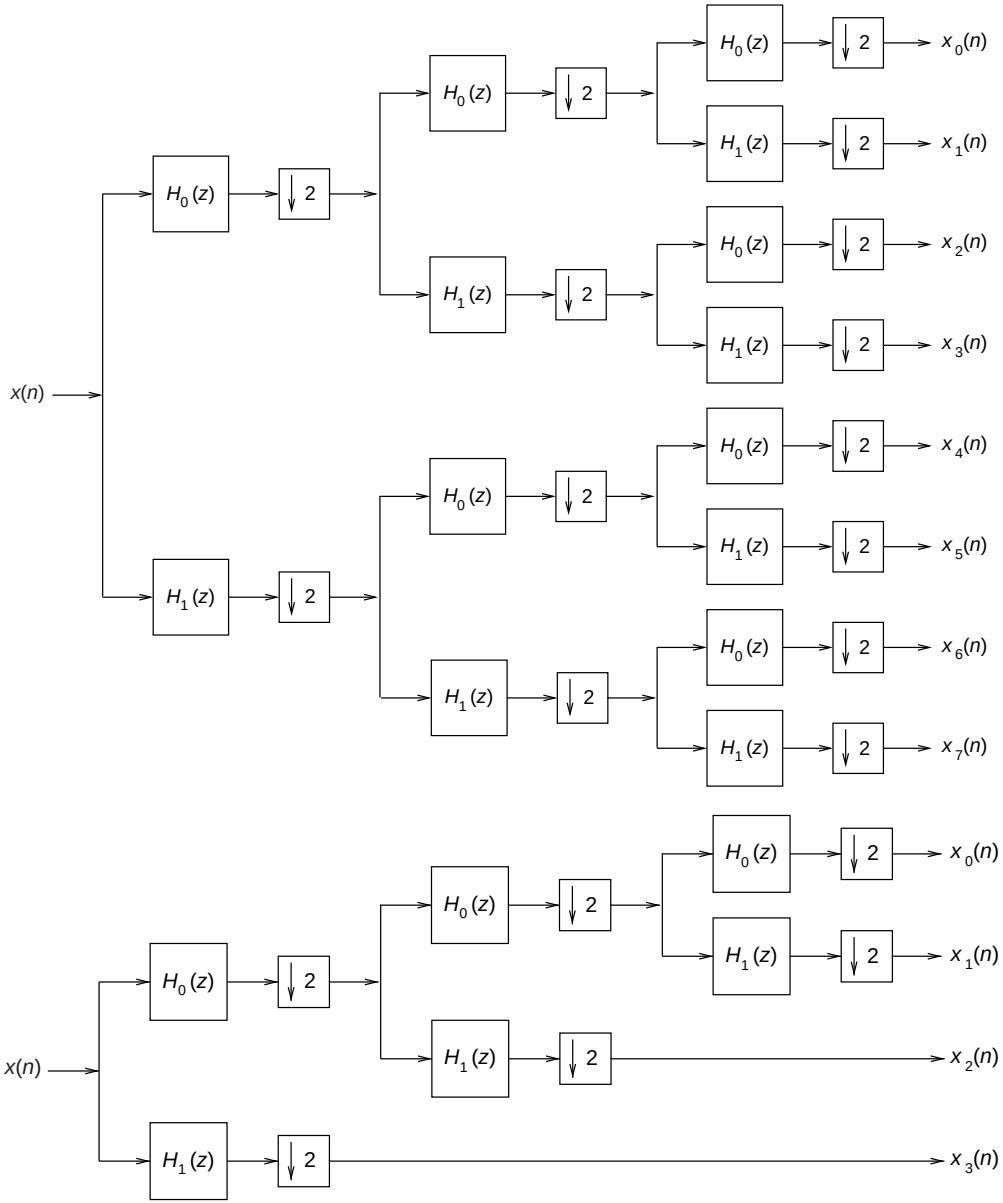

Figure 1: Hierarchical decompositions: (a) 8-band uniform; (b) 3-stage octave-band.

Wavelets

- Consider the octave-band analysis and synthesis filter banks depicted in Figure 2, where the lowpass bands are recursively decomposed into lowpass and highpass channels.
- In this framework, the outputs of the lowpass channels after an $(S+1)$-stage decomposition are $x_{S,n}$, and the outputs of the highpass channels are $c_{S,n}$, with $S \geq 1$.

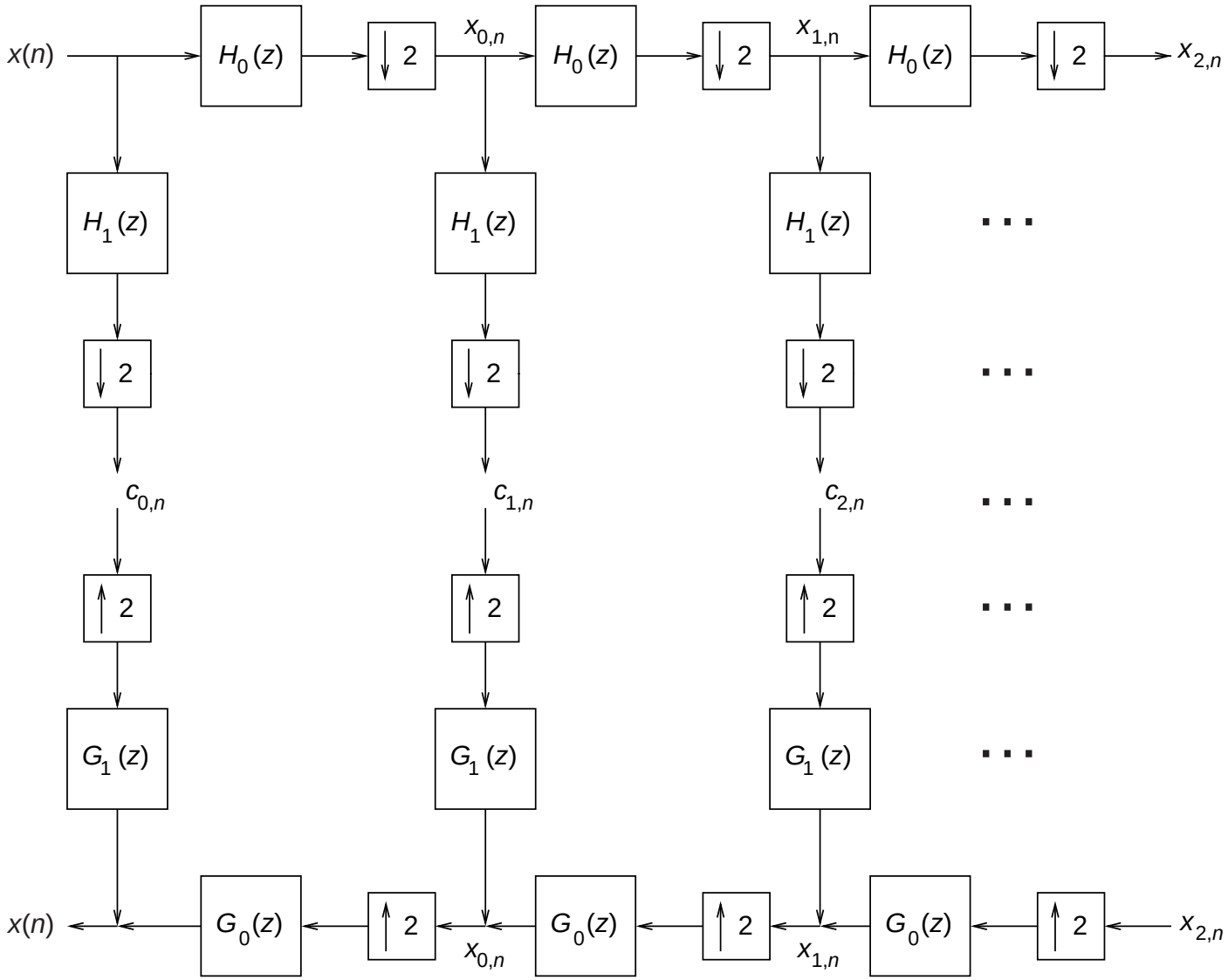

Figure 2: Octave-band analysis and synthesis filter banks.

Wavelets

- Applying the noble identities to Figure 2, we arrive at Figure 3.
- After $(S+1)$ stages, and before decimation by a factor of $2^{(S+1)}$, the z transforms of the analysis lowpass and highpass channels, $H_{low}^{(S)}(z)$ and $H_{high}^{(S)}(z)$, are

$$H_{low}^{(S)}(z) = \frac{X_S(z)}{X(z)} = \prod_{k=0}^{S} H_0(z^{2^k}) \tag{1}$$

$$H_{high}^{(S)}(z) = \frac{C_S(z)}{X(z)} = H_1(z^{2^S}) H_{low}^{(S-1)}(z) \tag{2}$$

respectively.

Wavelets

- For the synthesis channels, the results are analogous, that is

$$G_{low}^{(S)}(z) = \prod_{k=0}^{S} G_0(z^{2^k}) \tag{3}$$

$$G_{high}^{(S)}(z) = G_1(z^{2^S}) G_{low}^{(S-1)}(z) \tag{4}$$

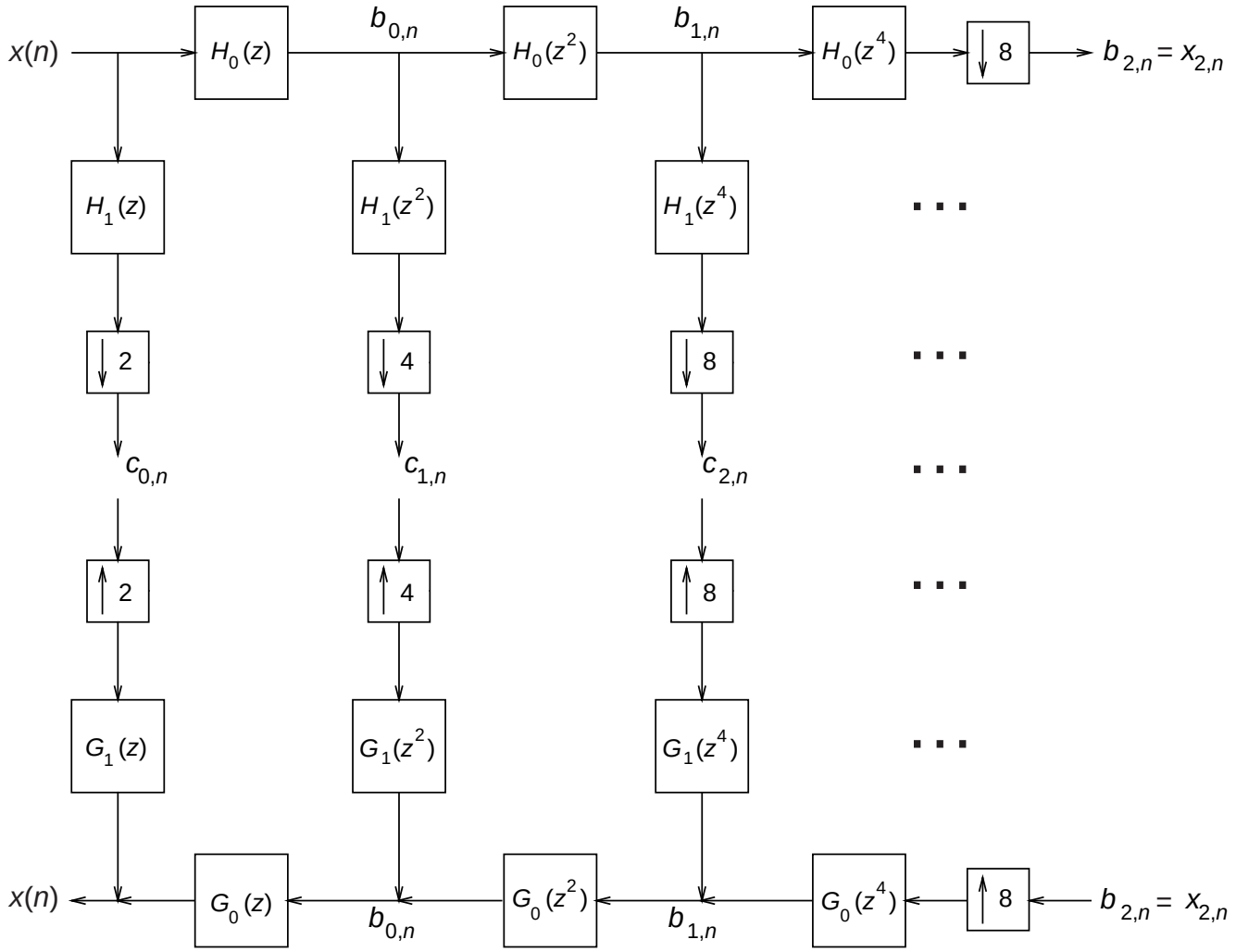

Figure 3: Octave-band analysis and synthesis filter banks after the application of the noble identities.

Wavelets

- If $H_0(z)$ has enough zeros at $z = -1$, it can be shown that the envelope of the impulse response of the filters in equation (2) has the same shape for all S.
- In other words, this envelope can be represented by expansions and contractions of a single function $\psi(t)$, as seen in Figure 4 for the analysis filter bank.

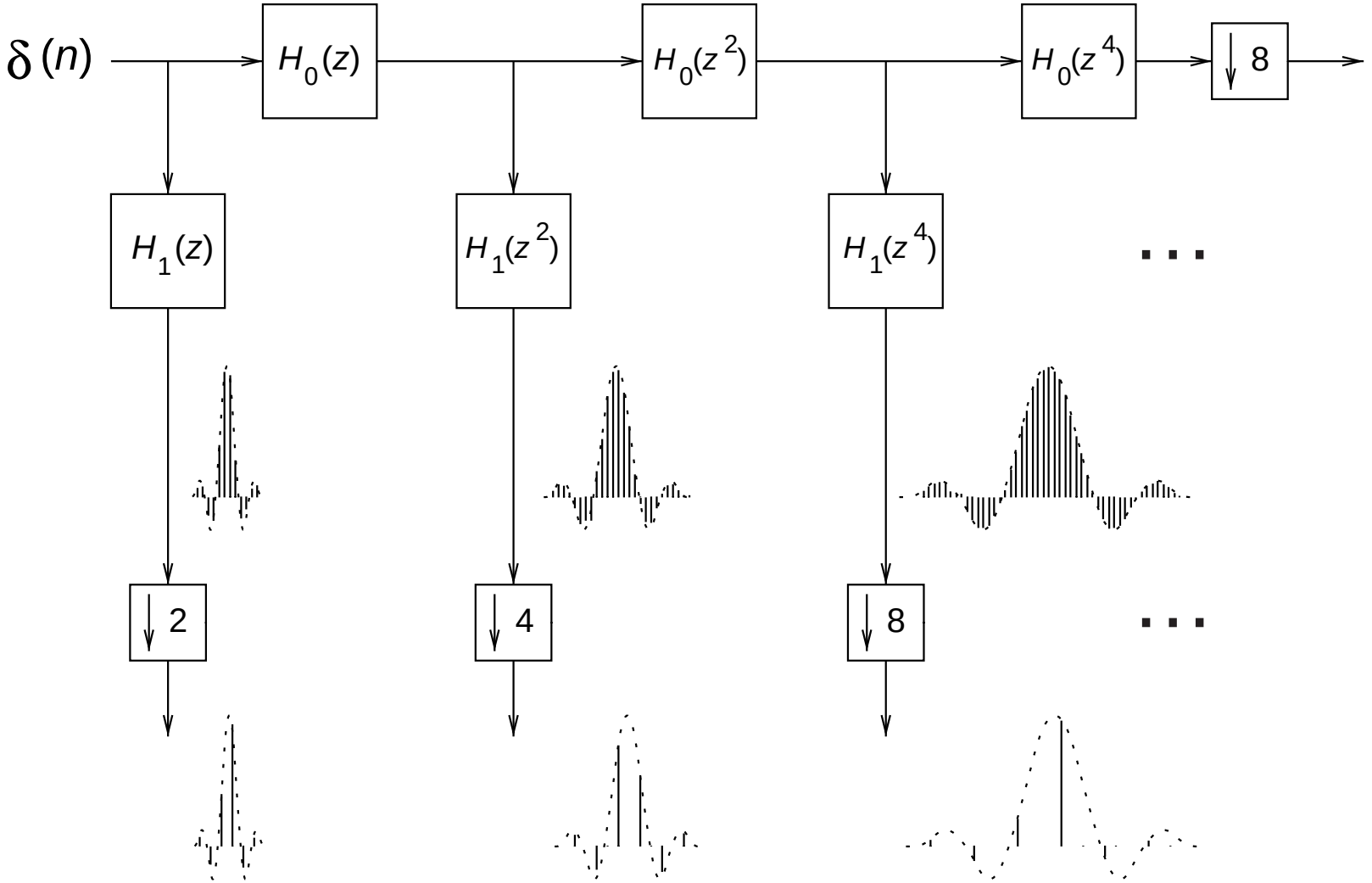

Figure 4: The impulse responses of the filters from equation (2) have the same shape for every stage.

Wavelets

- In fact, in this setup, the envelopes before and after the decimators are the same.
- However, it must be noted that, after decimation, we can not refer to impulse responses in the usual way, because the decimation operation is not time invariant.
- If Ω_s is the sampling rate at the input of the system in Figure 4, we have that this system has the same output as the one in Figure 5, where the boxes represent continuous-time filters with impulse responses equal to the envelopes of these signals in Figure 4.
- Note that in this case, sampling with frequency $\frac{\Omega_s}{k}$ is equivalent to decimating by k.

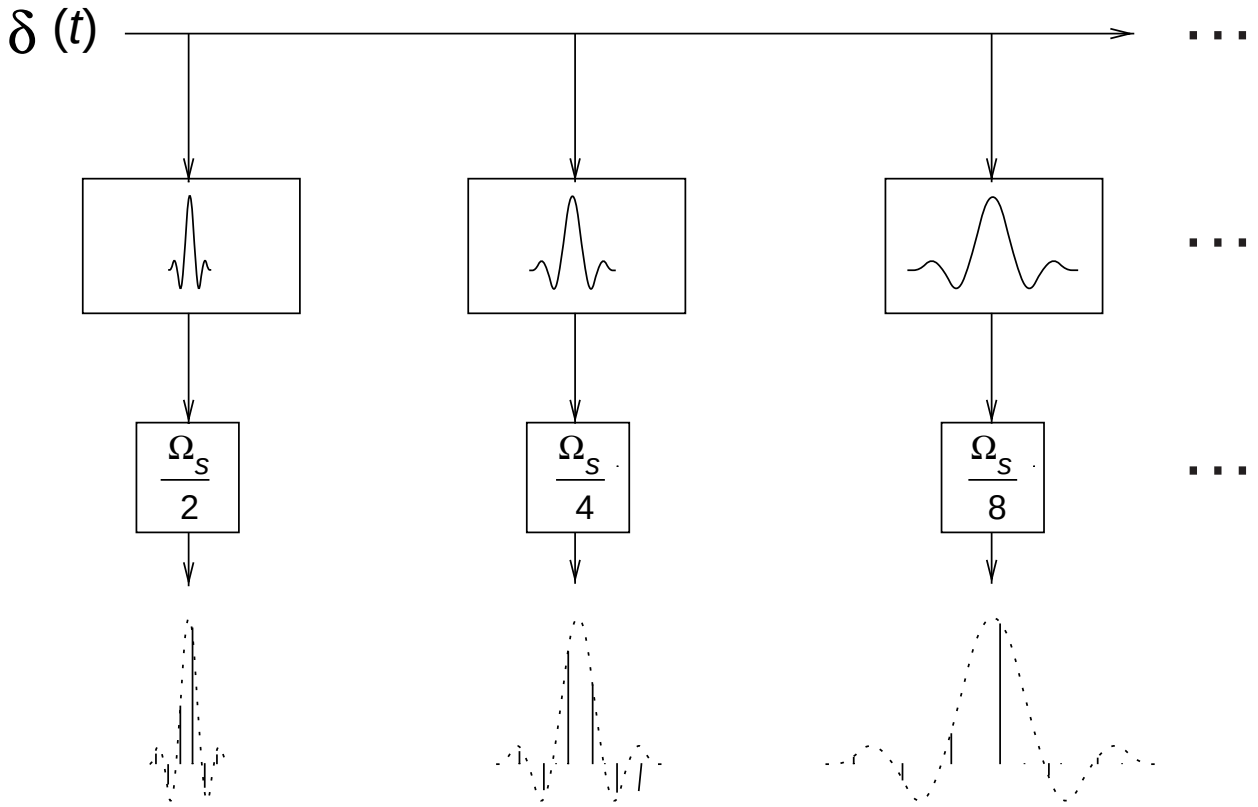

Figure 5: Equivalent system to the one in Figure 4.

Wavelets

- We then observe that the impulse responses of the continuous-time filters of Figure 5 are expansions and contractions of a single mother function $\psi(t)$, with the highest sampling rate being $\frac{\Omega_s}{2}$, as stated above.
- Then, each channel added to the right has an impulse response with double the width, and a sampling rate half of the previous one.
- There is no impediment in adding channels also to the left of the channel with sampling frequency $\frac{\Omega_s}{2}$.
  - In such cases, each new channel to the left has an impulse response with half the width, and a sampling rate twice the one to the right.
- If we keep adding channels to both the right and the left indefinitely, we arrive at Figure 6, where the input is $x(t)$, and the output is referred to as the wavelet transform of $x(t)$.
- The mother function $\psi(t)$ is called the wavelet, or, more specifically, the analysis wavelet.

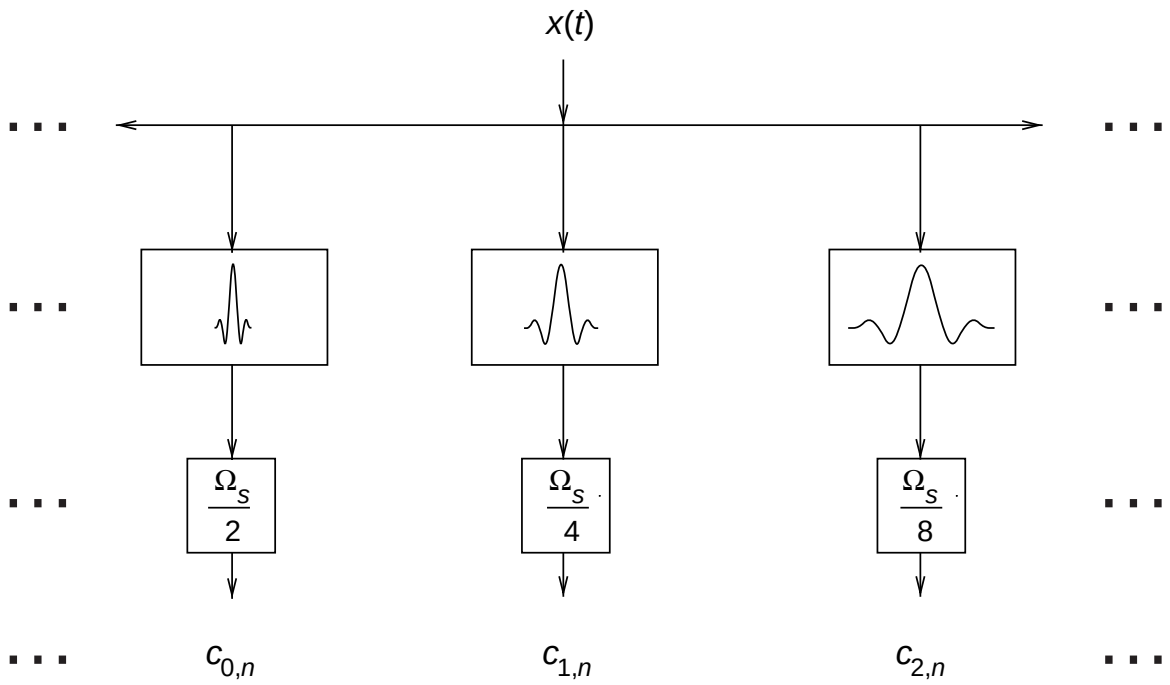

Figure 6: Wavelet transform of a continuous signal $x(t)$.

Wavelets

- Assuming, without loss of generality, that $\Omega_s = 2\pi$ (that is, $T_s = 1$), it is straightforward to derive from Figure 6 that the wavelet transform of a signal $x(t)$ is given by

  (Actually, in this expression, the impulse response of the filters are expansions and contractions of $\psi^*(-t)$. In addition, the constant $2^{-\frac{m}{2}}$ is included because, if $\psi(t)$ has unit energy, which can be assumed without loss of generality, $2^{-\frac{m}{2}}\psi(2^{-m}t - n)$ will also have unit energy.)

$$c_{m,n} = \int_{-\infty}^{\infty} 2^{-\frac{m}{2}}\psi^*(2^{-m}t - n)x(t)dt \tag{5}$$

- From Figures 3–6 and equation (2), one can see that the wavelet $\psi(t)$ is a bandpass function, because each channel is a cascade of several lowpass filters and a highpass filter with superimposing passbands.

Wavelets

- Also, when the wavelet is expanded in time by two, its bandwidth decreases by two, as seen in Figure 7.

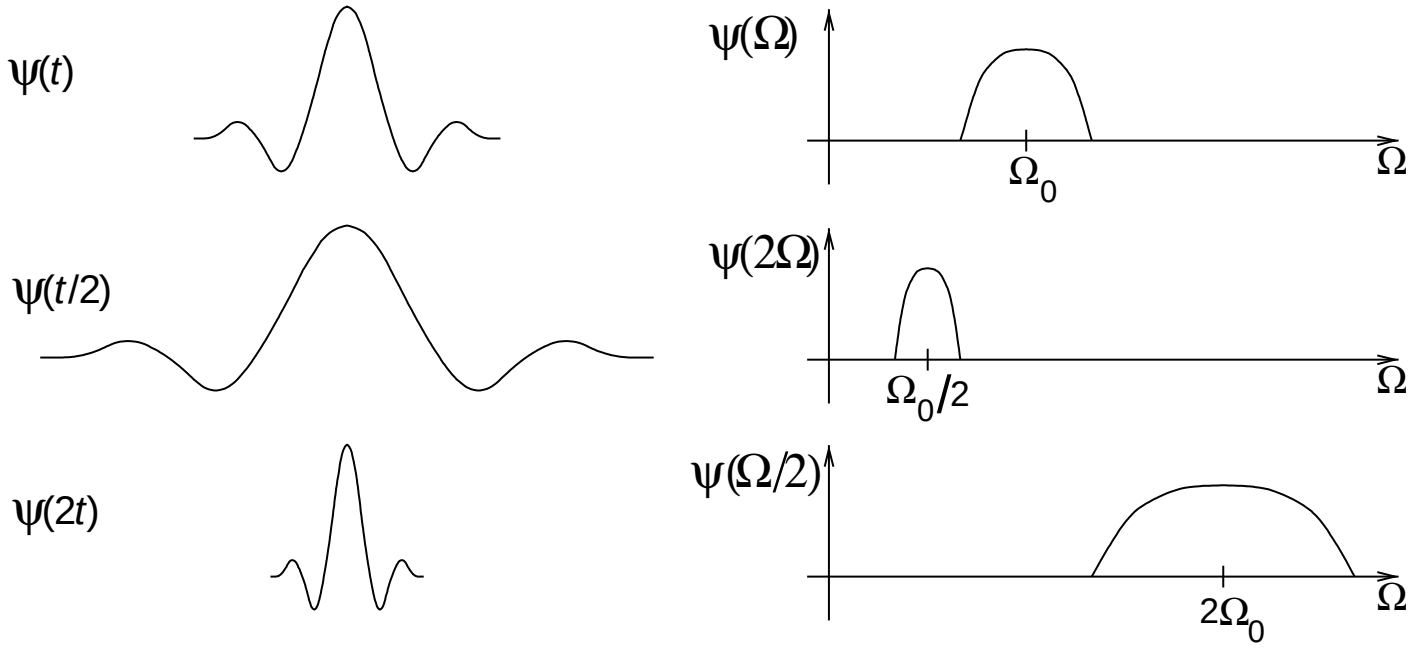

Figure 7: Expansions and contractions of the wavelet in the time and frequency domains.

Wavelets

- Therefore, the decomposition in Figure 6 and equation (5) is, in the frequency domain, as shown in Figure 8.

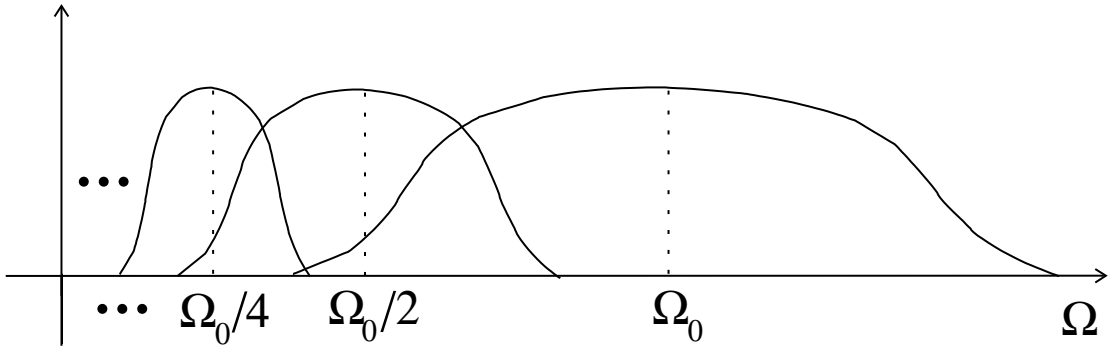

Figure 8: Wavelet transform in the frequency domain.

- In a similar manner, the envelopes of the impulse responses of the equivalent synthesis filters after interpolation (see Figure 3 and equation (4)) are expansions and contractions of a single mother function $\overline{\psi}(t)$.

Wavelets

- Using similar reasoning to that leading to Figures 4–6, one can obtain the continuous-time signal $x(t)$ from the wavelet coefficients $c_{m,n}$ as

$$x(t) = \sum_{m=-\infty}^{\infty} \sum_{n=-\infty}^{\infty} c_{m,n} 2^{-\frac{m}{2}} \overline{\psi}(2^{-m}t - n) \tag{6}$$

- Equations (5) and (6) represent the direct and inverse wavelet transforms of a continuous-time signal $x(t)$.

- The wavelet transform of the corresponding discrete-time signal $x(n)$ is merely the octave-band decomposition in Figures 2 and 3.

- A natural question to ask at this point is:
  How are the continuous-time signal $x(t)$ and the discrete-time signal $x(n)$ related, if they generate the same wavelet coefficients?
  In addition, how can the analysis and synthesis wavelets be derived from the filter bank coefficients and vice versa?

- These questions can be answered using the concept of scaling functions, seen next.

Scaling functions

- By examining Figure 6 and equations (5) and (6), we observe that the values of m which are associated with the "width" of the filters range from $-\infty$ to $+\infty$.
- Since all signals encountered in practice are somehow band-limited, one can assume, without loss of generality, that the output of the filters with impulse responses $\psi(2^{-\mathrm{m}}\mathrm{t})$ are zero, for $\mathrm{m} < 0$.
- Therefore, in practice, m can then vary only from 0 to $+\infty$.
- Examining Figures 2–4, we observe that $\mathrm{m} \rightarrow +\infty$ means that the lowpass channels will be indefinitely decomposed.
- However, in practice, the number of stages of decomposition is finite and, after S stages, we have S bandpass channels and one lowpass channel.
- Therefore, if we restrict the number of decomposing stages in Figures 2–6, and add a lowpass channel, we can modify equation (6) so that m assumes only a finite number of values.

Scaling functions

- This can be done by noting that if $H_0(z)$ has enough zeros at $z = -1$, the envelopes of the analysis lowpass channels given in equation (1) will also be expansions and contractions of a single function $\phi(t)$, which is called the analysis scaling function.
- Likewise, the envelopes of the synthesis lowpass channels are expansions and contractions of the synthesis scaling function $\overline{\phi}(t)$.

Scaling functions

- Therefore, if we make an $(S+1)$-stage decomposition, equation (6) becomes

$$x(t) = \sum_{m=0}^{S-1} \sum_{n=-\infty}^{\infty} c_{m,n} 2^{-\frac{m}{2}} \overline{\psi}(2^{-m}t - n) + \sum_{n=-\infty}^{\infty} x_{S,n} 2^{-\frac{S}{2}} \overline{\phi}(2^{-S}t - n) \tag{7}$$

  where

$$x_{S,n} = \int_{-\infty}^{\infty} 2^{-\frac{S}{2}} \phi^*(2^{-S}t - n) x(t) dt \tag{8}$$

- Hence, the wavelet transform is, in practice, described as in equations (5), (7), and (8).

- The summations in n will, in general, depend on the supports (that is, the regions where the functions are nonzero) of the signal, wavelets, and scaling functions.

Relation between $x(t)$ and $x(n)$

- Equation (8) shows how to compute the coefficients of the lowpass channel after an $(S+1)$-stage wavelet transform.
- In Figure 2, $x_{S,n}$ are the outputs of a lowpass filter $H_0(z)$ after $(S+1)$ stages.
- Since in Figure 3 the discrete-time signal $x(n)$ can be regarded as the output of a lowpass filter after "zero" stages, we can say that $x(n)$ would be equal to $x_{-1,n}$.
- In other words, equivalence of the outputs of the octave-band filter bank of Figure 2 and the wavelet transform given by equations (5) and (6) occurs only if the digital signal input to the filter bank of Figure 2 is equal to $x_{-1,n}$.
- From equation (8), this means

$$x(n) = \int_{-\infty}^{\infty} \sqrt{2}\phi^*(2t-n)x(t)dt \tag{9}$$

- Such an equation can be interpreted as $x(n)$ being the signal $x(t)$ digitized with a band-limiting filter having $\sqrt{2}\phi(-2t)$ as its impulse response.

Relation between $x(t)$ and $x(n)$

- Therefore, a possible way to compute the wavelet transform of a continuous-time signal $x(t)$ is depicted in Figure 9, in which $x(t)$ is passed through a filter having as impulse response the scaling function contracted-in-time by 2 and sampled with $T_s = 1$, or equivalently $\Omega_s = 2\pi$.
- The resulting digital signal is then the input to the octave-band filter bank in Figure 2 whose filter coefficients will be as determined later on in Section 77 by equations (125) and (127).
- At this point, it is important to note that, strictly speaking, the wavelet transform is only defined for continuous-time signals.
- However, it is common practice to refer to the wavelet transform of a discrete-time signal $x(n)$ as the output of the filter bank in Figure 2.

Relation between $x(t)$ and $x(n)$

- One should also note that, in order for the output signals in Figures 4 and 5 to be entirely equivalent, the input signal in Figure 4 must not be the discrete-time impulse, but the sampled impulse response of the filter $\sqrt{2}\phi(-2t)$.
- This is nothing less than a sampled version of the scaling function contracted-in-time by 2.

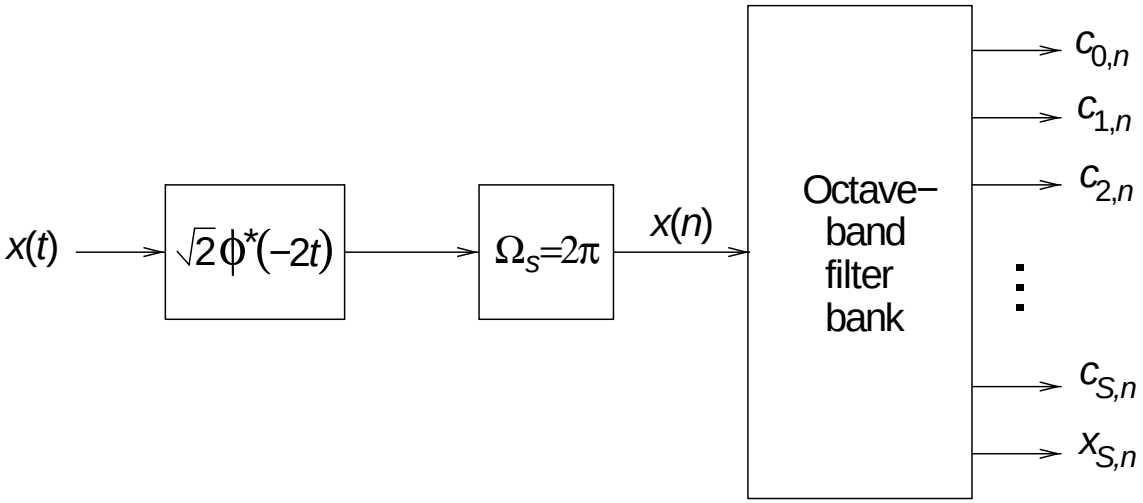

Figure 9: Practical way to compute the wavelet transform of a continuous-time signal.

Wavelet transforms and time-frequency analysis

- In time-frequency analysis one is interested to know how the frequency content of a signal varies in time.
- Wavelet transforms are a powerful tool for that purpose, and here we approach the wavelet transform from a time-frequency analysis point of view.
- We do so by first analyzing the short-time Fourier transform, highlighting its limitations using the uncertainty principle.
- Then we introduce the continuous-time wavelet transform as a way to overcome some of the limitations of the short-time Fourier transform.
- Finally, we arrive at the wavelet transform by sampling the continuous-time wavelet transform.

The short-time Fourier transform

- A common form of signal representation and analysis is through its decomposition into its frequency components.
- A classical way of doing so is through the Fourier transform $X(\Omega)$ of a function $x(t)$ defined as

$$X(\Omega) = \int_{-\infty}^{\infty} x(t) e^{-j\Omega t} dt \tag{10}$$

- The Fourier transform computes the frequency content of a signal taking into consideration its entire duration, from $t = -\infty$ to $t = \infty$.
- However, it is sometimes interesting to compute the frequency content of a signal only around a certain time location.
- For example, if someone speaks “The baby wants a ball”, one may be interested in analyzing the frequency content only of the article “a”, and not of the phrase as a whole.

The short-time Fourier transform

- Clearly, the Fourier transform is not suitable for such an analysis, for it will always take into account the full duration of the signal.
- Therefore, a tool for analyzing the local frequency content of a signal is desirable.
- A generalization of the Fourier transform, the short-time Fourier transform (STFT) is such a tool. It can be defined as:

$$X_F(\Omega_0, b) = \int_{-\infty}^{\infty} x(t)g(t-b)e^{-j\Omega_0 t}dt \tag{11}$$

- The STFT is equivalent to the Fourier transform of the windowed function $x(t)g(t-b)$.
- The window function $g(t)$ is in general "concentrated" around $t = 0$, and its purpose is to isolate the values of the function $x(t)$ around $t = b$ prior to the computation of the Fourier transform.
- Figure 10 shows a typical window $g(t)$.

The short-time Fourier transform

- The STFT has two independent variables, the frequency Ω and the position b of the data window.
- For each value of b, the STFT gives the spectral content $X_F(\Omega, b)$ of $x(t)$ around $t = b$.

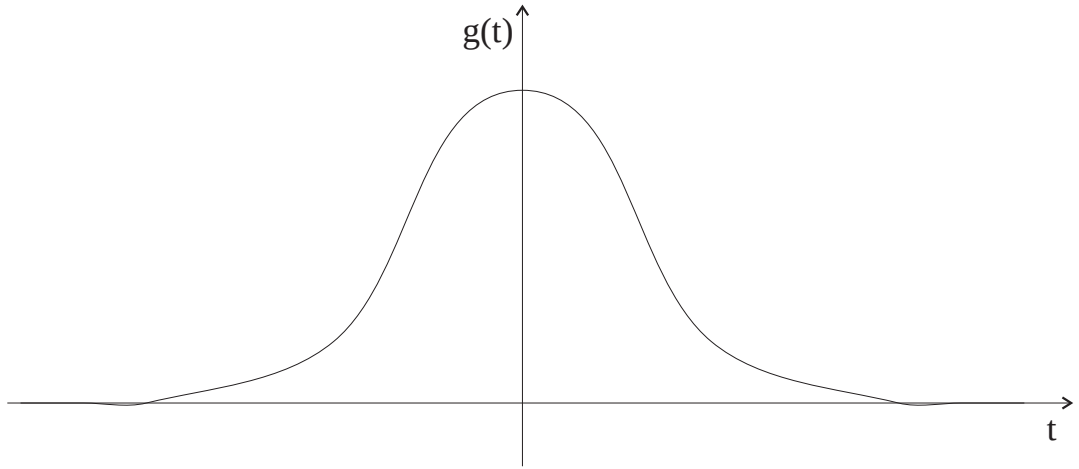

Figure 10: Typical window function for the STFT.

The short-time Fourier transform

- The STFT has also a dual interpretation. If $G(\Omega)$ is the Fourier transform of $g(t)$, one can use the Parseval's theorem to show that equation (11) is equivalent to

$$X_F(\Omega_0, b) = \frac{1}{2\pi} \int_{-\infty}^{\infty} X(\Omega) G(\Omega - \Omega_0) e^{-j\Omega b} d\Omega \qquad (12)$$

- Therefore, for each Ω_0, the STFT also gives how the frequency components of $x(t)$ around $\Omega = \Omega_0$ (as filtered by $G(\Omega - \Omega_0)$) evolve in time.
- Besides being concentrated around $t = 0$, the window function $g(t)$ is in general chosen such that $G(\Omega)$ is also concentrated around $\Omega = 0$.
- A common choice for $g(t)$ is a Gaussian function, which is concentrated around zero in both the time and frequency domains.
- A good estimate of the "width" of both $g(t)$ and $G(\Omega)$ is provided, respectively, by their standard deviations σ_b and σ_Ω.

The short-time Fourier transform

- The respective variances are given by:

$$\sigma_b^2 = \frac{\int_{-\infty}^{\infty} t^2 |g(t)|^2 dt}{\int_{-\infty}^{\infty} |g(t)|^2 dt} \tag{13}$$

$$\sigma_\Omega^2 = \frac{\int_{0}^{\infty} \Omega^2 |G(\Omega)|^2 d\Omega}{\int_{0}^{\infty} |G(\Omega)|^2 d\Omega} \tag{14}$$

- Examining equation (11), one can observe that the computation of $X_F(\Omega_0, b)$ depends mainly on the values of $x(t)$ in the interval $t \in [b - \sigma_b, b + \sigma_b]$.

- Alternatively, equation (12) shows that $X_F(\Omega_0, b)$ depends mainly on the values of $X(\Omega)$ in the interval $[\Omega - \sigma_\Omega, \Omega + \sigma_\Omega]$.

The short-time Fourier transform

- This is equivalent to saying that the STFT analyzes slices of the signal, having duration $2\sigma_b$, through filters of constant bandwidth, equal to $2\sigma_\Omega$.
- From the above, we can conclude that, the smaller the σ_b, the better a feature can be localized in the time domain; in other words, the better the time resolution of the STFT.
- Alternatively, the smaller the σ_Ω, the better the frequency resolution of the STFT.
- This implies that the time and frequency resolutions of the STFT depend only on $g(t)$, and are therefore fixed, independent of the particular point (b, Ω) in the time-frequency space, as illustrated in Figure 11.

The short-time Fourier transform

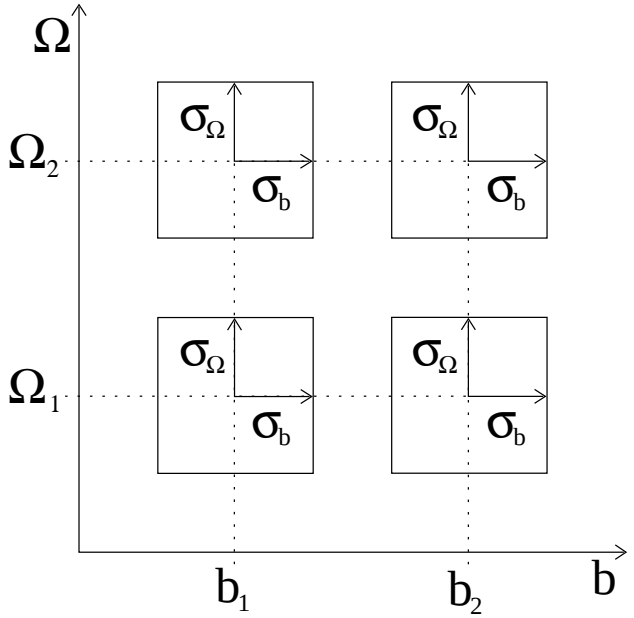

Figure 11: Resolution cells in the time $\times$ frequency plane for the STFT.

- It is important to point out that the time and frequency resolutions of the STFT, as defined in equations (13) and (14), can not be arbitrarily small, as stated below.

The short-time Fourier transform

UNCERTAINTY PRINCIPLE

Whenever $g(t)$ decays faster than $\frac{1}{\sqrt{t}}$ for $t \to \pm\infty$, then

$$\sigma_\Omega^2 \sigma_b^2 \geq \frac{1}{4} \tag{15}$$

- This result implies that there is a maximum resolution that can be jointly achieved in frequency and time by any linear transform.
- The equality holds for Gaussian signals, that is, for

$$g(t) = \alpha e^{-\kappa t^2} \tag{16}$$

The short-time Fourier transform

Outline of the Proof

- Using the Schwartz inequality,

$$\left|\int_{-\infty}^{\infty} t g(t) \frac{dg(t)}{dt} dt\right|^2 \leq \int_{-\infty}^{\infty} |tg(t)|^2 dt \int_{-\infty}^{\infty} \left|\frac{dg(t)}{dt}\right|^2 dt \qquad (17)$$

- Since the Fourier transform of $\frac{dg(t)}{dt}$ is $j\Omega G(\Omega)$, one can apply Parseval's theorem in the third integral to get

$$\int_{-\infty}^{\infty} \left|\frac{dg(t)}{dt}\right|^2 dt = \frac{1}{2\pi} \int_{-\infty}^{\infty} |\Omega G(\Omega)|^2 \, d\Omega \qquad (18)$$

and therefore equation (17) becomes

$$\left|\int_{-\infty}^{\infty} t g(t) \frac{dg(t)}{dt} dt\right|^2 \leq \frac{1}{2\pi} \int_{-\infty}^{\infty} |tg(t)|^2 dt \int_{-\infty}^{\infty} |\Omega G(\Omega)|^2 \, d\Omega \qquad (19)$$

The short-time Fourier transform

Since

$$2g(t)\frac{dg(t)}{dt} = \frac{d[g^2(t)]}{dt} \tag{20}$$

we have that

$$\begin{aligned}\int_{-\infty}^{\infty} tg(t)\frac{dg(t)}{dt}dt &= \frac{1}{2}\int_{-\infty}^{\infty} t\frac{d[g^2(t)]}{dt}dt \\ &= \frac{1}{2}tg^2(t)\Big|_{-\infty}^{\infty} - \frac{1}{2}\int_{-\infty}^{\infty} g^2(t)dt \end{aligned} \tag{21}$$

- Since $g(t)$ decays faster than $\frac{1}{\sqrt{t}}$ for $t \to \pm\infty$, we have that

$$\lim_{t\to\pm\infty} tg^2(t) = 0 \tag{22}$$

and then, supposing $g(t)$ real, equation (21) becomes

$$\int_{-\infty}^{\infty} tg(t)\frac{dg(t)}{dt}dt = -\frac{1}{2}\int_{-\infty}^{\infty} g^2(t)dt = -\frac{1}{2}\int_{-\infty}^{\infty} |g(t)|^2 dt \tag{23}$$

The short-time Fourier transform

- Substituting the above equation in equation (19), we get

$$\left|\frac{1}{2}\int_{-\infty}^{\infty}|g(t)|^2dt\right|^2 \leq \frac{1}{2\pi}\int_{-\infty}^{\infty}|tg(t)|^2dt\int_{-\infty}^{\infty}|\Omega G(\Omega)|^2\,d\Omega \tag{24}$$

- Using again Parseval's theorem we have that

$$\int_{-\infty}^{\infty}|g(t)|^2dt = \frac{1}{2\pi}\int_{-\infty}^{\infty}|G(\Omega)|^2\,d\Omega \tag{25}$$

and therefore

$$\left|\int_{-\infty}^{\infty}|g(t)|^2dt\right|^2 = \frac{1}{2\pi}\int_{-\infty}^{\infty}|G(\Omega)|^2\,d\Omega\int_{-\infty}^{\infty}|g(t)|^2dt \tag{26}$$

- Replacing the above expression into equation (24), we conclude that

$$\frac{1}{8\pi}\int_{-\infty}^{\infty}|g(t)|^2dt\int_{-\infty}^{\infty}|G(\Omega)|^2d\Omega \leq \frac{1}{2\pi}\int_{-\infty}^{\infty}|tg(t)|^2dt\int_{-\infty}^{\infty}|\Omega G(\Omega)|^2\,d\Omega \tag{27}$$

The short-time Fourier transform

and therefore

$$\left(\frac{\int_{-\infty}^{\infty}|t|^2|g(t)|^2dt}{\int_{-\infty}^{\infty}|g(t)|^2dt}\right)\left(\frac{\int_{-\infty}^{\infty}|\Omega|^2|G(\Omega)|^2d\Omega}{\int_{-\infty}^{\infty}|G(\Omega)|^2d\Omega}\right)\geq\frac{1}{4} \tag{28}$$

which, from the definitions of equations (13) and (14), gives the desired result.

- If $g(t)$ is a Gaussian, that is,

$$g(t)=\alpha e^{-\kappa t^2} \tag{29}$$

we have that

$$G(\Omega)=\alpha\sqrt{\frac{\pi}{\kappa}}e^{-\frac{\Omega^2}{4\kappa}} \tag{30}$$

and then

$$g^2(t)=\alpha^2e^{-2\kappa t^2};\qquad G^2(\Omega)=\alpha^2\frac{\pi}{\kappa}e^{-\frac{\Omega^2}{2\kappa}} \tag{31}$$

The short-time Fourier transform

- Since $g^2(t)$ and $G^2(\Omega)$ are still Gaussian, then $\sigma_b^2 = \frac{1}{4\kappa}$ and $\sigma_\Omega^2 = \kappa$, in such a way that

$$\sigma_b^2 \sigma_\Omega^2 = \frac{1}{4} \tag{32}$$

- Therefore, for the Gaussian window function, relationship (15) holds with the equality sign, indicating that it represents the best possible time-frequency resolution compromise.

- Note that the requirements of the window in this case are different from the ones in Chapter 5.

- There, we want $g(t)$ to be concentrated as much as possible in the frequency domain, while having ripples with the smallest amplitude possible.

- This is so because in that case we are interested only in the frequency domain properties, while in the STFT we want the best compromise between time- and frequency-domain representations.

The short-time Fourier transform

- In some cases, the fixed spatial and frequency resolutions of the STFT become in general a major drawback.
- This usually happens with highly non-stationary signals, that have features of very different sizes and in varying degrees of resolution.
- This is so because, once the function $g(t)$ is fixed, its time and frequency resolutions are also fixed, and only those features of size comparable to that of $g(t)$ can be conveniently analyzed.
- Therefore, it is desirable to have a transform with windows of different sizes, so that it can adapt to the features to be analyzed.
- Wavelet transforms are a class of transforms that have exactly this property.

The continuous-time wavelet transform

- The continuous wavelet transform of a signal $x(t)$ belonging to $L^2\{\mathbb{R}\}$, the space of square integrable functions in $\mathbb{R}$, is its decomposition into a set of basis functions comprising expansions and translations of a mother function $\psi(t)$.

- Therefore, by defining the basis functions $\psi_{a,b}(t)$ as

$$\psi_{a,b}(t) = \frac{1}{\sqrt{a}}\psi\left(\frac{t-b}{a}\right) \tag{33}$$

  the continuous wavelet transform can be written as

$$X_W(a,b) = \int_{-\infty}^{\infty} x(t)\psi^*_{a,b}(t)dt \tag{34}$$

  where "$*$" denotes complex conjugation.

- Throughout this discussion, wavelets will be assumed to be real, and so $\psi(t) = \psi^*(t)$.

The continuous-time wavelet transform

- Alternatively, if the Fourier transform of $\psi_{a,b}(t)$ is $\Psi_{a,b}(\omega)$, equation (34) can be rewritten in the frequency domain, using Parseval's theorem, as

$$X_W(a,b) = \frac{1}{2\pi}\int_{-\infty}^{\infty} \Psi^*_{a,b}(\omega)X(\omega)d\omega \tag{35}$$

- It can be shown that $x(t)$ can be recovered from its wavelet transform $X_W(a,b)$ using the following expression:

$$x(t) = C_\psi^{-1}\int_0^\infty \frac{da}{a^2}\int_{-\infty}^{\infty} X_W(a,b)\psi_{a,b}(t)db \tag{36}$$

where the constant C_ψ is such that

$$C_\psi = 2\pi\int_0^\infty \frac{|\Psi(\omega)|^2}{|\omega|}d\omega = 2\pi\int_{-\infty}^0 \frac{|\Psi(\omega)|^2}{|\omega|}d\omega < \infty \tag{37}$$

The continuous-time wavelet transform

- If $\psi(t)$ is continuous, equation (37) can only be satisfied if

$$\int_{-\infty}^{\infty} \psi(t)dt = 0 \tag{38}$$

- The above equation is equivalent to $\Psi(0) = 0$, which implies that $\psi(t)$ must be a band-pass function.
- The factor a is called the *scale* of the basis function.
  - The larger it is, the wider the basis function is in the time domain, and therefore the narrower it is in the frequency domain.
  - Conversely, the smaller the scale a, the narrower the basis function is in the time domain and the wider it is in the frequency domain.
- Figure 7 illustrates this point.
- From this, one can infer that in the wavelet transform time and frequency resolutions vary, and there is a trade-off between both.

The continuous-time wavelet transform

- In order to be more precise, we first note that, from equation (38), $\psi(t)$ must be band-pass.
- Supposing that $\psi(t)$ is real, then $\Psi(\Omega)$ is conjugate symmetric.
- Now let t_0 and Ω_0 be such that

$$\int_{-\infty}^{\infty} (t - t_0)|\psi(t)|^2 dt = 0 \quad (39)$$

$$\int_{0}^{\infty} (\Omega - \Omega_0)|\Psi(\Omega)|^2 d\Omega = 0 \quad (40)$$

The continuous-time wavelet transform

- We can define, similarly to equations (13) and (14), the variances of $\psi(t)$ and of the positive frequencies of its Fourier transform $\Psi(\omega)$ as:

$$\sigma_b^2 = \frac{\int_{-\infty}^{\infty} (t - t_0)^2 |\psi(t)|^2 dt}{\int_{-\infty}^{\infty} |\psi(t)|^2 dt} \tag{41}$$

$$\sigma_\Omega^2 = \frac{\int_0^{\infty} (\Omega - \Omega_0)^2 |\Psi(\Omega)|^2 d\Omega}{\int_0^{\infty} |\Psi(\Omega)|^2 d\Omega} \tag{42}$$

- Note that $\psi(t)$ is usually chosen such that $t_0 = 0$.
- The above equations imply that the standard deviations of $\psi_{a,b}(t)$ and its Fourier transform are $a\sigma_b$ and $\frac{\sigma_\Omega}{a}$, respectively.
- Also, the center frequency of $\Psi_{a,b}(\Omega)$ is $\frac{\Omega_0}{a}$.

The continuous-time wavelet transform

- Therefore, from equation (34), the wavelet transform $X_W(a, b)$ depends mainly on the values of $x(t)$ in the interval $t \in [b - a\sigma_b, b + a\sigma_b]$.
- From equation (35), $X_W(a, b)$ depends mainly on the values of $X(\Omega)$ in the frequency interval $\Omega \in [\frac{\Omega_0}{a} - \frac{\sigma_\Omega}{a}, \frac{\Omega_0}{a} + \frac{\sigma_\Omega}{a}]$.
- This implies that for large a, that is, for small frequencies, the wavelet transform has low time resolution and high frequency resolution.
- Conversely, for small values of a, which correspond to large frequencies, the wavelet transform has high time resolution and low frequency resolution.
- This can be illustrated by the resolution cells in Figure 12, where one may note that the uncertainty principle from relation (15) still holds.

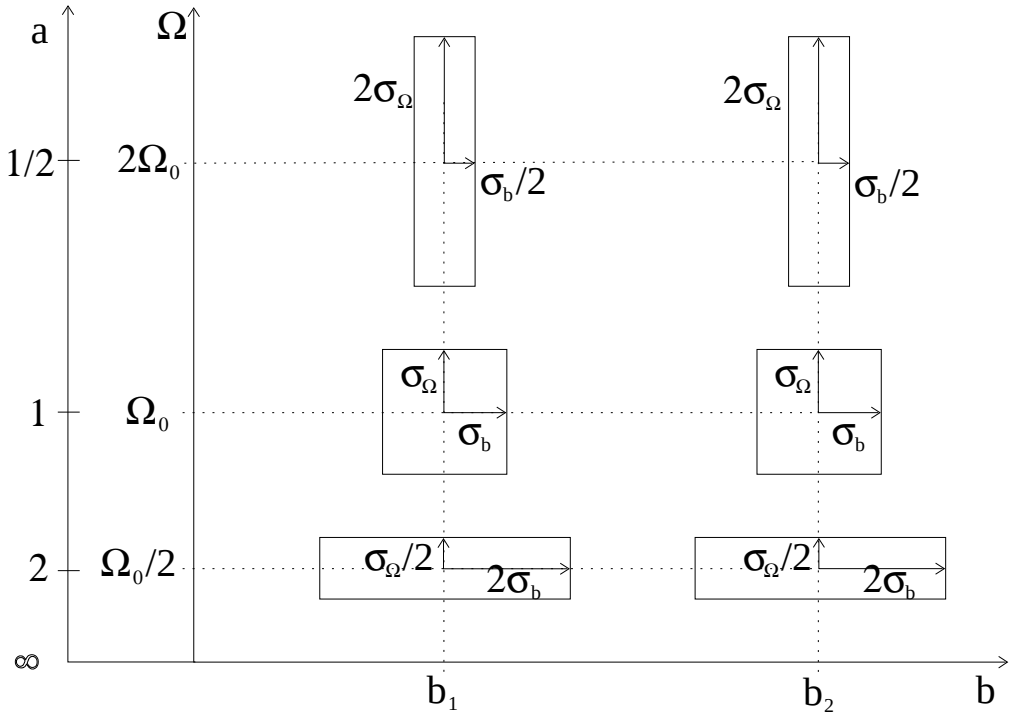

Figure 12: Resolution cells in the time $\times$ frequency plane for the wavelet transform.

- From the above analysis, one can see that the wavelet transform is adequate for analyzing signals having features of different sizes.
- For each feature size, there is a scale a in which it will be best analyzed or represented.
- This is particularly useful in image processing, which is thoroughly explored later.

The continuous-time wavelet transform

- There is another way of interpreting the fact that the wavelet transform depends mainly on values of $X(\Omega)$ within the interval $[\frac{\Omega_0}{a} - \frac{\sigma_\Omega}{a}, \frac{\Omega_0}{a} + \frac{\sigma_\Omega}{a}]$.
- Since $\psi(t)$ can be viewed as the impulse response of a band-pass filter, this is equivalent to stating that the wavelet $\psi_{a,b}(t)$ is the impulse response of a band-pass filter having center frequency $\frac{\Omega_0}{a}$ and bandwidth $\frac{2\sigma_\Omega}{a}$.
- Thus, the $\psi_{a,b}(t)$ functions represent a set of band-pass filters whose values of the quality factor Q (defined as the ratio between the center frequency Ω_0 to the filter bandwidth $2\sigma_\Omega$) are independent of the scale a.
- Therefore, a wavelet transform is equivalent to the analysis of a signal in the frequency domain using band-pass filters having variable center frequencies, which depend on the scale a, but with constant Q.

Sampling the continuous-time wavelet transform: The discrete wavelet transform

- As can be seen from equation (34), the wavelet transform maps a one-dimensional function into a two-dimensional function.
- This dimensionality increase makes it extremely redundant.
- Thus, it looks natural that the original signal can be recovered from the wavelet transform computed only on a discrete grid.
- This is indeed the case, and Ingrid Daubechies has made an extensive investigation of this problem.

Sampling the continuous-time wavelet transform: The discrete wavelet transform

- By looking at the resolution cells in Figure 12, we can see that when the scale a increases, the central frequency and the width of the resolution cells in the frequency direction decrease, and so more resolution cells are needed to cover that region of the $\Omega \times b$ plane.
- Therefore, a natural choice for the discretization of a would be $a = a_0^m$, with $a_0 > 1$ and $m \in \mathbb{Z}$.
- Since the discretization of b corresponds to a sampling in time, its sampling frequency must be proportional to the bandwidth of the signal to be sampled, which in turn is inversely proportional to the scale a.

Sampling the continuous-time wavelet transform: The discrete wavelet transform

- Therefore, it is intuitive to choose $b = nb_0a_0^m$.
- With these choices of a and b, the discrete wavelet transform $X_W(m,n)$ of $x(t)$ becomes

$$X_W(m,n) = a_0^{-m/2} \int_{-\infty}^{\infty} \psi^*_{m,n}(t)x(t)\,dt \tag{43}$$

$$\psi_{m,n}(t) = a_0^{-m/2}\psi(a_0^{-m}t - nb_0) \tag{44}$$

- If $a_0 = 2$ and $b_0 = 1$, there are choices of $\psi(t)$ such that the functions $\psi_{m,n}(t)$, for $m,n \in \mathbb{Z}$, form an orthonormal basis of $L^2\{\mathbb{R}\}$, the space of square integrable functions in $\mathbb{R}$.

Sampling the continuous-time wavelet transform: The discrete wavelet transform

- This implies that any function $x(t) \in L^2\{\mathbb{R}\}$ can be expressed as

$$x(t) = \sum_{m=-\infty}^{\infty} \sum_{n=-\infty}^{\infty} c_{m,n} \psi_{m,n}(t) \tag{45}$$

$$c_{m,n} = \int_{-\infty}^{\infty} \psi_{m,n}^*(t) x(t)\, dt \tag{46}$$

- The $c_{m,n}$ are the wavelet transform coefficients of $x(t)$. Note that the above equations are the same as equations (5) and (6), in the case that $\overline{\psi}(t) = \psi(t)$.

- This is so because the diagram depicted in Figure 6 implements exactly the discretization of the continuous-time wavelet transform given by equations (43) and (44) when $a_0 = 2$ and $b_0 = 1$.

Sampling the continuous-time wavelet transform: The discrete wavelet transform

- This implies that the samples of a continuous-time wavelet transform can be computed using the scheme in Figure 9, provided that the envelopes of the iterated filter banks in Figure 4 correspond to expansions and translations of $\psi(t)$.
- It is interesting to observe that in this discretization of the wavelet transform, for every increment in m, the value of a doubles.
- This implies doubling the width in the time domain and halving the width in the frequency domain.
- The equivalent sampling grid is shown in Figure 13.
- By referring to equation (35), this is equivalent to having a signal analyzed in frequency channels having widths of one octave, as illustrated in Figure 8.

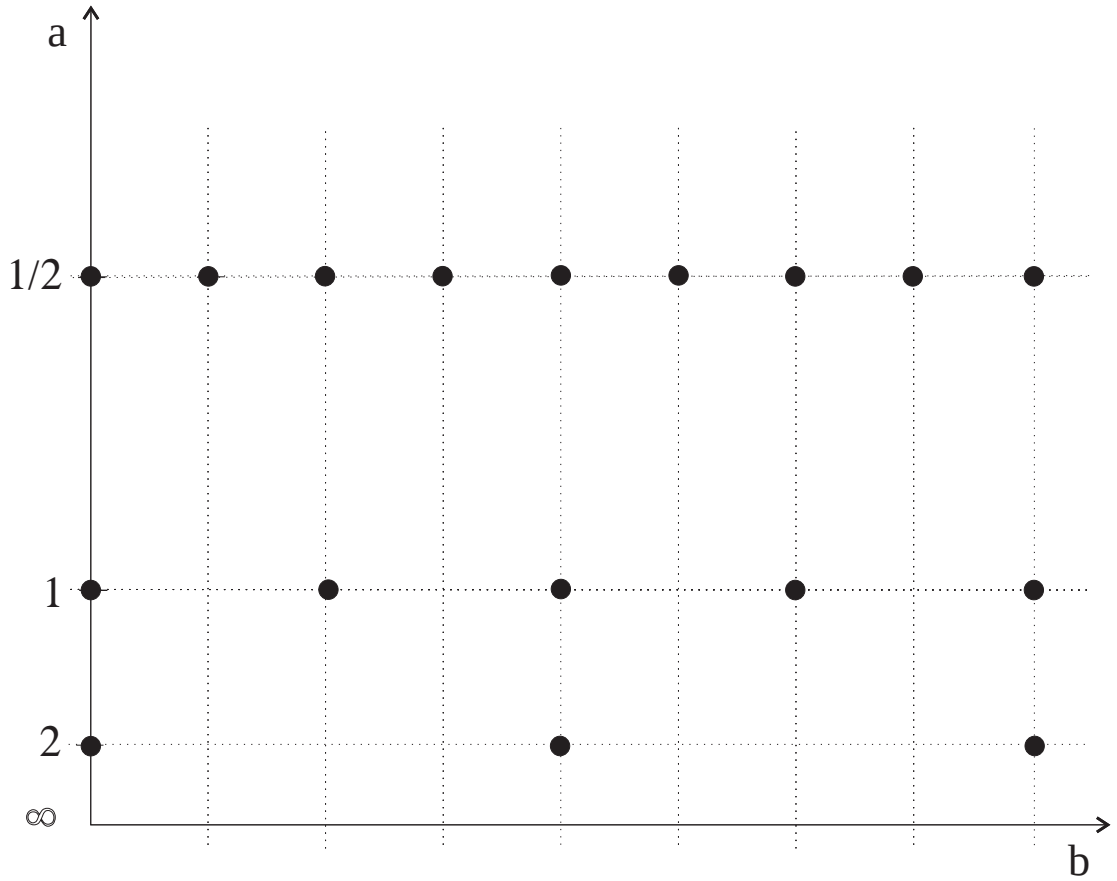

Figure 13: Discretization of the wavelet transform in equations (43) and (44) for $a_0 = 2$ and $b_0 = 1$.

Sampling the continuous-time wavelet transform: The discrete wavelet transform

- If $x(t)$ is equal to $\psi_{k,l}(t)$, then equation (45) becomes

$$\psi_{k,l}(t) = \sum_{m=-\infty}^{\infty} \sum_{n=-\infty}^{\infty} c_{m,n} \psi_{m,n}(t) \tag{47}$$

- In order for the above equation to be valid, one must have $c_{m,n} = \delta(m-k)\delta(n-l)$. In this case, equation (46) implies that

$$\int_{-\infty}^{\infty} \psi^*_{m,n}(t)\psi_{k,l}(t)\,dt = \delta(m-k)\delta(n-l) \tag{48}$$

- This is equivalent to saying that the functions $\psi_{m,n}(t)$, for all $m, n \in \mathbb{Z}$, are orthonormal.

Sampling the continuous-time wavelet transform: The discrete wavelet transform

- As detailed in Chapter 3, orthonormality is usually expressed using the inner product notation as

$$\langle \psi_{k,l}(t), \psi_{m,n}(t) \rangle = \delta(m-k)\delta(n-l) \tag{49}$$

where the inner product $\langle g(t), f(t) \rangle$ between the two functions $f(t)$ and $g(t)$ is defined as

$$\langle g(t), f(t) \rangle = \int_{-\infty}^{\infty} f^*(t) g(t)\, dt \tag{50}$$

- Since equations (45) and (46) are valid for any function $x(t) \in L^2\{\mathbb{R}\}$, then it can be said that the functions $\psi_{m,n}(t)$, for all $m, n \in \mathbb{Z}$, form an orthonormal basis of $L^2\{\mathbb{R}\}$.

- Other choices of a_0 can lead to other orthonormal bases. For example, Kovačević has described in some discrete wavelet transforms using fractional values of a_0.

Sampling the continuous-time wavelet transform: The discrete wavelet transform

- However, we will restrict our presentation to the dyadic cases, that is, to wavelet transforms in which $a_0 = 2$ and $b_0 = 1$.
- The wavelet transform as defined by equations (5) and (6), that is,

$$x(t) = \sum_{m=-\infty}^{\infty} \sum_{n=-\infty}^{\infty} c_{m,n} \overline{\psi}_{m,n}(t) \tag{51}$$

$$c_{m,n} = \int_{-\infty}^{\infty} x(t) \psi^*_{m,n}(t) dt \tag{52}$$

where

$$\psi_{m,n}(t) = 2^{-m/2} \psi(2^{-m}t - n) \tag{53}$$

$$\overline{\psi}_{m,n}(t) = 2^{-m/2} \overline{\psi}(2^{-m}t - n) \tag{54}$$

is not orthogonal. In this case, we refer to it as a biorthogonal wavelet transform (refer to Chapter 9 for a discussion on orthogonality and biorthogonality).

Sampling the continuous-time wavelet transform: The discrete wavelet transform

- Biorthogonal wavelet transforms are characterized by two wavelets, the analysis wavelet, $\psi(t)$, and the synthesis one, $\overline{\psi}(t)$.
- Equations (51)–(54) indicate that any function $x(t) \in L^2\{\mathbb{R}\}$ can be decomposed as a linear combination of contractions, expansions and translations of the synthesis wavelet, $\overline{\psi}(t)$.
- The weights of the expansion can be computed via the inner product of $x(t)$ with expansions, contractions, and translations of the analysis wavelet, $\psi(t)$.
- Functions $\psi_{m,n}(t)$ do not comprise an orthogonal set, so neither do the functions $\overline{\psi}_{m,n}(t)$.
- However, functions $\psi_{m,n}(t)$ are orthogonal to $\overline{\psi}_{m,n}(t)$
- This means that

$$\langle \psi_{m,n}(t), \overline{\psi}_{k,l}(t) \rangle = \delta(m-k)\delta(n-l) \tag{55}$$

Multiresolution representation

- The concept of multiresolution signal representation provides interesting insights on wavelet transforms, as well as a deeper understanding of their connection with filter banks.
- Suppose a function $\phi(t)$ such that the set $\phi(t-n)$, for all $n \in \mathbb{Z}$, is orthonormal.
- Define V_0 as the space generated by this set. Analogously, define V_m as the space generated by $2^{-m/2}\phi(2^{-m}t-n)$.
- Suppose also that $\phi(t)$ is the solution of the following two-scale difference equation:

$$\phi(t) = \sum_{n=-\infty}^{\infty} c_n \sqrt{2}\phi(2t-n) \tag{56}$$

- Since the orthonormality of the set $\phi(t-n)$ along t implies the orthonormality of the set $\sqrt{2}\phi(2t-n)$, we have that c_n is related to $\phi(t)$ by the following equation:

$$c_n = \int_{-\infty}^{\infty} \phi(t)\sqrt{2}\phi^*(2t-n)\,dt \tag{57}$$

Multiresolution representation

- From equation (56), it follows immediately by induction that, if $i, j \in \mathbb{Z}$, with $i > j$, there are constants α_n^{ij} such that

$$\phi(2^{-i}t) = \sum_{n=-\infty}^{\infty} \alpha_n^{ij} \phi(2^{-j}t - n) \tag{58}$$

- This means that the functions that generate the space V_i are also in V_j.
- This implies that $V_i \subset V_j$, for $i > j$. By induction, then,

$$\ldots \supset V_{-2} \supset V_{-1} \supset V_0 \supset V_1 \supset \ldots \tag{59}$$

- Interpreting V_0 as the space of functions having resolution 2^0, V_{-1} can be interpreted as the space of functions having the higher resolution 2^1, which contains V_0; V_1 can be interpreted as the space of functions having the lower resolution 2^{-1}, which is contained in V_0.
- Hence, the V_m, for increasing m, can be viewed as spaces of decreasing resolution.

Multiresolution representation

- The function $\phi(t)$ in equation (56) must also be such that

$$\bigcup_{j=-\infty}^{\infty} V_j = L^2\{\mathbb{R}\} \tag{60}$$

$$\bigcap_{j=-\infty}^{\infty} V_j = \{0\} \tag{61}$$

- Defining now W_j as the orthogonal complement of V_j in V_{j-1}, that is,

$$W_j \perp V_j \text{ and } W_j \oplus V_j = V_{j-1} \tag{62}$$

where $\oplus$ denotes the orthogonal sum operation, which corresponds to the linear closure of two orthogonal spaces. In this context, W_j can be seen as the amount of "detail" added when going from resolution V_j to the larger resolution V_{j-1}. This hierarchy of spaces is depicted in Figure 14.

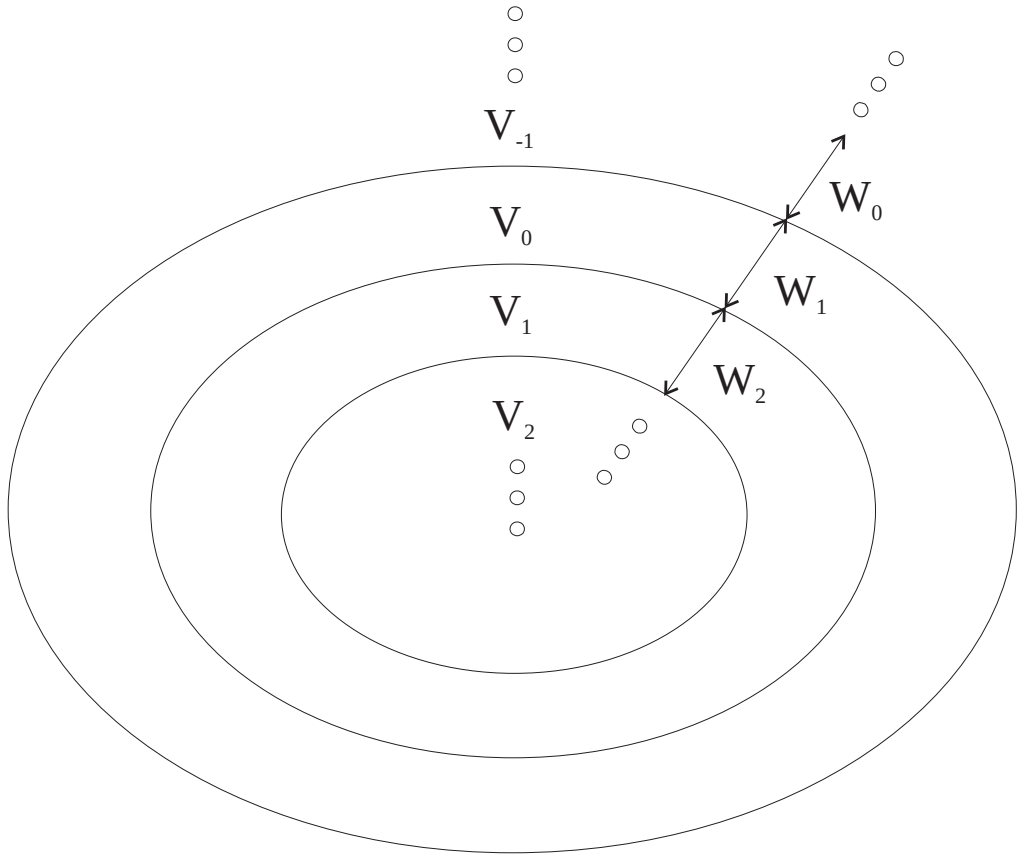

Figure 14: Geometric representation of multiresolution spaces.

- From equations (59) and (62), any function $g(t) \in W_0$ also belongs to V_{-1}, as also seen in Figure 14.

Multiresolution representation

- Therefore, such $g(t)$ can be expressed as

$$g(t) = \sum_{n=-\infty}^{\infty} d_n \sqrt{2}\phi(2t-n) \tag{63}$$

- If we define $\psi(t) \in V_{-1}$ as

$$\psi(t) = \sum_{n=-\infty}^{\infty} (-1)^n c_{1-n} \sqrt{2}\phi(2t-n) \tag{64}$$

  where the c_n are as in equation (56), it can be shown that $\psi(t) \in W_0$, and $\psi(t-n)$, for all $n \in \mathbb{Z}$, is an orthonormal basis for W_0

- More generally, $2^{-m/2}\psi(2^{-m}t-n)$ is an orthonormal basis for W_m.

- From equation (62), this implies that the functions $\psi(t-n)$ are orthogonal to the functions $\phi(t-m)$.

Multiresolution representation

- Summarizing the orthogonality conditions, we have:

$$\langle \phi(t-m), \phi(t-n) \rangle = \delta(m-n) \quad (65)$$

$$\langle \psi(t-m), \psi(t-n) \rangle = \delta(m-n) \quad (66)$$

$$\langle \psi(t-m), \phi(t-n) \rangle = 0 \quad (67)$$

- From equations (60)–(62) one can derive that:

$$\cdots \oplus W_{-2} \oplus W_{-1} \oplus W_0 \oplus W_1 \cdots = L^2\{\mathbb{R}\} \quad (68)$$

- Thus, the functions $\psi_{m,n}(t) = 2^{-m/2}\psi(2^{-m}t - n)$, for all $m, n \in \mathbb{Z}$, constitute an orthonormal basis of $L^2\{\mathbb{R}\}$.

Multiresolution representation

- This is equivalent to saying that any $f(t) \in L^2\{\mathbb{R}\}$ can be written as

$$f(t) = \sum_{m=-\infty}^{\infty} \sum_{n=-\infty}^{\infty} \alpha_{m,n} \psi_{m,n}(t) \tag{69}$$

$$\alpha_{m,n} = \int_{-\infty}^{\infty} \psi^*_{m,n}(t) f(t)\, dt \tag{70}$$

- These equations are the same as equations (45) and (46), respectively, indicating that they represent a discrete wavelet transform of $f(t)$ with mother wavelet $\psi(t)$.
- The wavelet transform coefficients $\alpha_{m,n}$ correspond to the projection of $f(t)$ onto a "detail space" W_m of resolution m.
- Therefore, a wavelet transform performs the decomposition of a signal into spaces of different resolutions.
- In the literature, these kinds of decompositions are in general referred to as multiresolution decompositions.

Multiresolution representation

- They are another way of stating the property that wavelet transforms can conveniently represent features of different sizes, that is, in different resolutions, as discussed in Section 42.
- In the frequency domain the multiresolution decompositions can be understood in the following way:
  - V_0 is the space generated by $\phi(t-n)$ and V_{-1} is the space generated by $\sqrt{2}\phi(2t-n)$, which has double the bandwidth of $\phi(t-n)$.
  - Therefore, V_{-1} also contains functions with double the frequency content than V_0, which means double the time resolution.
  - W_0 is composed by the functions that are in V_{-1} but not in V_0, and is therefore contained in the bandpass region between the passbands of $\phi(t-n)$ and $\sqrt{2}\phi(2t-n)$, which should be the passband of $\psi(t-n)$.
- This spectral reasoning is clarified in Figure 15.

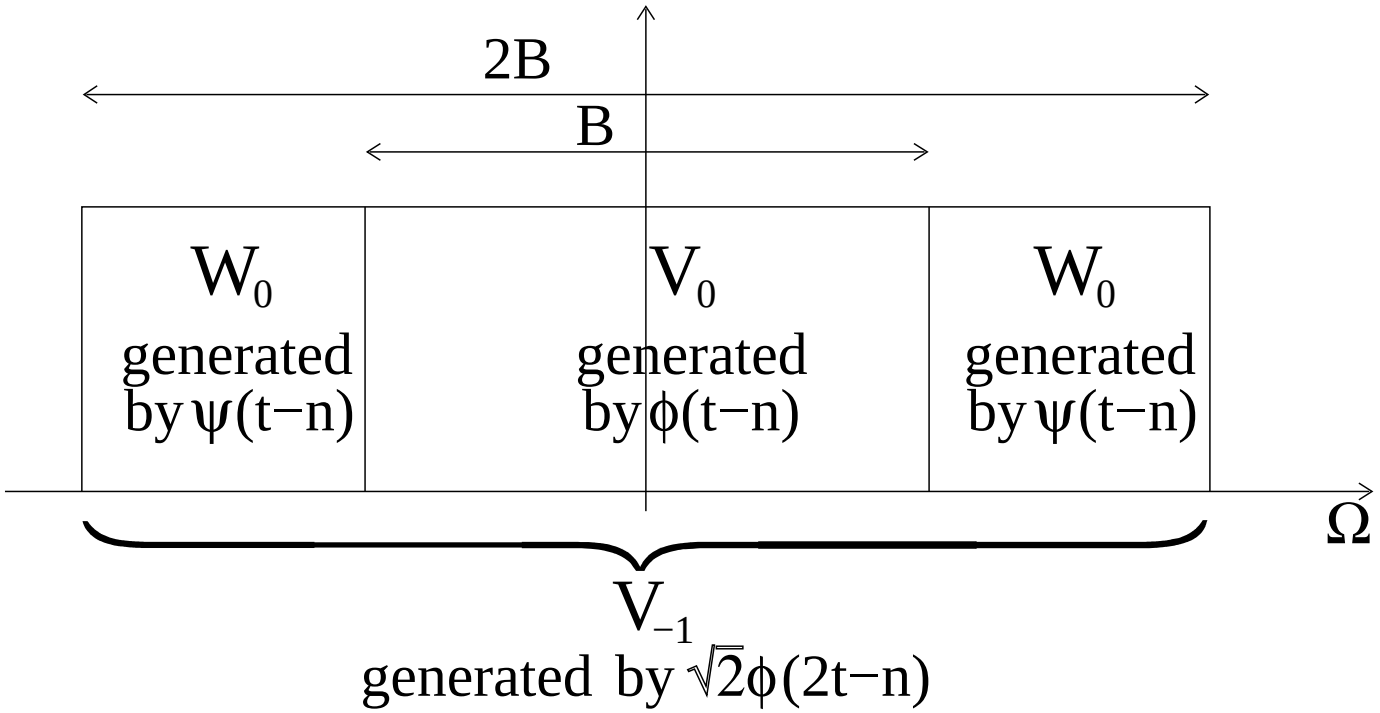

Figure 15: Multiresolution decomposition in the frequency domain.

- Note that the function $\phi(t)$ is the same as the scaling function defined earlier.
- It is often referred to as the scaling function of the multiresolution representation, while $\psi(t)$ is referred to as its wavelet.

Multiresolution representation

- Despite having nice properties, orthogonal wavelet transforms have an important limitation.
- As we have seen earlier, orthogonal filter banks can not have linear phase.
- Since wavelets are the envelope of the impulse response of iterated filter banks (see Figures 2–6), the wavelet $\psi(t)$ can not, at the same time, be orthogonal and be the impulse response of a linear phase filter.
- This is particularly significant in image processing applications, because the phase of an image signal carries very important information
- Thus, it is beneficial to use the biorthogonal wavelet transforms described in equations (51)–(55), that can have linear phase.
- In the sequel we analyze the biorthogonal multiresolution representation.

Biorthogonal multiresolution representation

- Let $\psi(t)$ and $\overline{\psi}(t)$ be the analysis and synthesis wavelets, respectively, and $\phi(t)$ and $\overline{\phi}(t)$ the corresponding analysis and synthesis scaling functions, respectively.
- Analogously to the orthogonal case, let $\phi(t)$ and $\overline{\phi}(t)$ be such that

$$\phi(t) = \sum_{n=-\infty}^{\infty} c_n \sqrt{2}\phi(2t-n) \tag{71}$$

$$\overline{\phi}(t) = \sum_{n=-\infty}^{\infty} \overline{c}_n \sqrt{2}\,\overline{\phi}(2t-n) \tag{72}$$

- Supposing also that

$$\left\langle 2^{-m/2}\phi(2^{-m}t-n), 2^{-m/2}\overline{\phi}(2^{-m}t-k)\right\rangle = \delta(n-k) \tag{73}$$

Biorthogonal multiresolution representation

we have

$$c_n = \int_{-\infty}^{\infty} \phi(t)\sqrt{2}\,\overline{\phi}^*(2t-n)\,dt \tag{74}$$

$$\overline{c}_n = \int_{-\infty}^{\infty} \overline{\phi}(t)\sqrt{2}\phi^*(2t-n)\,dt \tag{75}$$

- Functions $\phi(t)$ and $\overline{\phi}(t)$ defined this way generate two hierarchies of subspaces as the one in equation (59):

$$\phi(t): \quad \ldots \supset V_{-2} \supset V_{-1} \supset V_0 \supset V_1 \ldots \tag{76}$$

$$\overline{\phi}(t): \quad \ldots \supset \overline{V}_{-2} \supset \overline{V}_{-1} \supset \overline{V}_0 \supset \overline{V}_1 \ldots \tag{77}$$

Biorthogonal multiresolution representation

- Suppose also that, for the V_j and $\overline{V}_j$,

$$\bigcup_{j=-\infty}^{\infty} V_j = L^2\{\mathbb{R}\} \tag{78}$$

$$\bigcap_{j=-\infty}^{\infty} V_j = \{0\} \tag{79}$$

$$\bigcup_{j=-\infty}^{\infty} \overline{V}_j = L^2\{\mathbb{R}\} \tag{80}$$

$$\bigcap_{j=-\infty}^{\infty} \overline{V}_j = \{0\} \tag{81}$$

Biorthogonal multiresolution representation

- Defining W_j and $\overline{W}_j$ such that

$$V_{j-1} = V_j + W_j \tag{82}$$

$$\overline{V}_{j-1} = \overline{V}_j + \overline{W}_j \tag{83}$$

$$W_j \perp \overline{V}_j \text{ and } \overline{W}_j \perp V_j \tag{84}$$

  where $A + B$ denotes the linear closure of A and B, or the subspace generated by all the linear combinations of functions in A and B.

- It must be noted that the linear closure $+$ in equations (82) and (83) differs from the orthogonal sum $\oplus$ operation in equation (62), because, in the biorthogonal multiresolution representation considered here, V_j and W_j are not orthogonal to each other.

- Once again, W_j can be interpreted as the amount of "detail" added when going from "resolution" V_j to V_{j-1}, and $\overline{W}_j$ is the amount of "detail" added when going from "resolution" $\overline{V}_j$ to $\overline{V}_{j-1}$. However, unlike the orthogonal case, the W_j in one set of spaces is orthogonal only to the $\overline{V}_j$ in the other set of spaces, and not to V_j.

Biorthogonal multiresolution representation

- Let $\psi(t)$ and $\overline{\psi}(t)$ be bases for W_j and $\overline{W}_j$, respectively. Since, from equations (82) and (83), $W_j \in V_{j-1}$ and $\overline{W}_j \in \overline{V}_{j-1}$, hence $\psi(t)$ and $\overline{\psi}(t)$ can be expressed as

$$\psi(t) = \sum_{n=-\infty}^{\infty} d_n \sqrt{2}\phi(2t-n) \tag{85}$$

$$\overline{\psi}(t) = \sum_{n=-\infty}^{\infty} \overline{d}_n \sqrt{2}\,\overline{\phi}(2t-n) \tag{86}$$

where, from equation (73),

$$d_n = \int_{-\infty}^{\infty} \psi(t)\sqrt{2}\,\overline{\phi}^*(2t-n)\,dt \tag{87}$$

$$\overline{d}_n = \int_{-\infty}^{\infty} \overline{\psi}(t)\sqrt{2}\,\phi^*(2t-n)\,dt \tag{88}$$

Biorthogonal multiresolution representation

- The functions $\phi(t)$, $\overline{\phi}(t)$, $\psi(t)$, and $\overline{\psi}(t)$ defined as above satisfy the following biorthogonality conditions:

$$\left\langle \phi(t), \overline{\phi}(t-m) \right\rangle = \delta(m) \tag{89}$$

$$\left\langle \psi(t), \overline{\psi}(t-m) \right\rangle = \delta(m) \tag{90}$$

$$\left\langle \phi(t), \overline{\psi}(t-m) \right\rangle = 0 \tag{91}$$

$$\left\langle \psi(t), \overline{\phi}(t-m) \right\rangle = 0 \tag{92}$$

- From equations (76)–(83), we also get that

$$\cdots + \overline{W}_{-2} + \overline{W}_{-1} + \overline{W}_0 + \overline{W}_1 + \cdots = L^2\{\mathbb{R}\} \tag{93}$$

- The above equation together with equations (51) and (54) imply that, as in the orthogonal case, a biorthogonal wavelet transform involves the projection of a function onto the detail spaces $\overline{W}_j$.

Biorthogonal multiresolution representation

- Next we use the concept of multiresolution decomposition to present how wavelet transforms of digital signals can be computed, as well as their relation to the 2-band perfect reconstruction filter banks described earlier.

Wavelet transforms and filter banks

- In the real world, every function is measured with a finite resolution.
- Without any loss of generality, we can assume that $\overline{V}_0$ is this resolution
  (Since orthogonal wavelet transforms are a special case of the biorthogonal wavelet transforms, only the biorthogonal case will be analyzed here..
- Since $\overline{V}_j$ is the space generated by the functions $2^{-j/2}\overline{\phi}(2^{-j}t-n)$, the projection $x_j(t)$ of $x(t)$ onto $\overline{V}_j$ is equal to

$$x_j(t) = \sum_{n=-\infty}^{\infty} x_{j,n} 2^{-j/2}\overline{\phi}(2^{-j}t-n) \tag{94}$$

$$x_{j,n} = \int_{-\infty}^{\infty} x(t) 2^{-j/2}\phi^*(2^{-j}t-n)dt \tag{95}$$

- Equation (95) can be interpreted as the coefficients $x_{j,n}$ being obtained by filtering $x(t)$ with a continuous-time filter having impulse response $2^{-j/2}\phi(-2^{-j}t)$, and sampling the resulting continuous-time function at the sampling times $t_n = 2^j n$.

Wavelet transforms and filter banks

- Referring to Figure 15, the filtering process would serve to reduce the bandwidth of $x(t)$, and consequently its time resolution.
- Therefore, the resulting function $x_j(t)$, having limited resolution, can be represented unambiguously by the coefficients $x_{j,n}$.

Wavelet transforms and filter banks

- Since, from equation (71), $\phi(t) = \sum_{k=-\infty}^{\infty} c_k \sqrt{2}\phi(2t-k)$, we have

$$2^{-j/2}\phi(2^{-j}t-n) = \sum_{k=-\infty}^{\infty} c_k 2^{\frac{1-j}{2}}\phi(2^{1-j}t-2n-k) \tag{96}$$

which, when substituted into equation (95), results in

$$\begin{aligned} x_{j,n} &= \int_{-\infty}^{\infty} x(t) \sum_{k=-\infty}^{\infty} c_k^* 2^{\frac{1-j}{2}}\phi^*(2^{1-j}t-2n-k)dt \\ &= \sum_{k=-\infty}^{\infty} c_k^* \int_{-\infty}^{\infty} x(t)2^{\frac{1-j}{2}}\phi^*(2^{1-j}t-2n-k)dt \end{aligned} \tag{97}$$

- The comparison of the above expression with equation (95) implies that

$$x_{j,n} = \sum_{k=-\infty}^{\infty} c_k^* x_{j-1,2n+k} \tag{98}$$

Wavelet transforms and filter banks

- By defining

$$h_0(k) = c^*_{-k} \tag{99}$$

equation (98) can be rewritten as

$$x_{j,n} = \sum_{k=-\infty}^{\infty} h_0(k) x_{j-1,2n-k} \tag{100}$$

- This equation means that the coefficients $x_{j,n}$ of the approximation of $x(t)$ at resolution 2^{-j} can be obtained, from the coefficients $x_{j-1,n}$ of the approximation of $x(t)$ at the higher resolution 2^{1-j}, by filtering them with a digital filter having impulse response $h_0(k)$, with $k \in \mathbb{Z}$, and sub-sampling the result by a factor of two, as depicted in Figure 2.

Wavelet transforms and filter banks

- This result is not surprising, because, since the resolution of the space V_j is half of the one of the space V_{j-1}, then V_j should roughly have half of the frequency content of V_{j-1} (as determined by the filtering operation with $h_0(k)$), and should therefore be represented by a non-redundant transform with only half of the number of coefficients (as yielded by the decimation-by-2 operation).

Wavelet transforms and filter banks

- Since $\overline{W}_j$ is the space generated by the functions $2^{-j/2}\overline{\psi}(2^{-j}t - n)$, the projection $\check{x}_j(t)$ of $x(t)$ onto $\overline{W}_j$ is equal to

$$\check{x}_j(t) = \sum_{n=-\infty}^{\infty} \check{x}_{j,n} 2^{-j/2}\overline{\psi}(2^{-j}t - n) \quad (101)$$

$$\check{x}_{j,n} = \int_{-\infty}^{\infty} x(t) 2^{-j/2}\psi^*(2^{-j}t - n)dt \quad (102)$$

- Similarly to equation (95), equation (102) can be interpreted as the coefficients $\check{x}_{j,n}$ being obtained by filtering $x(t)$ with a continuous-time filter having impulse response $2^{-j/2}\psi(-2^{-j}t)$, and sampling the resulting continuous-time function at the sampling times $t_n = 2^j n$.

Wavelet transforms and filter banks

- As, from equation (85), $\psi(t) = \sum_{k=-\infty}^{\infty} d_k \sqrt{2}\phi(2t-k)$, we have

$$2^{-j/2}\psi(2^{-j}t-n) = \sum_{k=-\infty}^{\infty} d_k 2^{\frac{1-j}{2}} \phi(2^{1-j}t-2n-k) \tag{103}$$

which, when substituted in equation (102), results in

$$\begin{aligned} \check{x}_{j,n} &= \int_{-\infty}^{\infty} x(t) \sum_{k=-\infty}^{\infty} d_k^* 2^{\frac{1-j}{2}} \phi^*(2^{1-j}t-2n-k)dt \\ &= \sum_{k=-\infty}^{\infty} d_k^* \int_{-\infty}^{\infty} x(t) 2^{\frac{1-j}{2}} \phi^*(2^{1-j}t-2n-k)dt \end{aligned} \tag{104}$$

- Comparing this expression to equation (102), we have that

$$\check{x}_{j,n} = \sum_{k=-\infty}^{\infty} d_k^* x_{j-1,2n+k} \tag{105}$$

Wavelet transforms and filter banks

- By defining

$$h_1(k) = d^*_{-k} \tag{106}$$

equation (105) can be rewritten as

$$\check{x}_{j,n} = \sum_{k=-\infty}^{\infty} h_1(k) x_{j-1,2n-k} \tag{107}$$

- This relationship indicates that the coefficients of the detail signal $\check{x}_j(t)$ can be obtained from the coefficients of $x_{j-1}(t)$ by filtering them with $h_1(k)$ and sub-sampling by a factor of two, as illustrated in Figure 2.
- Equations (100) and (107) show how to go from resolution 2^{1-j} to the smaller resolution 2^{-j}.

Wavelet transforms and filter banks

- Assuming that the digital representation of $x(t)$ is given by the coefficients $x_{-1,n}$, we have that the discrete wavelet transform of $x(t)$, the coefficients $\check{x}_{j,n}$, can be computed recursively from equations (100) and (107).
- This is again illustrated in Figure 2, where $\check{x}_{j,n} = c_{j,n}$.

Wavelet transforms and filter banks

- Now we will deal with the problem of going from resolution 2^{-j} to the higher resolution 2^{1-j}, with the help of the detail signal.
- Being able to do so is equivalent to being able to recover the digital representation of the signal from its wavelet coefficients.
- From equation (83), the projection $x_{j-1}(t)$ of $x(t)$ onto $\overline{V}_{j-1}$ can be decomposed as the sum of the projection $x_j(t)$ of $x(t)$ onto $\overline{V}_j$ and the projection $\check{x}_j(t)$ of $x(t)$ onto the detail space $\overline{W}_j$, that is,

$$x_{j-1}(t) = x_j(t) + \check{x}_j(t) \tag{108}$$

- Then, substituting equations (94) and (101) into equation (108), we have

$$x_{j-1}(t) = \sum_{k=-\infty}^{\infty} x_{j,k} 2^{-j/2} \overline{\phi}(2^{-j}t - k) + \sum_{k=-\infty}^{\infty} \check{x}_{j,k} 2^{-j/2} \overline{\psi}(2^{-j}t - k) \tag{109}$$

Wavelet transforms and filter banks

- However, since

$$x_{j-1}(t) = \sum_{l=-\infty}^{\infty} x_{j-1,l} 2^{\frac{1-j}{2}} \overline{\phi}(2^{1-j}t - l) \tag{110}$$

from equation (75) and then from equation (109), we have that

$$\begin{aligned} x_{j-1,l} &= \int_{-\infty}^{\infty} x_{j-1}(t) 2^{\frac{1-j}{2}} \phi^*(2^{1-j}t - l)dt \\ &= \sum_{k=-\infty}^{\infty} x_{j,k} \int_{-\infty}^{\infty} 2^{-j/2}\overline{\phi}(2^{-j}t - k) 2^{\frac{1-j}{2}} \phi^*(2^{1-j}t - l)dt \\ &\quad + \sum_{k=-\infty}^{\infty} \check{x}_{j,k} \int_{-\infty}^{\infty} 2^{-j/2}\overline{\psi}(2^{-j}t - k) 2^{\frac{1-j}{2}} \phi^*(2^{1-j}t - l)dt \end{aligned} \tag{111}$$

Wavelet transforms and filter banks

- From equations (72) and (86),

$$2^{-j/2}\overline{\phi}(2^{-j}t-k) = \sum_{n=-\infty}^{\infty} \overline{c}_n 2^{\frac{1-j}{2}} \overline{\phi}(2^{1-j}t-2k-n) \quad (112)$$

$$2^{-j/2}\overline{\psi}(2^{-j}t-k) = \sum_{n=-\infty}^{\infty} \overline{d}_n 2^{\frac{1-j}{2}} \overline{\phi}(2^{1-j}t-2k-n) \quad (113)$$

- Substituting the above equations into equation (111), we have

$$\begin{aligned} x_{j-1,l} = & \sum_{k=-\infty}^{\infty} x_{j,k} \int_{-\infty}^{\infty} \sum_{n=-\infty}^{\infty} \overline{c}_n 2^{\frac{1-j}{2}} \overline{\phi}(2^{1-j}t-2k-n) 2^{\frac{1-j}{2}} \phi^*(2^{1-j}t-l)dt \\ & + \sum_{k=-\infty}^{\infty} \check{x}_{j,k} \int_{-\infty}^{\infty} \sum_{n=-\infty}^{\infty} \overline{d}_n 2^{\frac{1-j}{2}} \overline{\phi}(2^{1-j}t-2k-n) 2^{\frac{1-j}{2}} \phi^*(2^{1-j}t-l)dt \end{aligned} \quad (114)$$

Wavelet transforms and filter banks

- From equation (89),

$$\left\langle 2^{\frac{1-j}{2}}\phi(2^{1-j}t-n), 2^{\frac{1-j}{2}}\overline{\phi}(2^{1-j}t-m)\right\rangle = \delta(m-n) \tag{115}$$

then, equation (114) becomes

$$\begin{aligned} x_{j-1,l} &= \sum_{k=-\infty}^{\infty} x_{j,k} \sum_{n=-\infty}^{\infty} \overline{c}_n \delta(2k+n-l) + \sum_{k=-\infty}^{\infty} \check{x}_{j,k} \sum_{n=-\infty}^{\infty} \overline{d}_n \delta(2k+n-l) \\ &= \sum_{k=-\infty}^{\infty} x_{j,k}\overline{c}_{l-2k} + \sum_{k=-\infty}^{\infty} \check{x}_{j,k}\overline{d}_{l-2k} \end{aligned} \tag{116}$$

- By defining

$$\overline{c}_n = g_0(n) \tag{117}$$

$$\overline{d}_n = g_1(n) \tag{118}$$

Wavelet transforms and filter banks

equation (116) can be rewritten as

$$x_{j-1,l} = \sum_{k=-\infty}^{\infty} x_{j,k} g_0(l-2k) + \sum_{k=-\infty}^{\infty} \check{x}_{j,k} g_1(l-2k) \qquad (119)$$

- This equation means that the coefficients of the approximation $x_{j-1,l}$ of a signal at resolution 2^{1-j} can be obtained from the coefficients of the approximation of the signal at the smaller resolution 2^{-j} and the coefficients of the corresponding detail signal.

- In order to accomplish this, it suffices to up-sample the coefficients of the approximation $x_{j,k}$ by a factor of two and to filter them with a digital filter having impulse response $g_0(k)$, summing the result to the coefficients of the detail signal, $\check{x}_{j,k}$, up-sampled by a factor of two and filtered by a digital filter with impulse response $g_1(k)$, as represented in Figure 2.

Wavelet transforms and filter banks

- Summarizing equations (99), (100), (106), (107), (118), and (119), we have

$$
\left.
\begin{aligned}
c_n^* &= h_0(-n) \\
d_n^* &= h_1(-n) \\
\overline{c}_n &= g_0(n) \\
\overline{d}_n &= g_1(n) \\
x_{j,n} &= \sum_{k=-\infty}^{\infty} h_0(k) x_{j-1,2n-k} \\
\check{x}_{j,n} &= \sum_{k=-\infty}^{\infty} h_1(k) x_{j-1,2n-k} \\
x_{j-1,n} &= \sum_{k=-\infty}^{\infty} x_{j,k} g_0(n-2k) + \sum_{k=-\infty}^{\infty} \check{x}_{j,k} g_1(n-2k)
\end{aligned}
\right\} \quad (120)
$$

Wavelet transforms and filter banks

- From the above equations, we have that equations (71)–(75) and (85)–(88) become

$$\phi(t) = \sum_{n=-\infty}^{\infty} h_0^*(n)\sqrt{2}\phi(2t+n) \quad (121)$$

$$\overline{\phi}(t) = \sum_{n=-\infty}^{\infty} g_0(n)\sqrt{2}\overline{\phi}(2t-n) \quad (122)$$

$$\psi(t) = \sum_{n=-\infty}^{\infty} h_1^*(n)\sqrt{2}\phi(2t+n) \quad (123)$$

$$\overline{\psi}(t) = \sum_{n=-\infty}^{\infty} g_1(n)\sqrt{2}\overline{\phi}(2t-n) \quad (124)$$

Wavelet transforms and filter banks

- Therefore, the filter coefficients can be obtained from the wavelets and scaling functions by the following expressions:

$$h_0(n) = \int_{-\infty}^{\infty} \phi^*(t)\sqrt{2}\overline{\phi}(2t+n)dt \quad (125)$$

$$g_0(n) = \int_{-\infty}^{\infty} \overline{\phi}(t)\sqrt{2}\phi^*(2t-n)dt \quad (126)$$

$$h_1(n) = \int_{-\infty}^{\infty} \psi^*(t)\sqrt{2}\overline{\phi}(2t+n)dt \quad (127)$$

$$g_1(n) = \int_{-\infty}^{\infty} \overline{\psi}(t)\sqrt{2}\phi^*(2t-n)dt \quad (128)$$

- From the above equations, we can confirm that, in the orthogonal case, when $\phi(t) = \overline{\phi}(t)$ and $\psi(t) = \overline{\psi}(t)$, we have that $h_0(n) = g_0^*(-n)$ and $h_1(n) = g_1^*(-n)$.
- Note that this is similar to the condition for orthogonality of filter banks seen earlier.

Wavelet transforms and filter banks

- The Fourier transforms of the wavelets, scaling functions, and filters can be related by taking the Fourier transforms of equations (121)–(124).
- In the case of equation (121) we have that

$$\begin{aligned}
\Phi(\Omega) &= \sum_{n=-\infty}^{\infty} h_0^*(n) \frac{\sqrt{2}}{2} e^{j\frac{\Omega}{2}n} \Phi\left(\frac{\Omega}{2}\right) \\
&= \frac{1}{\sqrt{2}} \Phi\left(\frac{\Omega}{2}\right) \sum_{n=-\infty}^{\infty} h_0^*(n) e^{j\frac{\Omega}{2}n} \\
&= \frac{1}{\sqrt{2}} \Phi\left(\frac{\Omega}{2}\right) H_0^*(e^{j\frac{\Omega}{2}}) \qquad (129)
\end{aligned}$$

Wavelet transforms and filter banks

- Analogously, taking the Fourier transforms of equations (122)–(124) we have

$$\overline{\Phi}(\Omega) = \frac{1}{\sqrt{2}}\overline{\Phi}\left(\frac{\Omega}{2}\right) G_0(e^{j\frac{\Omega}{2}}) \quad (130)$$

$$\Psi(\Omega) = \frac{1}{\sqrt{2}}\Phi\left(\frac{\Omega}{2}\right) H_1^*(e^{j\frac{\Omega}{2}}) \quad (131)$$

$$\overline{\Psi}(\Omega) = \frac{1}{\sqrt{2}}\overline{\Phi}\left(\frac{\Omega}{2}\right) G_1(e^{j\frac{\Omega}{2}}) \quad (132)$$

Wavelet transforms and filter banks

and then, solving the recursions in equations (129)–(132), we get

$$\Phi(\Omega) = \prod_{n=1}^{\infty} \frac{1}{\sqrt{2}} H_0^*(e^{j\frac{\Omega}{2^n}}) \tag{133}$$

$$\overline{\Phi}(\Omega) = \prod_{n=1}^{\infty} \frac{1}{\sqrt{2}} G_0(e^{j\frac{\Omega}{2^n}}) \tag{134}$$

$$\Psi(\Omega) = \frac{1}{\sqrt{2}} H_1^*(e^{j\frac{\Omega}{2}}) \prod_{n=2}^{\infty} \frac{1}{\sqrt{2}} H_0^*(e^{j\frac{\Omega}{2^n}}) \tag{135}$$

$$\overline{\Psi}(\Omega) = \frac{1}{\sqrt{2}} G_1(e^{j\frac{\Omega}{2}}) \prod_{n=2}^{\infty} \frac{1}{\sqrt{2}} G_0(e^{j\frac{\Omega}{2^n}}) \tag{136}$$

- It is important to notice that, for the wavelet transform to be defined, the corresponding filter bank must provide perfect reconstruction.
- Also, it is interesting to note the similarity of the above equations with equations (1)–(4) for the iterated filters of an octave-band filter bank.

Relations between the filter coefficients

- Substituting equations (121) and (122) in equation (89), we have

$$\left\langle \sum_{k=-\infty}^{\infty} h_0^*(k)\sqrt{2}\phi(2t+k), \sum_{n=-\infty}^{\infty} g_0(n)\sqrt{2}\overline{\phi}(2t-2m-n) \right\rangle = \delta(m) \quad (137)$$

and then

$$\sum_{k=-\infty}^{\infty}\sum_{n=-\infty}^{\infty} h_0(k)g_0(n)\left\langle \sqrt{2}\phi(2t+k), \sqrt{2}\overline{\phi}(2t-2m-n) \right\rangle = \delta(m) \quad (138)$$

leading to

$$\sum_{k=-\infty}^{\infty}\sum_{n=-\infty}^{\infty} h_0(k)g_0(n)\delta(k+2m+n) = \delta(m) \quad (139)$$

Relations between the filter coefficients

- This implies that

$$\sum_{n=-\infty}^{\infty} h_0(-2m-n)g_0(n) = \delta(m) \tag{140}$$

  which is the same as writing

$$(h_0 * g_0)(-2m) = \delta(m) \tag{141}$$

  where $*$ denotes the convolution operation between two discrete-time sequences.

- Equation (141) means that all the even indexed elements of $(h_0 * g_0)$ are equal to zero with the exception of the 0^{th} element, which is equal to 1.

- This is equivalent to stating that the even powers of $H_0(z)G_0(z)$ are equal to zero with the exception of z^0, which is equal to 1.

- This implies that

$$H_0(z)G_0(z) + H_0(-z)G_0(-z) = 2 \tag{142}$$

Relations between the filter coefficients

- Now, substituting equations (123) and (124) in equation (90), we have

$$\left\langle \sum_{k=-\infty}^{\infty} h_1^*(k)\sqrt{2}\phi(2t+k), \sum_{n=-\infty}^{\infty} g_1(n)\sqrt{2}\overline{\phi}(2t-2m-n) \right\rangle = \delta(m) \quad \Rightarrow$$

$$\sum_{k=-\infty}^{\infty}\sum_{n=-\infty}^{\infty} h_1(k)g_1(n)\left\langle \sqrt{2}\phi(2t+k), \sqrt{2}\overline{\phi}(2t-2m-n) \right\rangle = \delta(m) \quad \Rightarrow$$

$$\sum_{k=-\infty}^{\infty}\sum_{n=-\infty}^{\infty} h_1(k)g_1(n)\delta(k+2m+n) = \delta(m) \tag{143}$$

this implies that

$$\sum_{n=-\infty}^{\infty} h_1(-2m-n)g_1(n) = \delta(m) \tag{144}$$

which can be rewritten as

$$(h_1 * g_1)(-2m) = \delta(m) \tag{145}$$

Relations between the filter coefficients

- Equation (145) means that all the even powers of $H_1(z)G_1(z)$ are equal to zero with the exception of z^0, which is equal to 1, that is,

$$H_1(z)G_1(z) + H_1(-z)G_1(-z) = 2 \tag{146}$$

Relations between the filter coefficients

- Substituting equations (121) and (124) in equation (91), we have

$$\left\langle \sum_{k=-\infty}^{\infty} h_0^*(k)\sqrt{2}\phi(2t+k), \sum_{n=-\infty}^{\infty} g_1(n)\sqrt{2}\overline{\phi}(2t-2m-n) \right\rangle = 0 \Rightarrow$$

$$\sum_{k=-\infty}^{\infty}\sum_{n=-\infty}^{\infty} h_0(k)g_1(n)\left\langle \sqrt{2}\phi(2t+k), \sqrt{2}\overline{\phi}(2t-2m-n) \right\rangle = 0 \Rightarrow$$

$$\sum_{k=-\infty}^{\infty}\sum_{n=-\infty}^{\infty} h_0(k)g_1(n)\delta(k+2m+n) = 0 \qquad (147)$$

this implies that,

$$\sum_{n=-\infty}^{\infty} h_0(-2m-n)g_1(n) = 0 \qquad (148)$$

which can be rewritten as

$$(h_0 * g_1)(-2m) = 0 \qquad (149)$$

Relations between the filter coefficients

- This is equivalent to saying that all the even powers of $H_0(z)G_1(z)$ are equal to zero, that is,

$$H_0(z)G_1(z) + H_0(-z)G_1(-z) = 0 \tag{150}$$

Relations between the filter coefficients

- Finally, substituting equations (122) and (123) in equation (92), we have

$$\left\langle \sum_{k=-\infty}^{\infty} h_1^*(k)\sqrt{2}\phi(2t+k), \sum_{n=-\infty}^{\infty} g_0(n)\sqrt{2}\overline{\phi}(2t-2m-n) \right\rangle = 0 \Rightarrow$$

$$\sum_{k=-\infty}^{\infty}\sum_{n=-\infty}^{\infty} h_1(k)g_0(n)\left\langle \sqrt{2}\phi(2t+k), \sqrt{2}\overline{\phi}(2t-2m-n) \right\rangle = 0 \Rightarrow$$

$$\sum_{k=-\infty}^{\infty}\sum_{n=-\infty}^{\infty} h_1(k)g_0(n)\delta(k+2m+n) = 0 \qquad (151)$$

this implies that

$$\sum_{n=-\infty}^{\infty} h_1(-2m-n)g_0(n) = 0 \qquad (152)$$

which can be rewritten as:

$$(h_1 * g_0)(-2m) = 0 \qquad (153)$$

Relations between the filter coefficients

- This is equivalent to saying that all the even powers of $H_1(z)G_0(z)$ are equal to zero, that is,

$$H_1(z)G_0(z) + H_1(-z)G_0(-z) = 0 \tag{154}$$

- Summarizing, equations (142), (146), (150), and (154) form the following system of equations:

$$\begin{aligned} H_0(z)G_0(z) + H_0(-z)G_0(-z) &= 2 && (155)\\ H_1(z)G_0(z) + H_1(-z)G_0(-z) &= 0 && (156)\\ H_0(z)G_1(z) + H_0(-z)G_1(-z) &= 0 && (157)\\ H_1(z)G_1(z) + H_1(-z)G_1(-z) &= 2 && (158) \end{aligned}$$

Relations between the filter coefficients

which can be written in matrix form as

$$\begin{bmatrix} H_0(z) & H_0(-z) \\ H_1(z) & H_1(-z) \end{bmatrix} \begin{bmatrix} G_0(z) \\ G_0(-z) \end{bmatrix} = \begin{bmatrix} 2 \\ 0 \end{bmatrix} \tag{159}$$

$$\begin{bmatrix} H_0(z) & H_0(-z) \\ H_1(z) & H_1(-z) \end{bmatrix} \begin{bmatrix} G_1(z) \\ G_1(-z) \end{bmatrix} = \begin{bmatrix} 0 \\ 2 \end{bmatrix} \tag{160}$$

Then, from equation (159),

$$\begin{bmatrix} G_0(z) \\ G_0(-z) \end{bmatrix} = \frac{1}{H_0(z)H_1(-z) - H_0(-z)H_1(z)} \begin{bmatrix} H_1(-z) & -H_0(-z) \\ -H_1(z) & H_0(z) \end{bmatrix} \begin{bmatrix} 2 \\ 0 \end{bmatrix} \tag{161}$$

Relations between the filter coefficients

and from equation (160),

$$\begin{bmatrix} G_1(z) \\ G_1(-z) \end{bmatrix} = \frac{1}{H_0(z)H_1(-z) - H_0(-z)H_1(z)} \begin{bmatrix} H_1(-z) & -H_0(-z) \\ -H_1(z) & H_0(z) \end{bmatrix} \begin{bmatrix} 0 \\ 2 \end{bmatrix} \tag{162}$$

- If one wants linear-phase filters, we should look for FIR filters, as thoroughly discussed earlier.
- If the solutions for $G_0(z)$ and $G_1(z)$ in equations (161) and (162) have to be FIR, the following condition must be satisfied

$$H_0(z)H_1(-z) - H_0(-z)H_1(z) = cz^{-r} \tag{163}$$

Relations between the filter coefficients

in such a way that, from equation (161), we have

$$G_0(z) = \frac{2}{c} z^r H_1(-z) \quad (164)$$

$$G_0(-z) = \frac{2}{c} z^r \left(-H_1(z)\right) \quad (165)$$

- Comparing equation (164) with equation (165) we conclude that

$$(-1)^r = -1 \Rightarrow r = 2l + 1, \text{ with } l \in \mathbb{Z} \quad (166)$$

equation (164) then becomes

$$G_0(z) = \frac{2}{c} z^{2l+1} H_1(-z) \quad (167)$$

Relations between the filter coefficients

- Now, from equation (162),

$$G_1(z) = \frac{2}{c} z^{2l+1} \left(-H_0(-z)\right) \tag{168}$$

$$G_1(-z) = \frac{2}{c} z^{2l+1} H_0(z) \tag{169}$$

- Therefore, the conditions that must satisfied by the filters $H_0(z)$, $H_1(z)$, $G_0(z)$, and $G_1(z)$, as given by equations (142), (167), and (168) can be summarized as

$$H_0(z)G_0(z) + H_0(-z)G_0(-z) = 2 \tag{170}$$

$$G_0(z) = \frac{2}{c} z^{2l+1} H_1(-z) \tag{171}$$

$$G_1(z) = -\frac{2}{c} z^{2l+1} H_0(-z) \tag{172}$$

- Note that these equations are very similar to the perfect reconstruction equations seen in Chapter 9.

Relations between the filter coefficients

- One important difference is that, in the present derivation, the overall delay has been forced to be zero by the biorthonormality of the wavelet transform.
- In fact, equations (171) and (172) can be obtained by making $\Delta = -\frac{1}{2}$ in the perfect reconstruction equations of Chapter 9, corresponding to an overall delay of $(2\Delta + 1) = 0$.

Relations between the filter coefficients

- These conditions are obviously valid for purely orthogonal systems, a special case of biorthogonal ones. As we have seen earlier, for orthogonal wavelets one has that $\phi(t) = \overline{\phi}(t)$ and $\psi(t) = \overline{\psi}(t)$, and then

$$h_0(n) = g_0^*(-n) \quad (173)$$

$$h_1(n) = g_1^*(-n) \quad (174)$$

- In the z-transform domain, the above conditions correspond to

$$G_0(z) = H_0^*((z^{-1})^*) \quad (175)$$

$$G_1(z) = H_1^*((z^{-1})^*) \quad (176)$$

in such a manner that the conditions given by equations (170) to (172) then become

$$H_0(z)H_0^*((z^{-1})^*) + H_0(-z)H_0^*(-(z^{-1})^*) = 2 \quad (177)$$

$$H_0^*((z^{-1})^*) = z^{2l+1}H_1(-z) \quad (178)$$

Relations between the filter coefficients

- Substituting z by $e^{j\omega}$, equation (177) can be rewritten as

$$\left|H_0(e^{j\omega})\right|^2 + \left|H_0(e^{j(\omega+\pi)})\right|^2 = 2 \tag{179}$$

- This is the power complementary condition that arises in the project of CQF filter banks, as detailed in Chapter 9.
- This is not surprising, since CQF filter banks are orthogonal, and therefore generate orthogonal wavelet transforms.

Regularity

- From equations (133)–(136), one can see that the wavelets and scaling functions are derived from the filter bank coefficients by infinite products.
- Therefore, in order for a wavelet to be defined, these infinite products must converge.
- In other words, a wavelet transform is not necessarily defined for every 2-band perfect reconstruction filter bank.
- In fact, there are cases in which the envelope of the impulse responses of the equivalent filters of equations (1)–(4) is not the same for every S.
- The regularity of a wavelet or scaling function is roughly speaking the number of continuous derivatives that a wavelet has.
- It gives a measure of the extent of convergence of the products in equations (133)–(136).

Regularity

- In order to define regularity more formally, we first define the following concept.

  DEFINITION

  A function $f(t)$ is Lipschitz continuous of order α, with $0 < \alpha \leq 1$, if for all $x, h \in \mathbb{R}$, we have

  $$|f(x+h) - f(x)| \leq ch^{\alpha} \tag{180}$$

  where c is a constant.

- Using this definition, we have the regularity concept.

  DEFINITION

  The Hölder regularity of a scaling function $\phi(t)$, such that $\frac{d^N \phi(t)}{dt^N}$ is Lipschitz continuous of order α, is $r = (N + \alpha)$, where N is integer and $0 < \alpha \leq 1$.

Regularity

- It can be shown that, in order for a scaling function $\phi(t)$ to be regular, $H_0(z)$ must have enough zeros at $z = -1$.
- In addition, supposing that $\phi(t)$ generated by $H_0(z)$, as given in equation (133), has regularity r, if we take

$$H_0'(z) = \left(\frac{1 + z^{-1}}{2}\right) H_0(z) \tag{181}$$

  then $\phi'(t)$ generated by $H_0'(z)$ will have regularity $(r + 1)$.
- The regularity of a wavelet is the same as the regularity of the corresponding scaling function.

Regularity

- If $\phi(t)$ and $\overline{\phi}(t)$ are regular, the products in equations (133) and (134) must converge.
- Using $\Omega = 0$ in equation (129), we have

$$\Phi(0) = \frac{1}{\sqrt{2}} H_0^*(1)\Phi(0) \Rightarrow H_0(1) = \sqrt{2} \tag{182}$$

and then, from equation (133), we get

$$\Phi(0) = 1 \tag{183}$$

- Analogously, using $\Omega = 0$ in equation (130), we have that

$$G_0(1) = \sqrt{2} \tag{184}$$

which, when substituted in equation (134), demands that

$$\overline{\Phi}(0) = 1 \tag{185}$$

Regularity

- Another condition can be imposed by substituting equations (182) and (184) in equation (170) for $z = 1$, leading to

$$H_0(-1)G_0(-1) = 0 \tag{186}$$

  indicating that the product $H_0(z)G_0(z)$ must have a zero at $z = -1$.

- In the orthogonal case, since from equation (175), $G_0(z) = H_0^*((z^{-1})^*)$, it can be concluded that the simple convergence of the product in equation (133) forces the presence of one zero at $z = -1$. On the other hand, in the biorthogonal case, equation (186) imposes a weaker condition, where only one of either $H_0(z)$ or $G_0(z)$ must have a zero at $z = -1$.

Regularity

- Below, however, we see that an additional constraint forces $H_0(z)$ and $G_0(z)$ to present a zero at $z = -1$ even in the biorthogonal case.
- As seen in equation (38), a wavelet $\psi(t)$ must present a bandpass response in such a way that its Fourier transform at $\Omega = 0$ must be zero, that is $\Psi(0) = 0$.
- Thus, substituting $\Omega = 0$ in equations (131) and (132), we have

$$\Psi(0) = \frac{1}{\sqrt{2}} H_1^*(1)\Phi(0) = 0 \quad (187)$$

$$\overline{\Psi}(0) = \frac{1}{\sqrt{2}} G_1(1)\overline{\Phi}(0) = 0 \quad (188)$$

- Since $\Phi(0) = \overline{\Phi}(0) = 1$, then both $H_1(1)$ and $G_1(1)$ must be zero.

Regularity

- Summarizing all results, for a regular wavelet, the filters must satisfy the following extra conditions:

$$H_0(-1) = 0 \tag{189}$$

$$G_0(-1) = 0 \tag{190}$$

$$H_0(1) = \sqrt{2} \tag{191}$$

$$G_0(1) = \sqrt{2} \tag{192}$$

- Equations (189) and (190) imply that the filters $H_0(z)$, $H_1(z)$, $G_0(z)$, and $G_1(z)$ have to be normalized in order to generate a wavelet transform.

- Remember that when deriving the wavelet transform from the octave-band filter bank in Section 6, it was supposed that the lowpass filters had enough zeros at $z = -1$.

- In fact, what was meant there was that the wavelets should be regular.

Regularity

- It is interesting to note that the conditions $H_0(1) = \sqrt{2}$ and $H_0(-1) = 0$ imply that $H_0(z)$ is a lowpass filter to a certain extent, the same being true for $G_0(z)$.
- These, together with equations (171) and (172), imply that $H_1(z)$ and $G_1(z)$ are highpass filters.
- Therefore, by referring once again to Figure 2, a wavelet transform can be viewed as an octave band sub-band analysis/synthesis system, in which the low frequency band is recursively divided in low and high frequency bands.
- This implies that, in the frequency domain, a wavelet transform is equivalent to the frequency decomposition depicted in Figure 8

A practical estimate of regularity

- There are several approaches to estimate the regularity of a scaling function or wavelet.
- Next we describe how to estimate the regularity of the synthesis wavelet and scaling function.
- The regularity of the analysis wavelet and scaling function follows by substituting $G_0(z)$ by $H_0(z)$.
- Supposing that $G_0(z)$ has at least $(N+1)$ zeros at $z=-1$, the auxiliary function $F_N(z)$ is defined such that

$$G_0(z) = G_0(1)\left(\frac{1+z}{2}\right)^N F_N(z) \tag{193}$$

A practical estimate of regularity

- Let $(f_N^j)_n$ be the sequence whose z transform $F_N^j(z)$ is given by the following expression:

$$F_N^j(z) = \prod_{k=1}^{j} F_N(z^{2^{k-1}}) \tag{194}$$

- Define α_N^j such that

$$2^{-j\alpha_N^j} = \max_{0 \le n \le 2^j - 1} \left\{ \sum_{k=-\infty}^{\infty} \left| (f_N^j)_{n+k2^j} \right| \right\} \tag{195}$$

- Then the Hölder regularity of the synthesis wavelet and scaling function is

$$r = N + \alpha_N \tag{196}$$

where $\alpha_N = \lim_{j \to \infty} \alpha_N^j$.

- The main advantage of this estimate is that it can be easily implemented in a digital computer, and it converges reasonably fast.

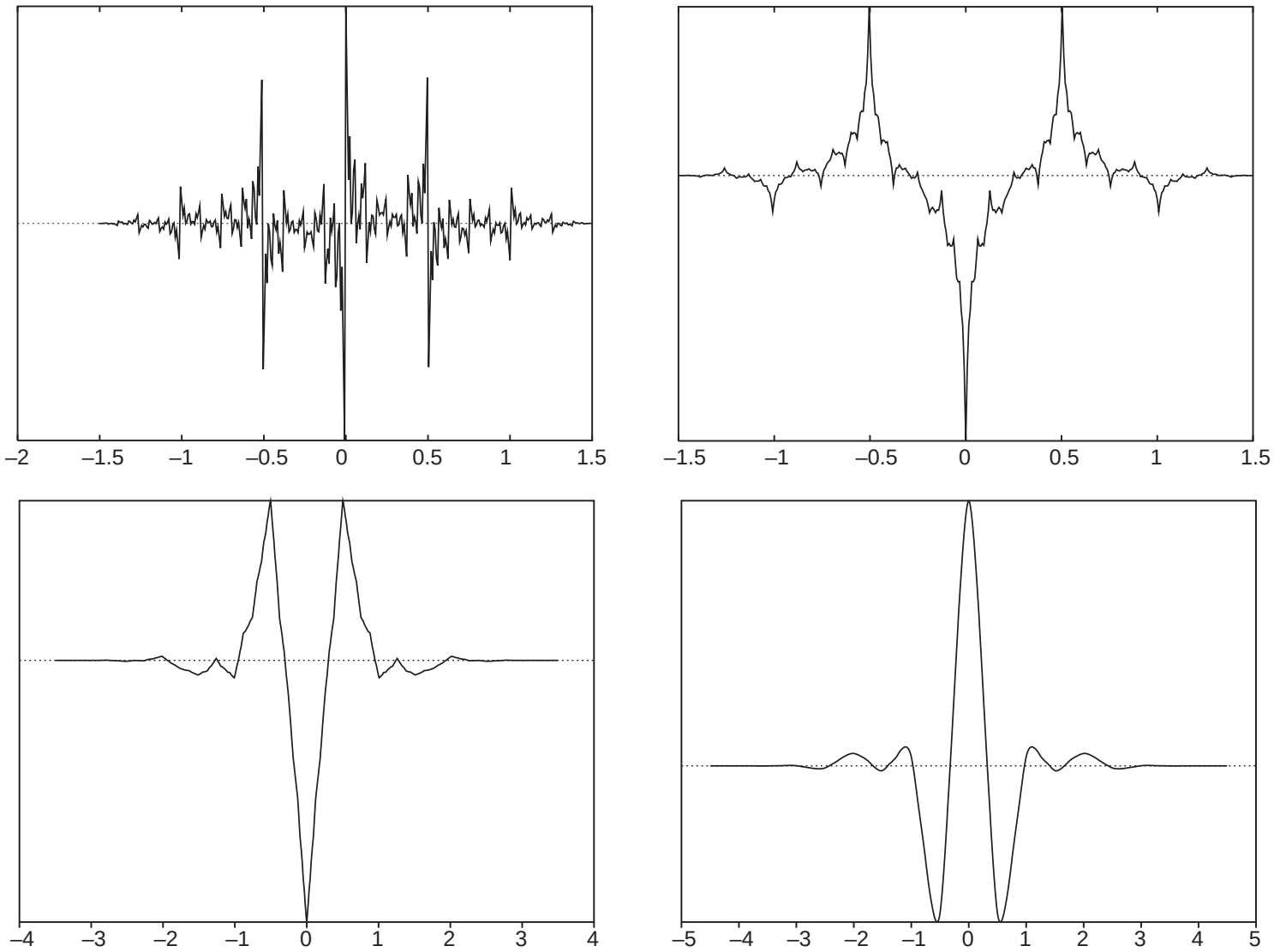

Figure 16: Examples of wavelets with different regularities. (a) regularity = -1; (b) regularity = 0; (c) regularity = 1; (d) regularity = 2.

A practical estimate of regularity

- In Figure 16, we see examples of wavelets with different regularities.
  - For example, Figure 16a corresponds to the analysis wavelet generated by the filter bank described by equations (9.135)–(9.138), and Figure 16b corresponds to the analysis wavelet generated by the filter bank described by equations (9.20)–(9.23).
- From these figures, we notice that higher values of regularity correspond to smoother wavelets, as described above.

Number of vanishing moments

- The presence of zeros at $z = -1$ for $H_0(z)$ and $G_0(z)$ lends an interesting property to the wavelets $\overline{\psi}(t)$ and $\psi(t)$, respectively, regarding their number of vanishing moments.
- Suppose that $H_0(z)$ has N zeros at $z = -1$, or, in an equivalent way, $H_0(e^{j\omega})$ has N zeros at $\omega = \pi$.
- From equation (172), this implies that $G_1(z)$ has N zeros at $z = 1$.
- Hence, $G_1(e^{j\omega})$ has N zeros at $\omega = 0$, and then

$$\left.\frac{d^n G_1(e^{j\omega})}{d\omega^n}\right|_{\omega=0} = 0, \quad \text{for } n = 0, 1, \ldots, (N-1) \tag{197}$$

Number of vanishing moments

- From equation (132), one has

$$\frac{d\overline{\Psi}(\Omega)}{d\Omega} = \frac{1}{2\sqrt{2}}\left[\frac{dG_1(e^{j\frac{\Omega}{2}})}{d\Omega}\overline{\Phi}\left(\frac{\Omega}{2}\right) + G_1(e^{j\frac{\Omega}{2}})\frac{d\overline{\Phi}\left(\frac{\Omega}{2}\right)}{d\Omega}\right] \tag{198}$$

  it then follows that

$$\left.\frac{d^n\overline{\Psi}(\Omega)}{d\Omega^n}\right|_{\Omega=0} = 0, \quad \text{for } n = 0, 1, \ldots, (N-1) \tag{199}$$

- By definition,

$$\overline{\Psi}(\Omega) = \int_{-\infty}^{\infty} \overline{\psi}(t)e^{-j\Omega t}dt \tag{200}$$

  such that

$$\frac{d^n\overline{\Psi}(\Omega)}{d\Omega^n} = \int_{-\infty}^{\infty} \overline{\psi}(t)(-jt)^n e^{-j\Omega t}dt = (-j)^n \int_{-\infty}^{\infty} t^n\overline{\psi}(t)e^{-j\Omega t}dt \tag{201}$$

Number of vanishing moments

- Therefore, conditions (199) correspond to

$$\int_{-\infty}^{\infty} t^n \overline{\psi}(t) dt = 0, \quad \text{for } n = 0, 1, \ldots, (N-1) \tag{202}$$

  which are equivalent to the synthesis wavelet $\overline{\psi}(t)$ having N vanishing moments.

- Applying a similar reasoning, one can conclude that if $G_0(z)$ has N zeros at $z = -1$, the analysis wavelet $\psi(t)$ has N vanishing moments.

- Referring to equation (52), this means that the wavelet coefficients of any polynomial function of degree less than or equal to N are zero.

- Also, by referring to equation (102), this implies that the coefficients $\check{x}_{j,n}$ of such a polynomial are equal to zero, and therefore the polynomial function $x(t)$ is represented only by the lowpass coefficients $x_{j,n}$, as given in equation (95).

Number of vanishing moments

- If a function $x(t)$ is analytic, it can be expanded into a Taylor series, as follows:

$$x(t) = \sum_{k=0}^{\infty} \frac{1}{k!} \left. \frac{d^k x(t)}{dt^k} \right|_{t=t_0} (t - t_0)^k \tag{203}$$

- Therefore, if the analysis wavelet has N vanishing moments, only the terms of the expansion for $k > N$ will generate non-zero wavelet coefficients.
- If these terms are negligible, the wavelet coefficients $\check{x}_{j,n}$ will be very small.
- This property can be useful in signal compression applications, because such functions could be represented by a few significant coefficients $x_{j,n}$ (equation (95)), and negligible $\check{x}_{i,n}$, for $i \leq j$ (equation (102).

Examples of wavelets

- Every 2-band perfect reconstruction filter bank with $H_0(z)$ having enough zeros at $z = -1$, has corresponding analysis and synthesis wavelets and scaling functions.
- For example, the filter bank described by equations (9.11–9.14), normalized such that the CQF design equation,

$$H_1(z) = -z^{-N} H_0(-z^{-1})$$

  is satisfied, generates the so-called Haar wavelet.
- It is the only orthogonal wavelet that has linear phase.
- The corresponding scaling function and wavelets are shown in Figure 17.

Examples of wavelets

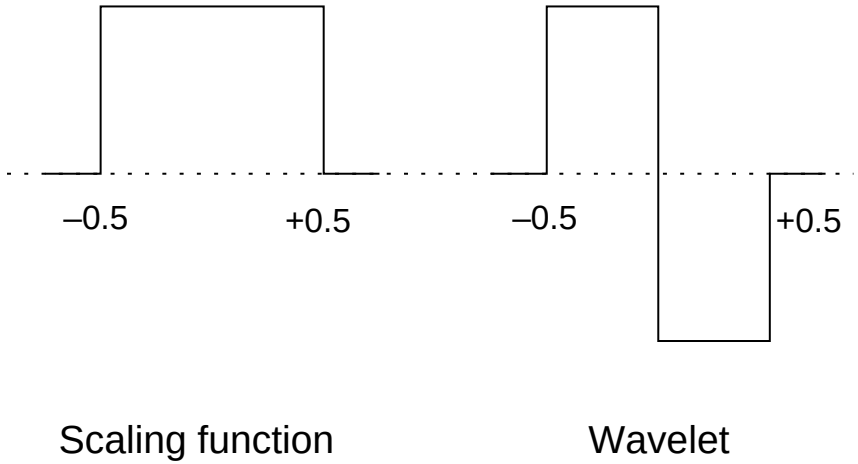

Figure 17: Haar wavelet and scaling function.

- The wavelets and scaling functions corresponding to the symmetric short-kernel filter bank, described by equations (9.20)–(9.23), are depicted in Figure 18.

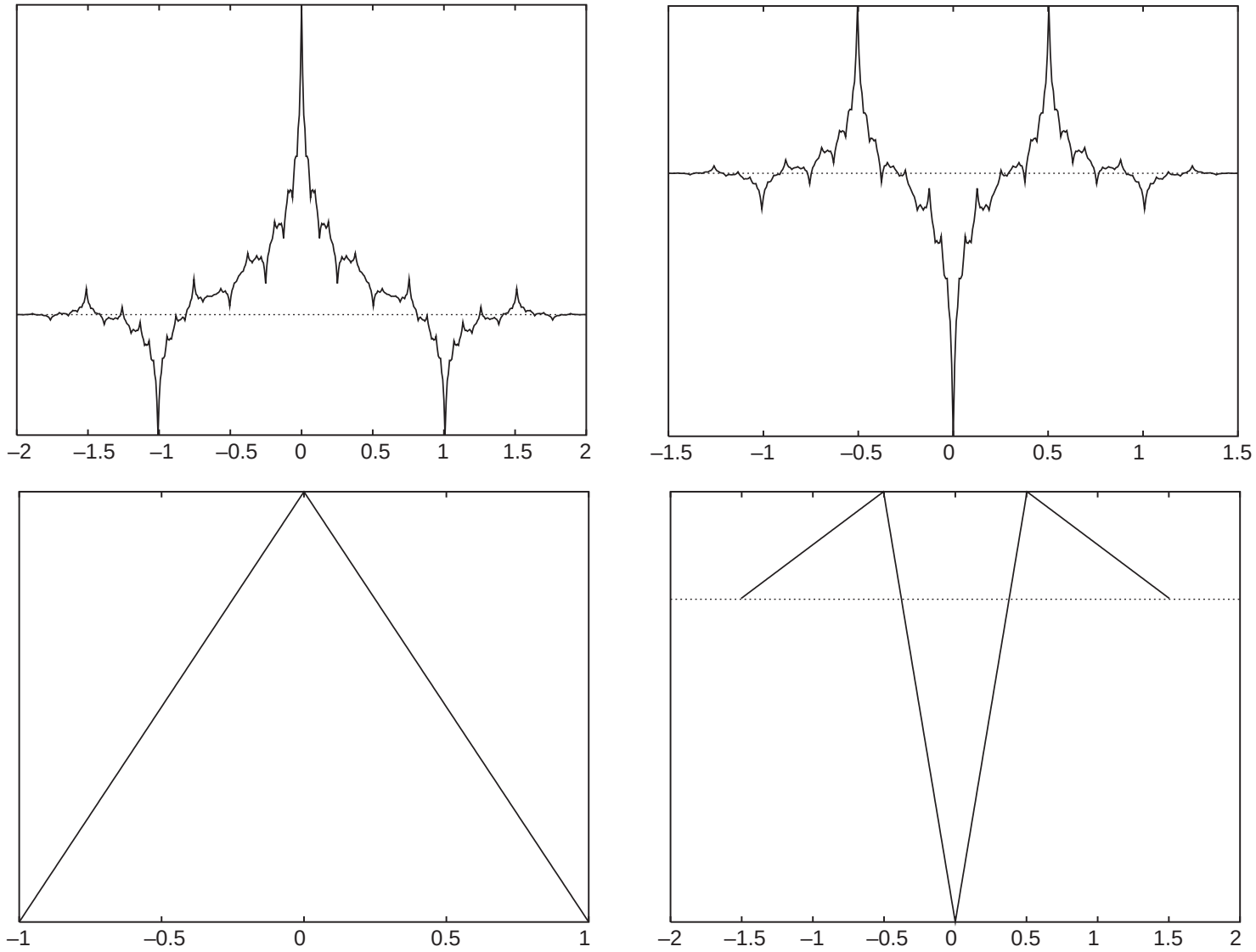

Figure 18: The "symmetric short-kernel" wavelet transform (equations (9.20–9.23)): (a) analysis scaling function; (b) analysis wavelet; (c) synthesis scaling function; (d) synthesis wavelet.

Examples of wavelets

- A good example of an orthogonal wavelet is the Daubechies wavelet whose filters have length 4.
  - They are also an example of CQF banks, seen in Chapter 9. The filters are

$$H_0(z) = +0.482\,9629 + 0.836\,5163z^{-1} + 0.224\,1439z^{-2} - 0.129\,4095z^{-3} \tag{204}$$

$$H_1(z) = -0.129\,4095 - 0.224\,1439z^{-1} + 0.836\,5163z^{-2} - 0.482\,9629z^{-3} \tag{205}$$

$$G_0(z) = -0.129\,4095 + 0.224\,1439z^{-1} + 0.836\,5163z^{-2} + 0.482\,9629z^{-3} \tag{206}$$

$$G_1(z) = -0.482\,9629 + 0.836\,5163z^{-1} - 0.224\,1439z^{-2} - 0.129\,4095z^{-3} \tag{207}$$

- Since the wavelet transform is orthogonal, the analysis and synthesis scaling functions and wavelets are the same.

Examples of wavelets

- These are depicted in Figure 19.
- It is important to notice that, unlike the biorthogonal wavelets in Figure 18, these orthogonal wavelets are nonsymmetric, and, therefore, do not have linear phase.

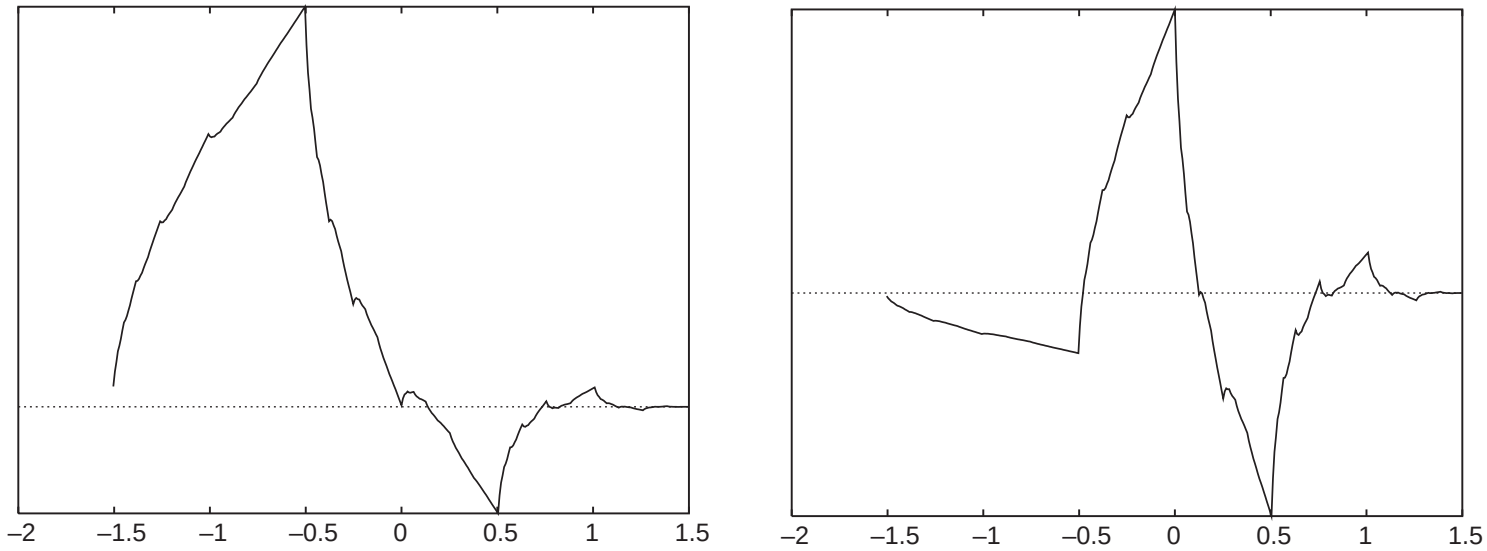

Figure 19: Daubechies wavelet transform of length 4 (equations (204)–(207)): (a) scaling function; (b) wavelet.

- Figure 20 shows the basis functions of a Daubechies wavelet of length 4, with several scales and displacements.

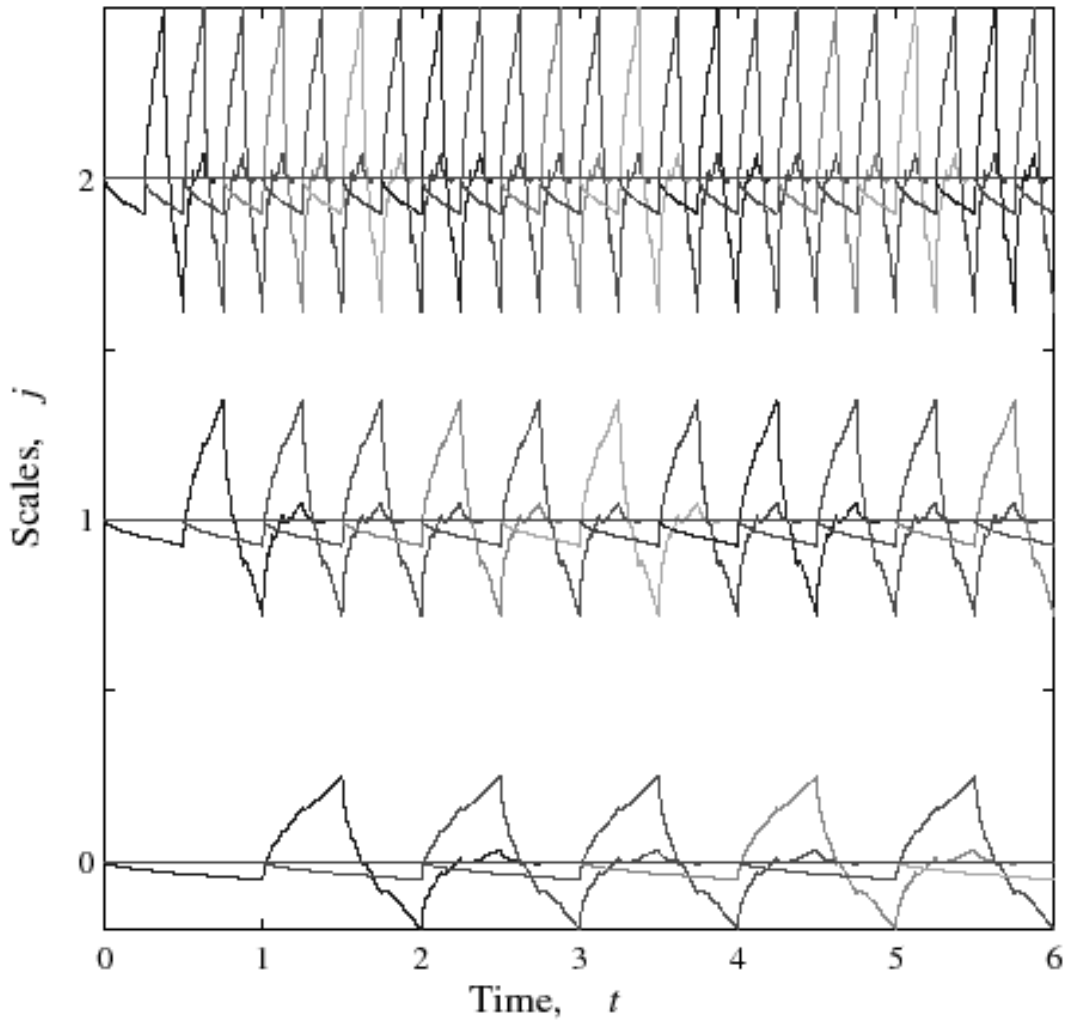

Figure 20: Basis functions of a Daubechies wavelet transform of length 4, showing several scales and displacements.

Examples of wavelets

- When implementing a wavelet transform using the scheme in Figure 2, it is essential that the delay introduced by each analysis/synthesis stage is compensated.
- Failure to do so may result in the loss of the perfect reconstruction property.

Wavelet transforms of images

- One application where wavelet transforms are extremely useful is image processing.
- The varying degrees of time and frequency resolutions provided by their basis functions are well suited to images in general, since images tend to have features of varying sizes.
  - For example, in a picture of a house with a person at the window, the basis function with a large scale will analyze conveniently the house as a whole.
  - The person at the window will be best analyzed at a smaller scale, and the eyes of the person at an even smaller scale.
- This property of images is illustrated in Figure 21.

Figure 21: Image showing features of different sizes.

Wavelet transforms of images

- For applying wavelet transforms to images, a two-dimensional wavelet transform should be defined.
- This can be done in a variety of ways.
- The simplest form is the separable one, where a two-dimensional wavelet transform is computed by applying one dimensional wavelet transforms to every row in the image and then applying one-dimensional wavelet transforms to every column of the result.
- It can therefore be implemented by using the filter banks, as in equations (125)–(128), in the horizontal and vertical directions of an image.

Wavelet transforms of images

- More precisely, the two-dimensional z transforms of the analysis and synthesis filter banks, $H_{ij}(z_1, z_2)$ and $G_{ij}(z_1, z_2)$, respectively, are defined as:

$$H_{00}(z_1, z_2) = H_0(z_1)H_0(z_2) \quad (208)$$

$$H_{01}(z_1, z_2) = H_0(z_1)H_1(z_2) \quad (209)$$

$$H_{10}(z_1, z_2) = H_1(z_1)H_0(z_2) \quad (210)$$

$$H_{11}(z_1, z_2) = H_1(z_1)H_1(z_2) \quad (211)$$

$$G_{00}(z_1, z_2) = G_0(z_1)G_0(z_2) \quad (212)$$

$$G_{01}(z_1, z_2) = G_0(z_1)G_1(z_2) \quad (213)$$

$$G_{10}(z_1, z_2) = G_1(z_1)G_0(z_2) \quad (214)$$

$$G_{11}(z_1, z_2) = G_1(z_1)G_1(z_2) \quad (215)$$

- In this framework, note that the variable z_1 corresponds to filtering the rows of the images, and z_2 to filtering its columns.

Wavelet transforms of images

- If the filter banks above are applied recursively to the sub-band resulting from the lowpass filtering and subsampling in the horizontal and vertical directions, we get an octave-band two-dimensional sub-band decomposition.
- Figure 22 below depicts the process of generating a 3-stage wavelet transform, that is, an octave-band sub-band decomposition.

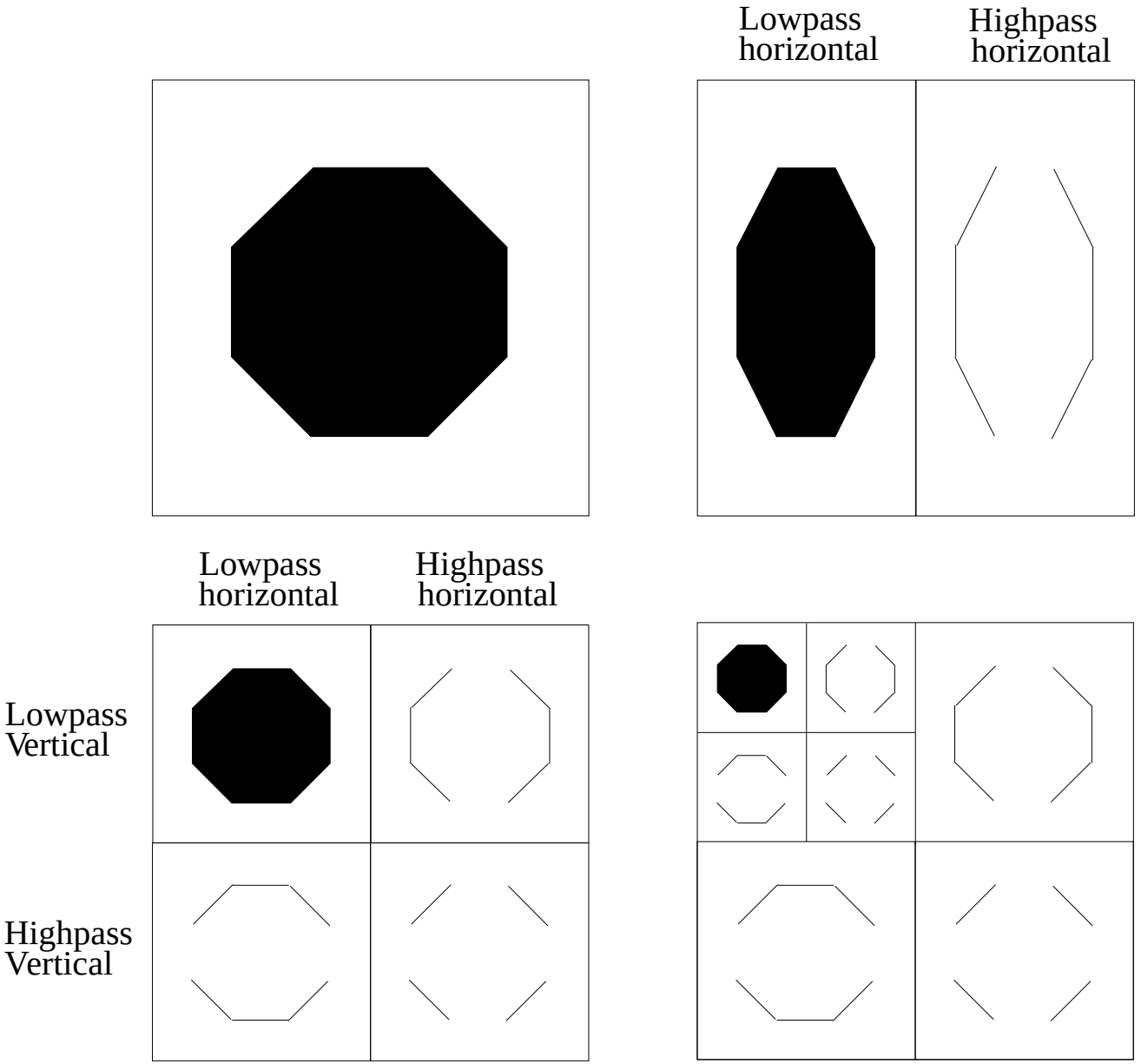

Figure 22: Process of generating a 3-stage wavelet transform of an image.

Wavelet transforms of images

- Therefore, the resulting two-dimensional separable wavelet transform is defined by one scaling function and three wavelets, for the analysis and synthesis cases.
- The analysis wavelets are then as below:

$$\phi_{00}(x_1, x_2) = \phi(x_1)\phi(x_2) \quad (216)$$

$$\psi_{01}(x_1, x_2) = \phi(x_1)\psi(x_2) \quad (217)$$

$$\psi_{10}(x_1, x_2) = \psi(x_1)\phi(x_2) \quad (218)$$

$$\psi_{11}(x_1, x_2) = \psi(x_1)\psi(x_2) \quad (219)$$

where x_1 corresponds to the horizontal direction and x_2 to vertical direction.

Wavelet transforms of images

- Similarly, the synthesis wavelets are:

$$\overline{\phi}_{00}(x_1, x_2) = \overline{\phi}(x_1)\overline{\phi}(x_2) \quad (220)$$

$$\overline{\psi}_{01}(x_1, x_2) = \overline{\phi}(x_1)\overline{\psi}(x_2) \quad (221)$$

$$\overline{\psi}_{10}(x_1, x_2) = \overline{\psi}(x_1)\overline{\phi}(x_2) \quad (222)$$

$$\overline{\psi}_{11}(x_1, x_2) = \overline{\psi}(x_1)\overline{\psi}(x_2) \quad (223)$$

- The scaling functions $\phi_{00}(x_1, x_2)$ and $\overline{\phi}_{00}(x_1, x_2)$ are impulse responses of two-dimensional filters that are lowpass both in the vertical and horizontal directions.
- The wavelets $\psi_{01}(x_1, x_2)$ and $\overline{\psi}_{01}(x_1, x_2)$ are impulse responses of two-dimensional filters that are lowpass in the horizontal direction and highpass in the vertical direction.
- This makes the corresponding wavelet coefficients to be mainly related to image information in the horizontal direction.

Wavelet transforms of images

- Similarly, the coefficients corresponding to the wavelets $\psi_{10}(x_1, x_2)$ and $\overline{\psi}_{10}(x_1, x_2)$ are related to image information in the vertical direction, and the coefficients corresponding to the wavelets $\psi_{11}(x_1, x_2)$ and $\overline{\psi}_{11}(x_1, x_2)$ are related to image information in the diagonal direction.

- The frequency decomposition obtained through such a wavelet transform is schematically represented in Figure 23, where H_i corresponds to coefficients in the vertical direction and resolution i (wavelet $\psi_{01}(\frac{x_1}{2^i}, \frac{x_2}{2^i})$).

- Analogously, V_i (wavelet $\psi_{10}\left(\frac{x_1}{2^i}, \frac{x_2}{2^i}\right)$) and D_i (wavelet $\psi_{11}\left(\frac{x_1}{2^i}, \frac{x_2}{2^i}\right)$) correspond to the horizontal and diagonal directions, respectively.

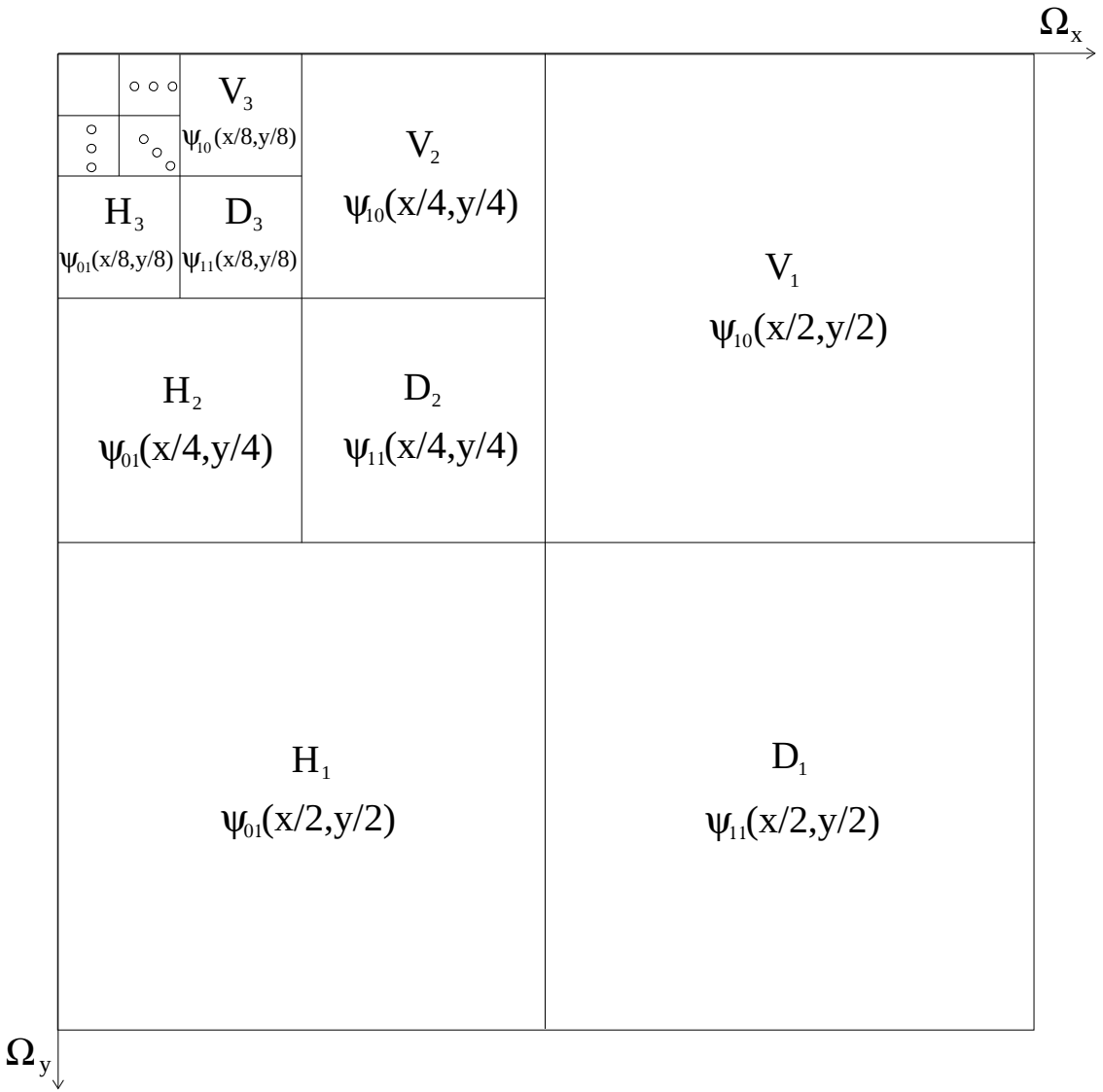

Figure 23: Frequency decomposition obtained with a two-dimensional separable wavelet transform.

Wavelet transforms of images

- The same reasoning can be extended to multiple dimensions, that is, a one-dimensional wavelet transform can be applied in each dimension, generating multidimensional separable wavelet transforms.
- The directionality of the sub-bands of a wavelet transform is represented schematically in Figure 22, where the horizontal, vertical and diagonal bands can be clearly identified.
- The original octagon image and its wavelet transform are shown in Figure 24. Note that, besides the predominantly horizontal, vertical, and diagonal orientations, the sub-bands of similar orientations tend to be similar to each other.

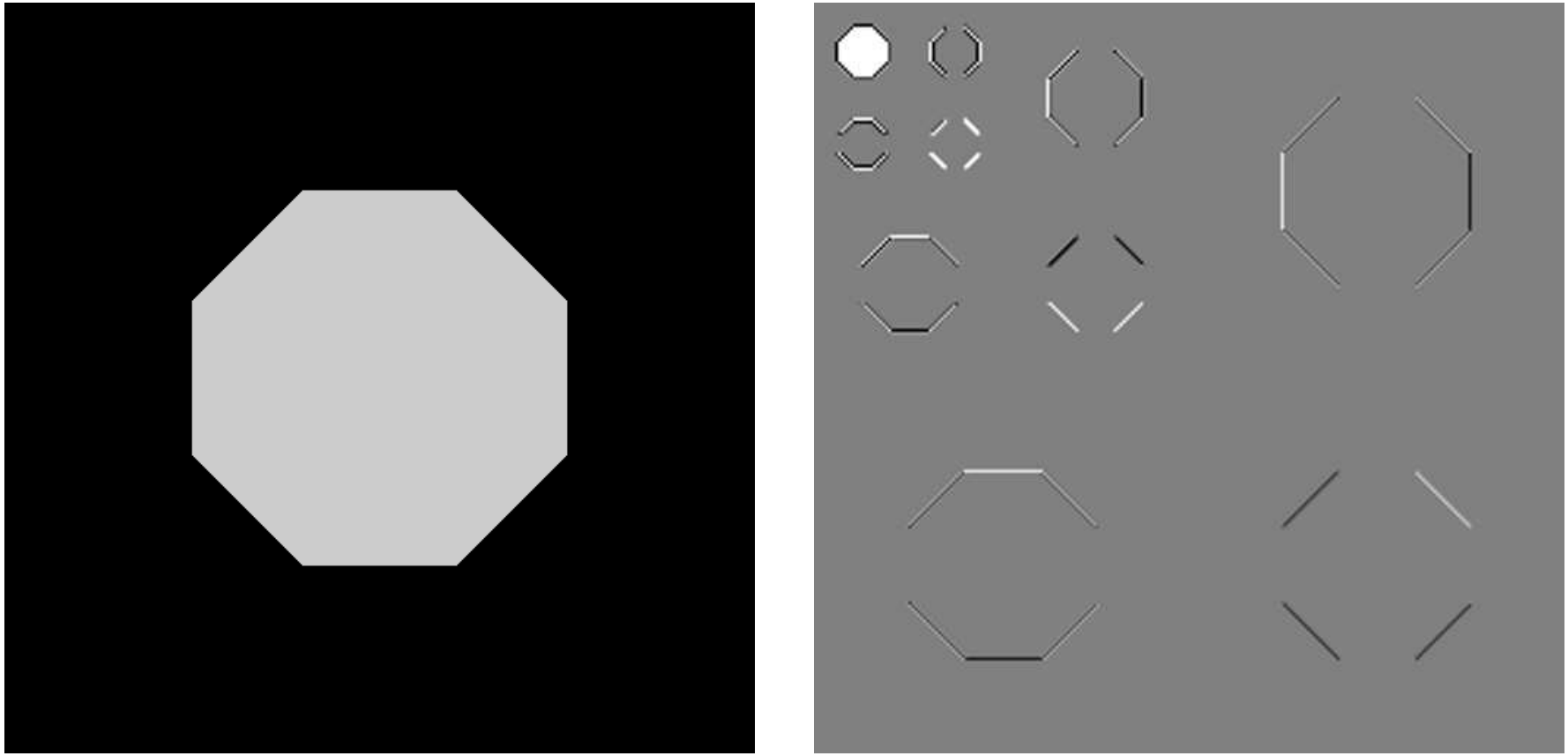

(a) (b)

Figure 24: (a) Original octagon image; (b) corresponding wavelet transform.

Wavelet transforms of images

- Figure 25 shows the wavelet transform of the image shown in Figure 21.
  - On the first plot, each scale has been normalized such that it occupies the full dynamic range.
  - On the second plot, its absolute value is displayed in logarithmic scale.
- We can note that the small scales (high frequency bands) tend to represent details more well localized in space, while the large scales (low frequency bands) tend to represent only larger objects, and therefore with worse localization in space.
- We can also note the directionality of the bands, as well as the similarity among the bands of similar orientations.
- In addition, by looking at the bands in logarithmic scale in Figure 25b, we can see that the wavelet transform is quite effective in concentrating the energy of an image in a small number of coefficients.
- This is one of the main reasons why it has been successfully used in image compression schemes.

Figure 25:

Figure 25

Wavelet transforms of finite-length signals

- Often the signals that one wants to filter have finite length.
- One example has been given on Section 135, where we have computed wavelet transforms of images, that are, by nature, finite-length.
- One problem that arises when one considers finite-length signals is that a length-N signal, when filtered by a length-K impulse response FIR filter, yields an output signal of length $(\mathrm{N}+\mathrm{K}-1)$.
- As seen above, in wavelet transforms, a 2-band filter bank is recursively applied to the lowpass band of the previous stage.
- Therefore, the lengths of the signals increase for each decomposition stage.
- As a consequence, the number of samples of the wavelet transform tends to be larger than the number of samples of the signal.

Wavelet transforms of finite-length signals

- This is particularly inconvenient when one uses wavelet transforms in order to generate compact representations, as is the case, for example, of the JPEG2000 standard for image compression.
- Therefore, a way to overcome this problem of increased number of samples in the wavelet transform is highly desirable.
- Here we analyze signal extensions as a way to compute wavelet transforms that have as much coefficients as signal samples.

Periodic signal extension

- The most straightforward way to avoid the increase in a signal length when it is filtered is to consider that it is periodic.
- This is so because, when one filters a periodic signal of period N, the filtered signal also has period N. Hence, for a periodic signal one needs to know the results for just one period, and, in this way, the effective signal length is not increased after filtering.
- The periodic extension of a length-N signal $x(n)$ is

$$x'(n) = x(n \bmod N) \tag{224}$$

- Such a periodic extension is illustrated at the top of Figure 26.

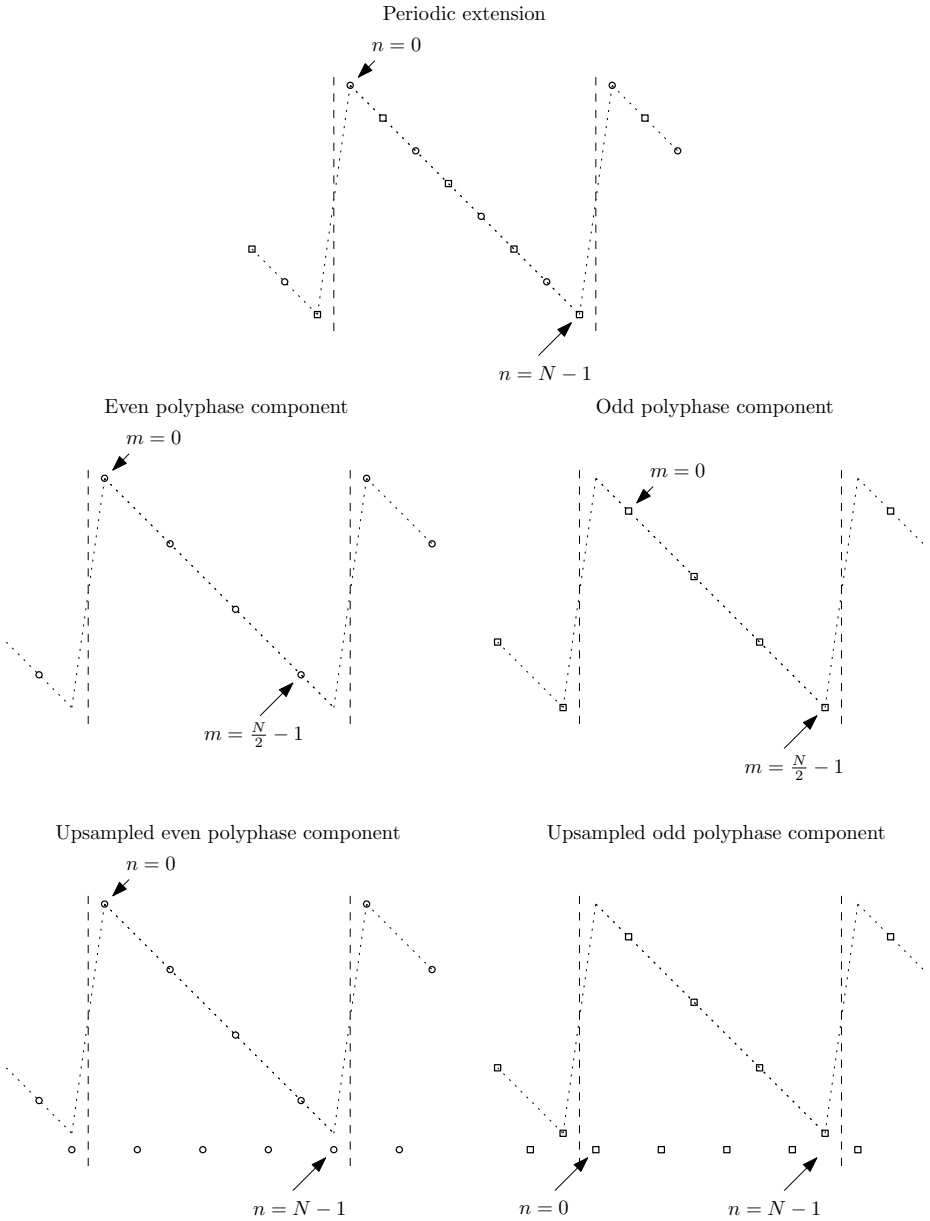
Periodic extension
$n = 0$
$n = N - 1$
Even polyphase component
$m = 0$
$m = \frac{N}{2} - 1$
Odd polyphase component
$m = 0$
$m = \frac{N}{2} - 1$
Upsampled even polyphase component
$n = 0$
$n = N - 1$
Upsampled odd polyphase component
$n = 0$
$n = N - 1$

Figure 26:

Periodic signal extension

- When computing the wavelet transform one performs subsampling of each band by a factor of two.
- Therefore, for such a scheme to work, it is important that, besides the filtered signal being periodic with period N, its subsampled versions should also be periodic.
- In other words, its even and odd polyphase components

$$e'_0(l) = x'(2l) \quad (225)$$

$$e'_1(l) = x'(2l+1) \quad (226)$$

respectively, must be also periodic with period N. From equation (224), if N is even, we have that,

$$e'_0\left(l+\frac{N}{2}\right) = x'(2l+N) = x'(2l) = e'_0(l) \quad (227)$$

$$e'_1\left(l+\frac{N}{2}\right) = x'(2l+N+1) = x'(2l+1) = e'_1(l) \quad (228)$$

and thus we conclude that the polyphase components are periodic with period $\frac{N}{2}$.

Periodic signal extension

- Since a sub-band is a filtered polyphase component, then the sub-bands are also periodic with period $\frac{N}{2}$, and thus the total number of samples in the two sub-bands is also equal to N.
- This is illustrated in the second row of Figure 26.
- Note that, if the number of samples N is odd, then the polyphase components are only periodic with period N, and thus the total number of samples in the sub-bands is $2N$.
- This is inefficient, and is one of the main reasons why periodic extensions of odd-length signals are seldom used.
- Because of this, we restrict ourselves to extensions of even-length signals.
- In the synthesis part of the process, the sub-bands are upsampled and filtered.
- As can be seen in at the bottom of Figure 26, the upsampled polyphase components are also periodic.

Periodic signal extension

- Therefore, no matter which component is chosen during subsampling, the signal resulting from synthesis is also periodic with period N, having only N independent samples.
- One drawback of the periodic extension can be understood by looking again at the top of Figure 26, that shows the original signal extended periodically. We see that the periodic extension will in general have discontinuities around $n = 0$ and $n = N - 1$ that are not part of the original signal.
- These discontinuities tend to appear with large energy in the detail bands of its wavelet transform (see Experiment 10.1), which is quite undesirable in many applications.

Periodic signal extension

- For example, as can be seen in Figure 25, the wavelet transform has the energy concentrated in a relatively small number of coefficients, yielding compact representations.
- However, if one uses periodic extensions, the discontinuities introduced will appear as high energy coefficients in the details bands, thus diminishing the energy compaction properties of the wavelet transform.
- Therefore, whenever possible, it is preferable to use symmetric extensions.
- Such extensions will be dealt with next.

Symmetric signal extensions

- A commonly used form of signal extension is the symmetric extension.
- It avoids the discontinuities that arise when performing a periodic extension.
- Discrete-time signals have two types of symmetry: whole-sample symmetry and half-sample symmetry.
  - In whole-sample symmetry, the axis of symmetry intersects a sample, while in half-sample symmetry it falls between samples.

Symmetric signal extensions

- Mathematically, a signal $x(n)$ is whole-sample symmetric around $n = K$ if

$$x(K - n) = x(K + n), \quad \text{for all } n \in \mathbb{Z} \tag{229}$$

- On the other hand, a signal is half-sample symmetric around "sample" $K - \frac{1}{2}$, with $K \in \mathbb{Z}$, if

$$x(K - 1 - n) = x(K + n), \quad \text{for all } n \in \mathbb{Z} \tag{230}$$

- Examples of the whole- and half-sample symmetries are depicted in Figures 27a and 27b, respectively.

Symmetric signal extensions

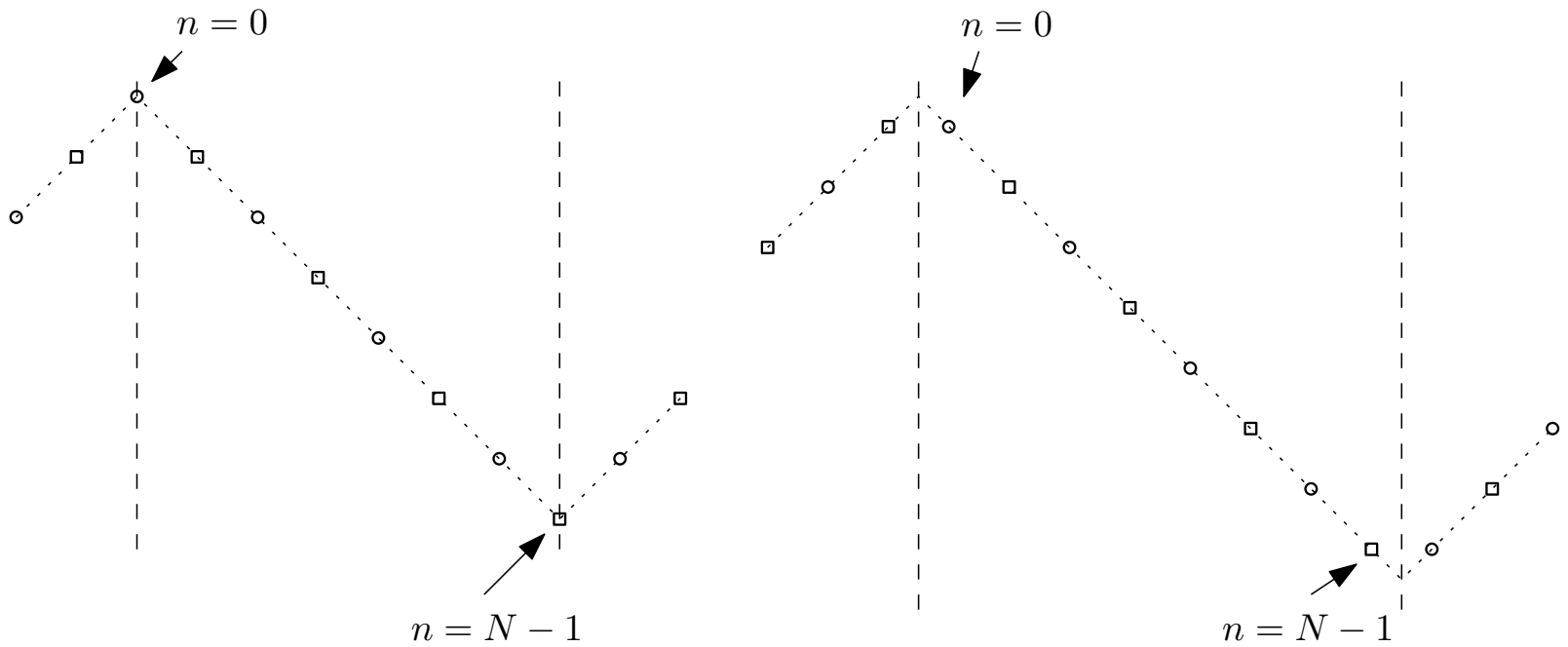

Figure 27: (a) Whole-sample symmetry; (b) half-sample symmetry.

Symmetric signal extensions

- From equation (229), if a signal $x(n)$ of length N is extended symmetrically with whole-sample symmetry around both $n = 0$ and $n = N - 1$, the resulting signal $x'(n)$ is a periodic signal with period $2N - 2$ that is given by

$$x'(n) = \begin{cases} x(n), & 0 \leq n \leq N-1 \\ x(-n), & -N+1 \leq n \leq 0 \\ x(2N-2-n), & N-1 \leq n \leq 2N-2 \end{cases} \tag{231}$$

- Likewise, from equation (230), if a signal $x(n)$ of length N is extended symmetrically with half-sample symmetry around both $n = 0$ and $n = N - 1$, the resulting signal $x'(n)$ is a periodic signal with period $2N$ such that

$$x'(n) = \begin{cases} x(n), & 0 \leq n \leq N-1 \\ x(-n-1), & -N \leq n \leq -1 \\ x(2N-1-n), & N \leq n \leq 2N-1 \end{cases} \tag{232}$$

Symmetric signal extensions

- If the jth polyphase components of $x(n)$ and $x'(n)$ are $e_j(l)$ and $e'_j(l)$, respectively, we have, from equation (231), that for whole-sample symmetry (as in the periodic case, we restrict ourselves to the case that N is even)

$$e'_0(l) = \begin{cases} x(2l) = e_0(l), & 0 \le l \le \frac{N}{2} - 1 \\ x(-2l) = e_0(-l), & -\frac{N}{2} + 1 \le l \le 0 \\ x(2N-2-n) = e_0(N-1-l), & \frac{N}{2} - 1 \le l \le N-1 \end{cases} \tag{233}$$

$$e'_1(l) = \begin{cases} x(2l+1) = e_1(l), & 0 \le l \le \frac{N}{2} - 1 \\ x(-2l-1) = e_1(-l), & -\frac{N}{2} \le l \le -1 \\ x(2N-2l-3) = e_1(N-2-l), & \frac{N}{2} - 1 \le l \le N-2 \end{cases} \tag{234}$$

Symmetric signal extensions

- Therefore, the above equations, with the help of equations (229)–(232), imply that for signals what are extended with whole-sample symmetry, the even polyphase component, $e'_0(l)$, is whole-sample symmetric around zero and half-sample symmetric around $\frac{N}{2} - 1$.
- Likewise, the odd polyphase component, $e'_1(l)$, is half-sample symmetric around zero and whole-sample symmetric around $\frac{N}{2} - 1$.
- This situation is illustrated in Figure 28.

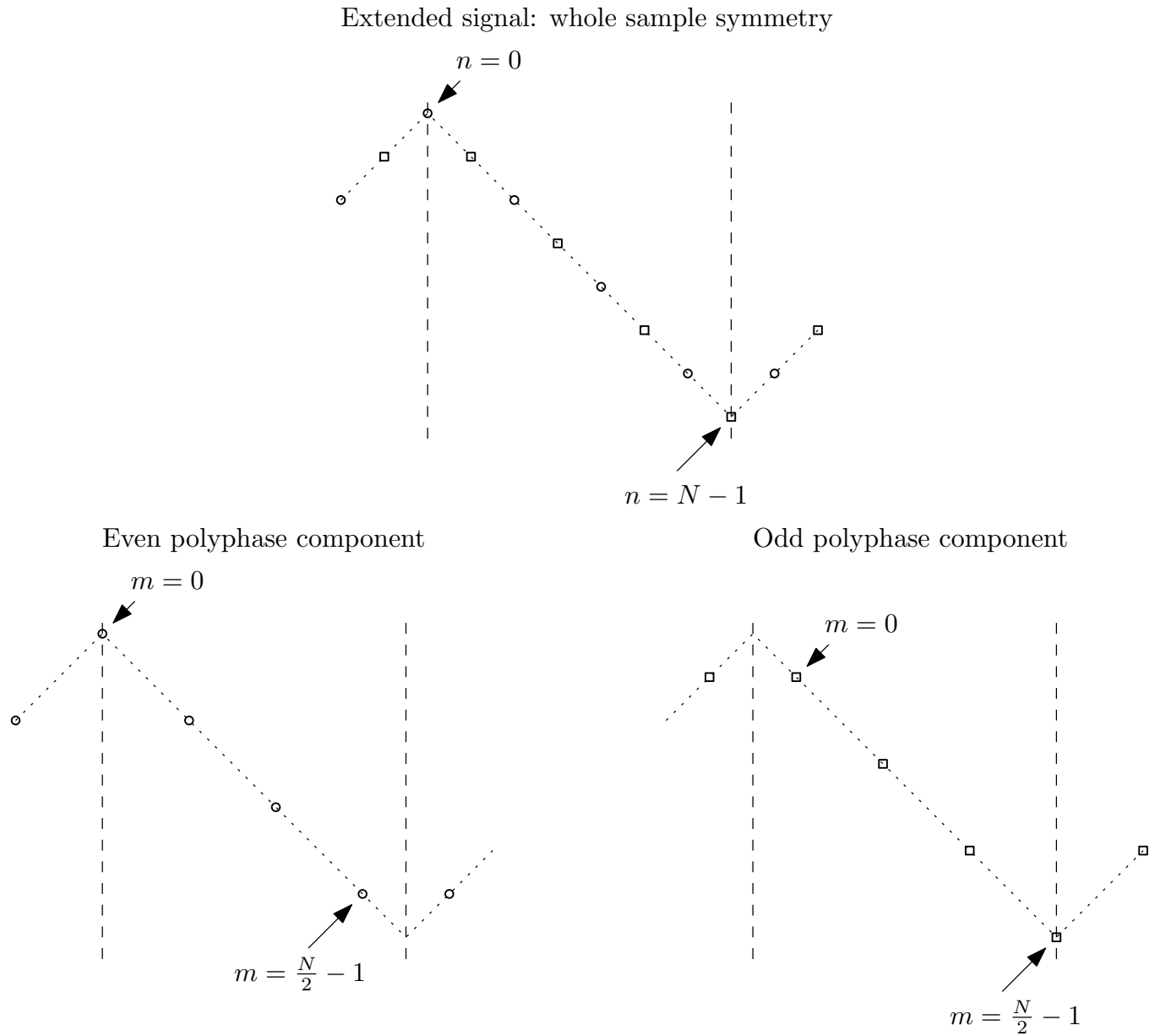
Extended signal: whole sample symmetry
$n = 0$
$n = N - 1$
Even polyphase component
$m = 0$
$m = \frac{N}{2} - 1$
Odd polyphase component
$m = 0$
$m = \frac{N}{2} - 1$

Figure 28:

Symmetric signal extensions

- On the other hand, we have, from equation (232), that for half-sample symmetry (again, N is restricted to be even),

$$e'_0(l) = \begin{cases} x(2l) = e_0(l), & 0 \leq l \leq \frac{N}{2} - 1 \\ x(-2l-1) = e_1(-l-1), & -\frac{N}{2} \leq l \leq -1 \\ x(2N-1-n) = e_1(N-1-l), & \frac{N}{2} \leq l \leq N-1 \end{cases} \tag{235}$$

$$e'_1(l) = \begin{cases} x(2l+1) = e_1(l), & 0 \leq l \leq \frac{N}{2} - 1 \\ x(-2l-2) = e_0(-l-1), & -\frac{N}{2} \leq l \leq -1 \\ x(2N-2l-2) = e_0(N-1-l), & \frac{N}{2} \leq l \leq N-1 \end{cases} \tag{236}$$

- Therefore, the above equations imply that, for signals what are extended with half-sample symmetry, neither of its polyphase components is symmetric, as illustrated in Figure 29.

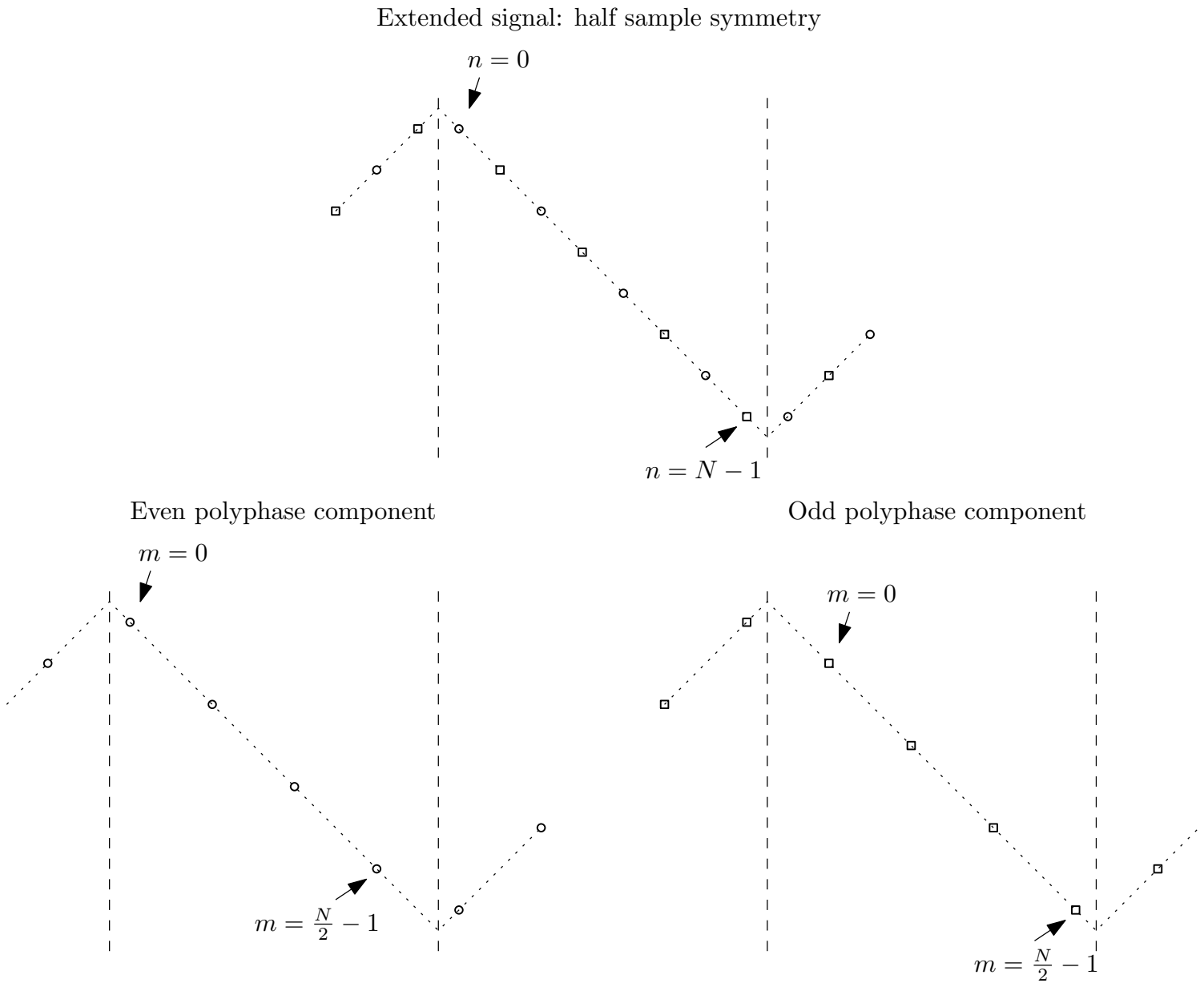
Extended signal: half sample symmetry
$n = 0$
$n = N - 1$
Even polyphase component
$m = 0$
$m = \frac{N}{2} - 1$
Odd polyphase component
$m = 0$
$m = \frac{N}{2} - 1$

Figure 29:

Symmetric signal extensions

- In order for a symmetric extension to be usable for the computation of a wavelet transform, three conditions must be satisfied:

  (a) The signal must remain symmetric after the application of the analysis filter.

  (b) The signal filtered by the analysis filters must remain symmetric after subsampling by a factor of two.

  (c) The upsampled signal must be symmetric before application of the synthesis filters.

- Condition a above demands that the analysis filters have linear phase, since they are the only ones that do not destroy the symmetry of signals input to it.

- As seen earlier, linear-phase filters can have either integer delays (even order) or an integer plus $\frac{1}{2}$ delay (odd order).

- It is important to notice that a signal with whole-sample symmetry, when delayed by an integer number of samples, remains whole-sample symmetric.

Symmetric signal extensions

- On the other hand, a signal with whole-sample symmetry becomes half-sample symmetric when delayed by half sample.
- Likewise, a signal with half-sample symmetry becomes whole-sample symmetric when delayed by half sample.
- Condition b demands that the output signals for the analysis filters have to be whole-sample symmetric around both zero and $N - 1$.
- This is so because, as seen above and illustrated in Figures 28 and 29, the polyphase components of half-sample symmetric signals are not symmetric.

Symmetric signal extensions

- Therefore, since the output of an analysis filter must be whole-sample symmetric, we have two cases, depending on the order of the analysis filters:
  - If its delay is integer (even order), then the signal must be extended with whole-sample symmetry;
  - If its delay is an integer plus $\frac{1}{2}$ (odd order), then the signal must be extended with half-sample symmetry.
- Condition c is automatically satisfied provided that the subsampled signals input to the interpolators are symmetric.
- This is illustrated in Figure 30.

Symmetric signal extensions

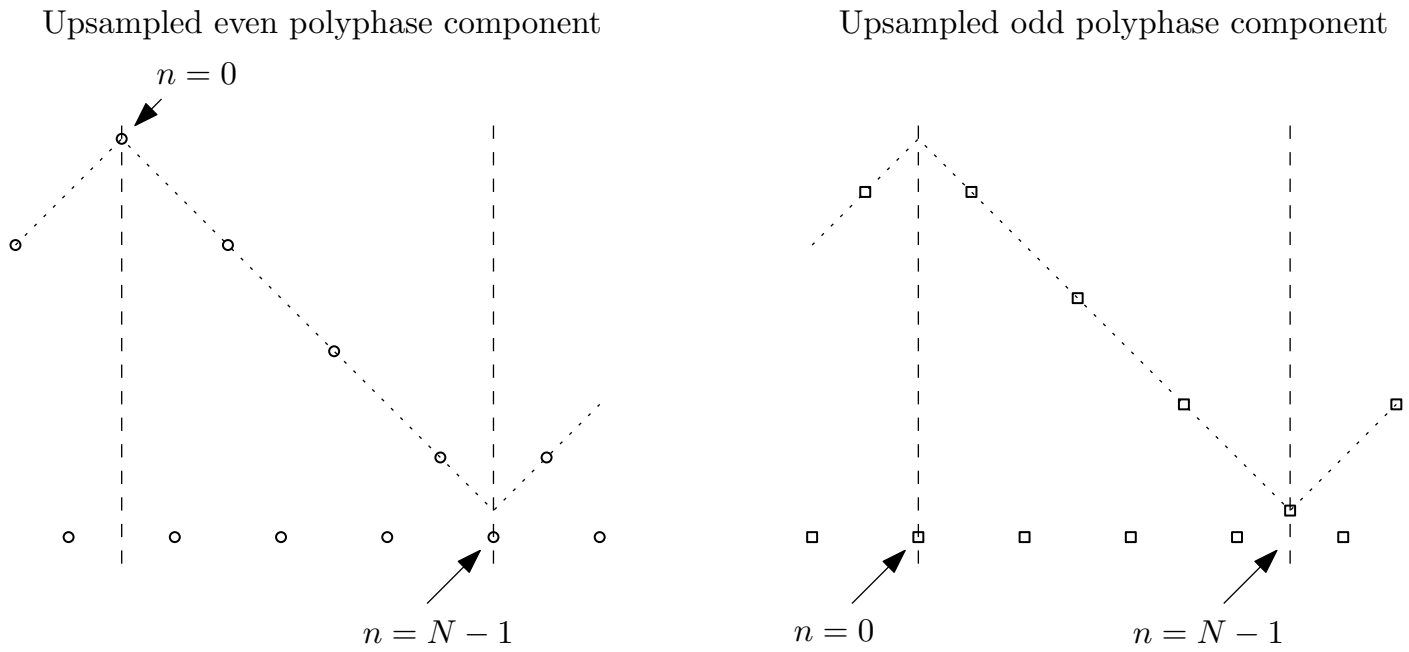

Figure 30:

- Note that for both polyphase components the symmetry of their interpolated versions is whole-sample.

Symmetric signal extensions

- From the design restrictions for the 2-band linear-phase filter banks, as presented earlier, we have that useful 2-band linear-phase filter banks should have either all filters with even orders or all filters with odd orders.
- Table 1 summarizes how the symmetric extensions in each stage of the 2-band filter bank process should be in the two cases. Note that once again we restrict ourselves to the case when the signal length N is even.

Symmetric signal extensions

Table 1: Types of symmetric extension in the two-band analysis and synthesis process for both even order and odd order filter banks.

Stage of the filtering process	Symmetry	
	Even order	Odd order
Before analysis filter	whole (0) / whole ($N-1$)	half (0) / half ($N-1$)
After analysis filter	whole (0) / whole ($N-1$)	whole (0) / whole ($N-1$)
Even polyphase component	whole (0) / half ($\frac{N}{2}-1$)	whole (0) / half ($\frac{N}{2}-1$)
Odd polyphase component	half (0) / whole ($\frac{N}{2}-1$)	half (0) / whole ($\frac{N}{2}-1$)
After upsampling	whole (0) / whole ($N-1$)	whole (0) / whole ($N-1$)
After synthesis	whole (0) / whole ($N-1$)	half (0) / half ($N-1$)

Symmetric signal extensions

- It is important to note that in wavelet transforms we have to apply a 2-band filter bank recursively to the lowpass bands.
- In the even-order case, for instance, if we take the even polyphase component as the signal after subsampling, it is whole-sample symmetric around zero and half-sample symmetric around $\frac{N}{2} - 1$.
- Although this is the signal that we must upsample to perform the synthesis stage, in order for us to further decompose it we have to generate a slightly different signal.
- For example, if we are going to use an even-order filter bank for the next stage, we must first generate from it a signal that is whole-sample symmetric at both ends.
- We do so by first taking its samples from $m = 0$ to $m = \frac{N}{2} - 1$ and extending them using whole-sample symmetry at both ends.

Do-it-yourself: Wavelet transforms

Experiment 10.1:

- Here we see how wavelets can be used to analyze nonstationary signals.
- We start by generating a signal composed of a sequence of five sinusoids of different frequencies, corrupted by spikes.
  - The beginning of each sinusoid is specified in `pos_sin` variable and the corresponding period is defined in `T_sin`.
  - For the spikes, their amplitude and time positions are as given by the `amp_imp` and `pos_imp` variables, respectively.

Do-it-yourself: Wavelet transforms

- The MATLAB code to generate it is as follows:

```
N = 2000; t = [0:N];
x = zeros(size(t));
pos_sin = [0 600 1080 1380 1680 2000];
T_sin = [100 40 20 10 5];
for i = 1:5,
   m = 1 + pos_sin(i); n = pos_sin(i+1);
   x(m:n) = sin(2*pi*t(1:n-m+1)/T_sin(i));
end;
amp_imp = [3 -2 2 2.5 -2.5];
pos_imp = [200 372 1324 1343 1802];
T_imp = [5 25 5 5 5 ];
for i = 1:5,
   m = 1 + pos_imp(i); n = 1 + pos_imp(i)+fix(T_imp(i)/2);
   x(m:n) = x(m:n) +
amp_imp(i)*sin(2*pi*t(1:n-m+1)/T_imp(i)).^2;
end;
```

Do-it-yourself: Wavelet transforms

- The resulting signal `x` has `(N+1)`=2001 samples, and the sinusoids have, in sequence, periods of 100, 40, 20, 10 and 5 samples.
- The spikes consist of one period of a sine-squared waveform.
- Four of them have duration of 3 samples, and another one (the second from left to right) has a period of 23 samples.
- The third and fourth spikes are very close, only 19 samples apart. The signal is depicted in Figure 31.

Do-it-yourself: Wavelet transforms

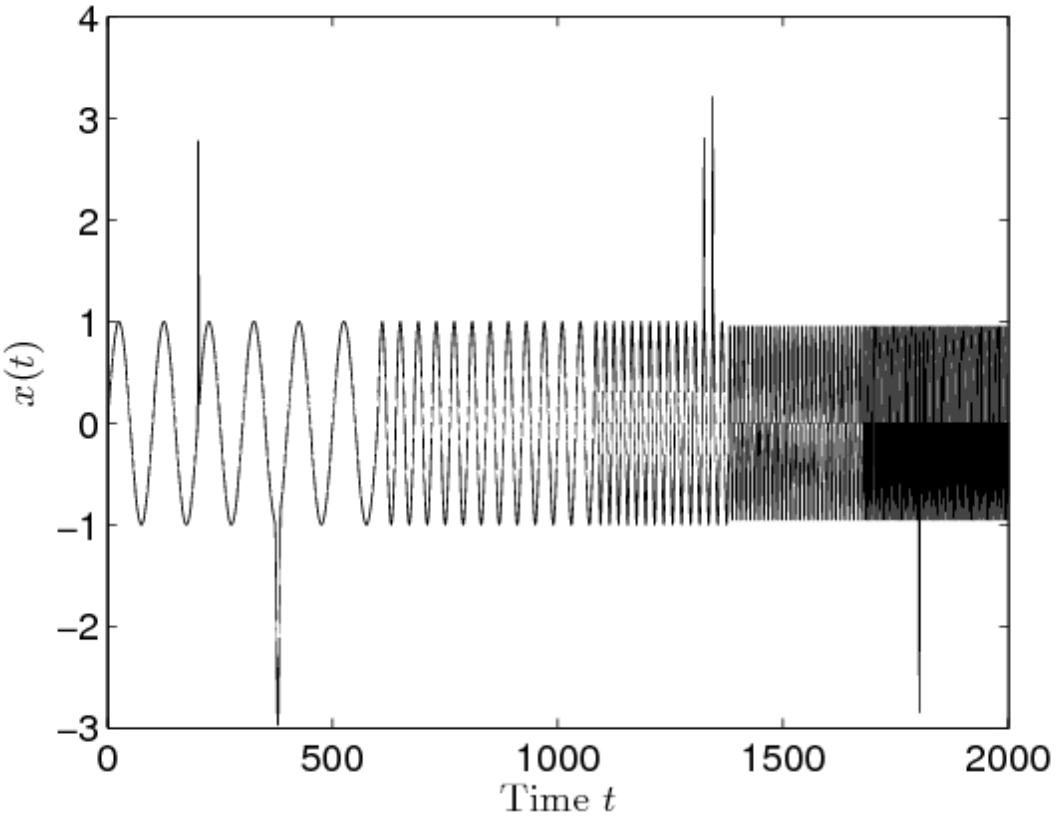

Figure 31: Signal for Experiment 10.1.

Do-it-yourself: Wavelet transforms

- In this experiment, we decompose the signals with the wavelet `bior4.4`, which is the biorthogonal linear-phase wavelet used in the JPEG2000 standard for image compression, also referred to as the 9-7 wavelet.
- The coefficients of the analysis and synthesis filters are shown in Table 2.

Do-it-yourself: Wavelet transforms

Table 2: Coefficients of the analysis and synthesis 9-7 (`bior4.4`) wavelet.

$h_0(0) = 0.0378$	$h_1(0) = -0.0645$	$g_0(0) = -0.0645$	$g_1(0) = -0.0378$
$h_0(1) = -0.0238$	$h_1(1) = 0.0407$	$g_0(1) = -0.0407$	$g_1(1) = -0.0238$
$h_0(2) = -0.1106$	$h_1(2) = 0.4181$	$g_0(2) = 0.4181$	$g_1(2) = 0.1106$
$h_0(3) = 0.3774$	$h_1(3) = -0.7885$	$g_0(3) = 0.7885$	$g_1(3) = 0.3774$
$h_0(4) = 0.8527$	$h_1(4) = 0.4181$	$g_0(4) = 0.4181$	$g_1(4) = -0.8527$
$h_0(5) = 0.3774$	$h_1(5) = 0.0407$	$g_0(5) = -0.0407$	$g_1(5) = 0.3774$
$h_0(6) = -0.1106$	$h_1(6) = -0.0645$	$g_0(6) = -0.0645$	$g_1(6) = 0.1106$
$h_0(7) = -0.0238$			$g_1(7) = -0.0238$
$h_0(8) = 0.0378$			$g_1(8) = -0.0378$

Do-it-yourself: Wavelet transforms

- In order to load the analysis and synthesis filters we use the MATLAB command

  ```
  [Lo_D,Hi_D,Lo_R,Hi_R] = wfilters('bior4.4');
  ```

  and compute the 5-stage wavelet transform using

  ```
  [C,S] = wavedec(x,5,Lo_D,Hi_D);
  ```

- Following this approach, vector `C` stores the wavelet coefficients and vector `S` stores the lengths of the sub-bands. We compute the detail sub-bands using the command `detcoef`, and the approximation coefficients (lowpass bands for each scale) using the command `appcoef`, as follows:

Do-it-yourself: Wavelet transforms

```
D1 = detcoef(C,S,1);
D2 = detcoef(C,S,2);
D3 = detcoef(C,S,3);
D4 = detcoef(C,S,4);
D5 = detcoef(C,S,5);
A1 = appcoef(C,S,Lo_R,Hi_R,1);
A2 = appcoef(C,S,Lo_R,Hi_R,2);
A3 = appcoef(C,S,Lo_R,Hi_R,3);
A4 = appcoef(C,S,Lo_R,Hi_R,4);
A5 = appcoef(C,S,Lo_R,Hi_R,5);
```

- The plots of the detail bands are shown in Figure 32, and the plots of the approximation bands are shown in Figure 33.
- Note that the sample scale has been normalized in order to make the comparison easier along the time axis.

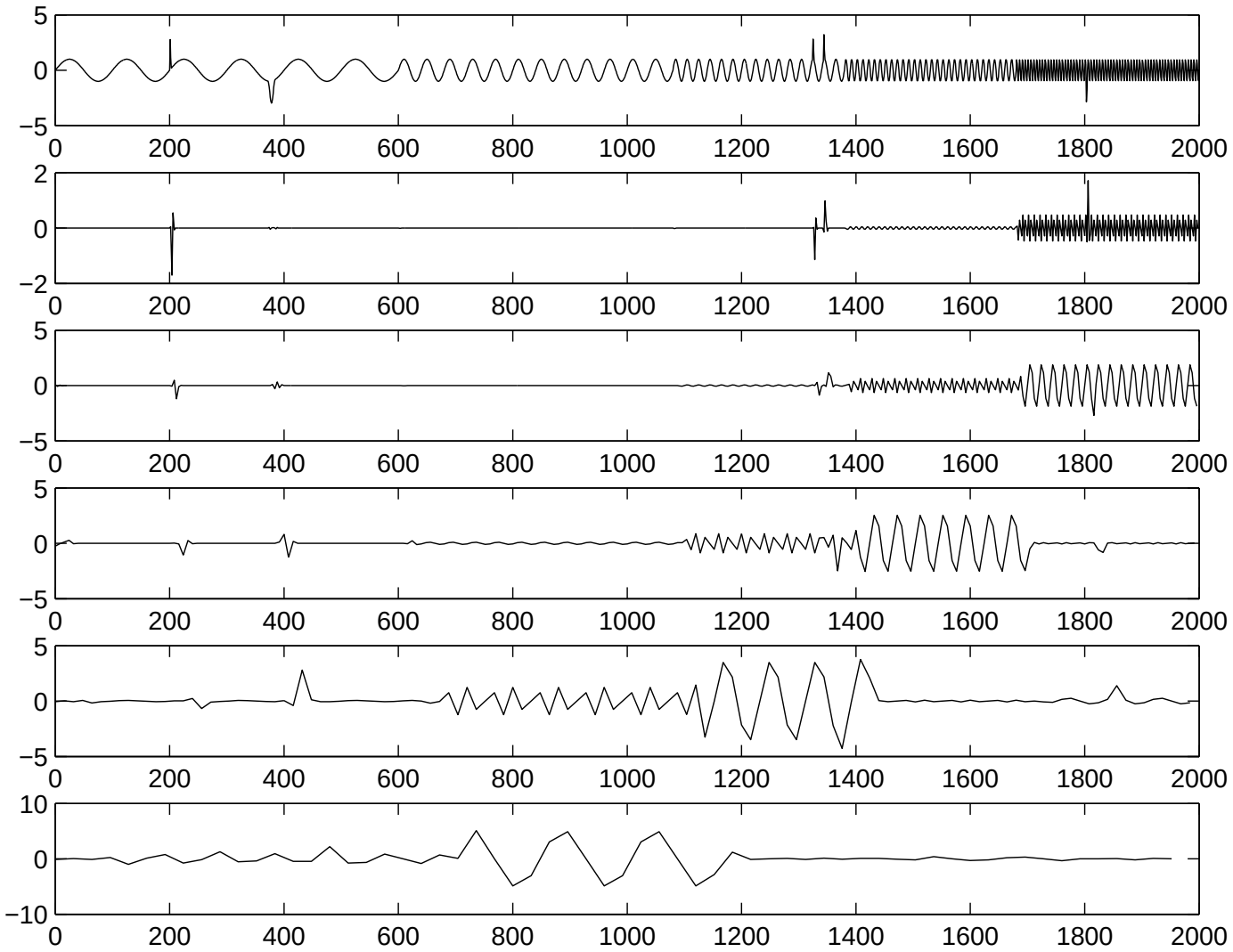

Figure 32: Detail bands for the signal from Experiment 10.1. The top plot corresponds to the original signal, and the details bands are shown, from top to bottom, in increasing scale (decreasing frequency) order.

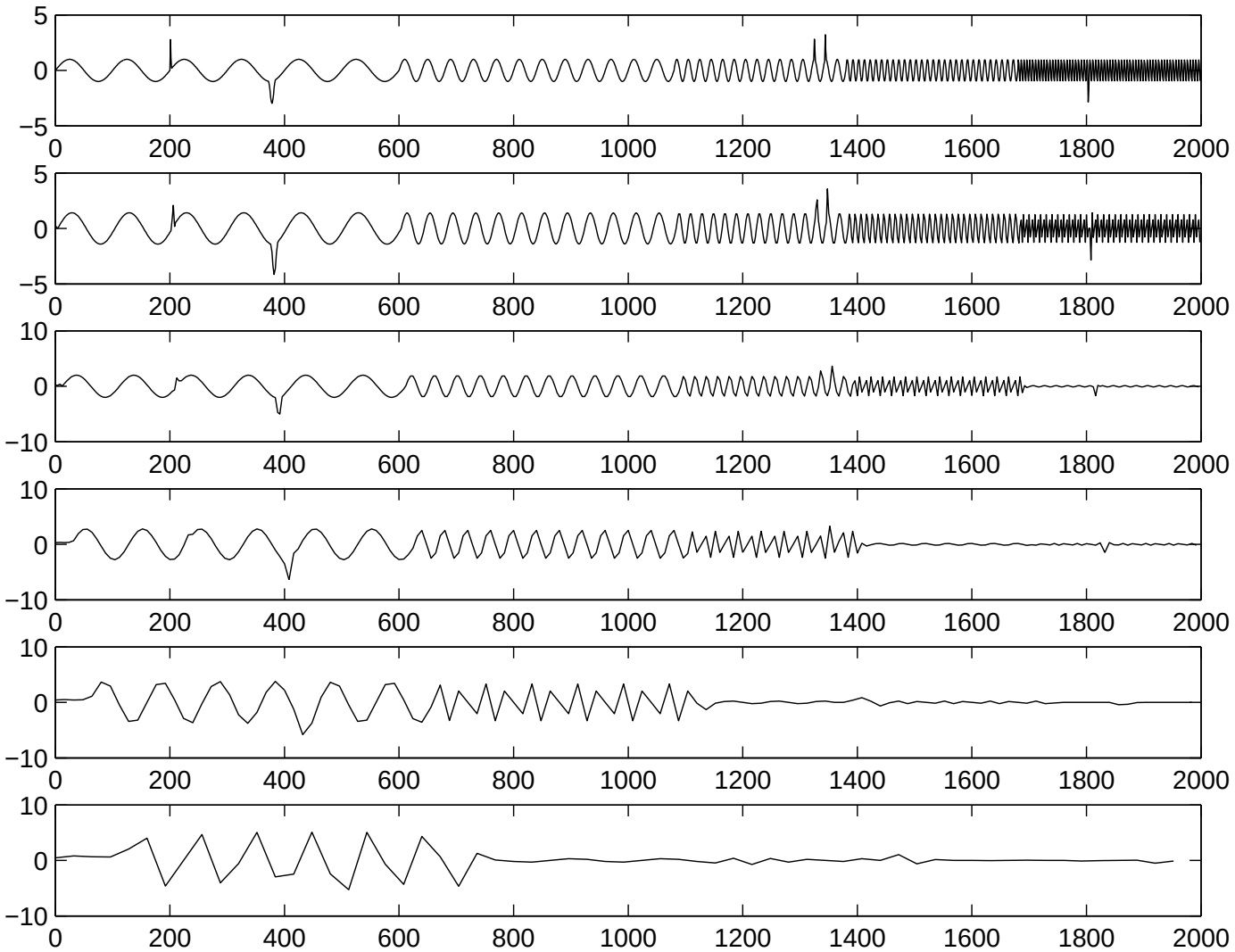

Figure 33: Approximation bands for the signal from Experiment 10.1. The top plot corresponds to the original signal, and the approximation bands are shown, from top to bottom, in increasing scale (decreasing frequency) order.

Do-it-yourself: Wavelet transforms

- By observing Figure 32, we can see that the highest frequency detail band (second plot from top) contains essentially the spikes of 3 samples duration.
- The wider spike does not appear in this band, since its resolution is not high enough for that.
- Note that, although some of the 5 sample period sinusoid is still present, by performing a simple thresholding in this band, one can easily have a signal composed only of these short duration spikes, and their locations can be easily determined.
- In addition, although there are traces of these spikes up to the fourth detail band, the two spikes that are closer together can only be distinguished up to the second band.
- Also, the wider spike can only be detected from the third band onwards. From these observations, we can see that the wavelet transform is good to detect transient phenomena.

Do-it-yourself: Wavelet transforms

- A good way to perform this is to look for correlation across bands.
- All the spikes in the signal tend to appear at least in three consecutive detail bands.
- Note also that each band shows preferentially one sinusoid, highlighting the bandpass nature of the detail bands.
- Figure 33 shows the approximation bands.
  - There, we can see the decreasing levels of details present in these bands as the scale increases (frequency decreases).
- This highlights the lowpass nature of these bands.

Do-it-yourself: Wavelet transforms

- The reader is encouraged to try different wavelets with this signal, and also different number of decomposition stages.
- The MATLAB Wavelet toolbox has several other signals that can be used for processing.
- They are usually under the directory `wavedemo` in the wavelet toolbox.
- Using these signals, the reader can play around with the wavelet transforms.
- This will help develop a good feeling of this important signal processing tool.

Do-it-yourself: Wavelet transforms

Experiment 10.2:

- In this experiment, we investigate the use of wavelet analysis to perform denoising of a given signal.
- We use as example the signal `leleccum` from the MATLAB wavelet toolbox. It can be loaded with the command

  ```
  load leleccum;
  ```

  which creates a variable `leleccum` of length 4320, as depicted in Figure 34.

Do-it-yourself: Wavelet transforms

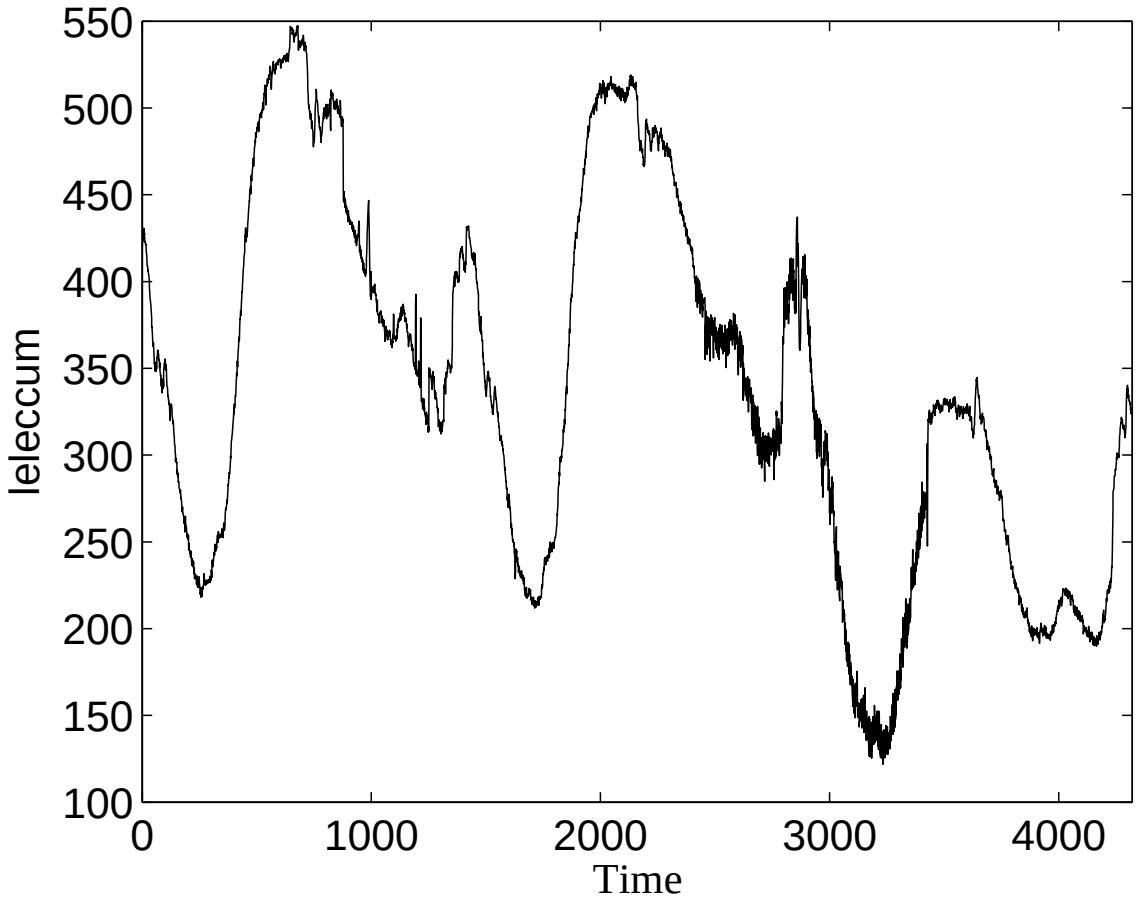

Figure 34: Signal for Experiment 10.

Do-it-yourself: Wavelet transforms

- This signal is corrupted by noise.
- Wavelet transforms can be successfully used to perform signal denoising.
- Since noise is usually wideband, the mere lowpass filtering of the corrupted signal is not the most effective way of reducing the noise.
- Let us start by computing the 5 stage wavelet transform of the signal, using the Daubechies 4 orthogonal filter bank.
- Its analysis and synthesis filters are shown in Table 3.

Do-it-yourself: Wavelet transforms

Table 3: Coefficients of the analysis and synthesis Daubechies 4 wavelet (db4).

$h_0(0) = -0.0106$	$h_1(0) = -0.2304$	$g_0(0) = 0.2304$	$g_1(0) = -0.0106$
$h_0(1) = 0.0329$	$h_1(1) = 0.7148$	$g_0(1) = 0.7148$	$g_1(1) = -0.0329$
$h_0(2) = 0.0308$	$h_1(2) = -0.6309$	$g_0(2) = 0.6309$	$g_1(2) = 0.0308$
$h_0(3) = -0.1870$	$h_1(3) = -0.0280$	$g_0(3) = -0.0280$	$g_1(3) = 0.1870$
$h_0(4) = -0.0280$	$h_1(4) = 0.1870$	$g_0(4) = -0.1870$	$g_1(4) = -0.0280$
$h_0(5) = 0.6309$	$h_1(5) = 0.0308$	$g_0(5) = 0.0308$	$g_1(5) = -0.6309$
$h_0(6) = 0.7148$	$h_1(6) = -0.0329$	$g_0(6) = 0.0329$	$g_1(6) = 0.7148$
$h_0(7) = 0.2304$	$h_1(7) = -0.0106$	$g_0(7) = -0.0106$	$g_1(7) = -0.2304$

Do-it-yourself: Wavelet transforms

- In order to load the analysis and synthesis filters we use the MATLAB command

```
[Lo_D,Hi_D,Lo_R,Hi_R] = wfilters('db4');
```

  and compute the 5-stage wavelet transform using

```
[C,S] = wavedec(leleccum,5,Lo_D,Hi_D);
```

- The detail bands as well as the fifth level approximation band can be computed using the following commands:

```
A5 = appcoef(C,S,Lo_R,Hi_R,5);
D1 = detcoef(C,S,1);
D2 = detcoef(C,S,2);
D3 = detcoef(C,S,3);
D4 = detcoef(C,S,4);
D5 = detcoef(C,S,5);
```

- The results from these commands are plotted on the left-hand side of Figure 35, with the scale increasing from top to bottom.

Do-it-yourself: Wavelet transforms

- The bottommost plot corresponds to the approximation band of the fifth stage.
- By looking at these plots, one can see that if we apply a magnitude threshold of around 20, then most of the noisy coefficients can be made null.
- We can perform this using the commands

```
Ct = zeros(size(C));
Ct(find(abs(C)>20)) = C(find(abs(C)>20));
xt = waverec(Ct,S,Lo_R,Hi_R);
```

- The reconstructed bands can be computed by

```
At5 = appcoef(Ct,S,Lo_R,Hi_R,5);
Dt1 = detcoef(Ct,S,1);
Dt2 = detcoef(Ct,S,2);
Dt3 = detcoef(Ct,S,3);
Dt4 = detcoef(Ct,S,4);
Dt5 = detcoef(Ct,S,5);
```

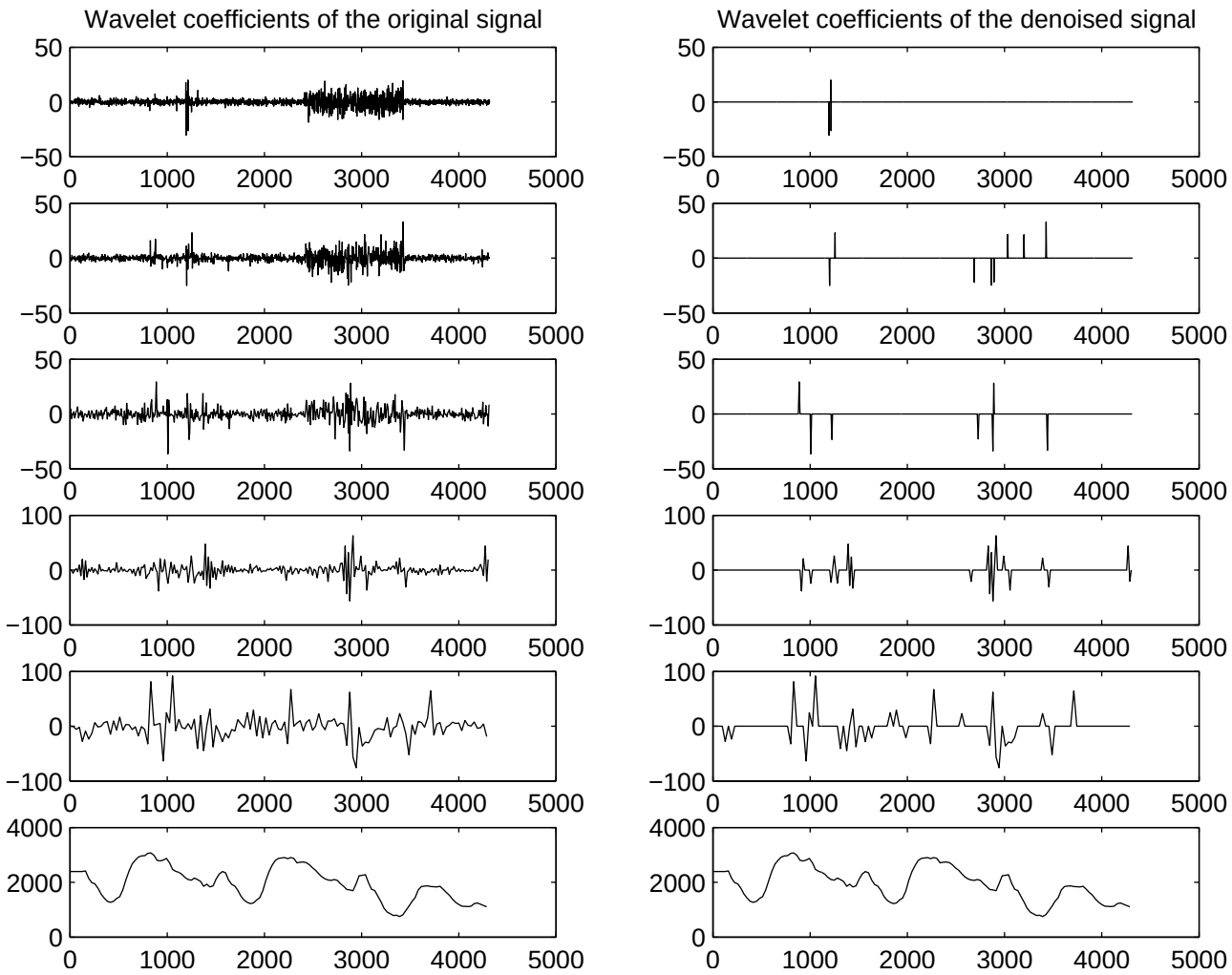

Figure 35: Fifth stage approximation band and detail bands for the signals from Experiment 10.2. Details bands are shown, from top to bottom, in increasing scale order. The bottommost plot corresponds to the approximation band. Left: original signal; right: denoised signal.

Do-it-yourself: Wavelet transforms

- The right-hand side of Figure 35 shows the sub-bands after applying the threshold.
- Figure 36 shows the denoised signal.

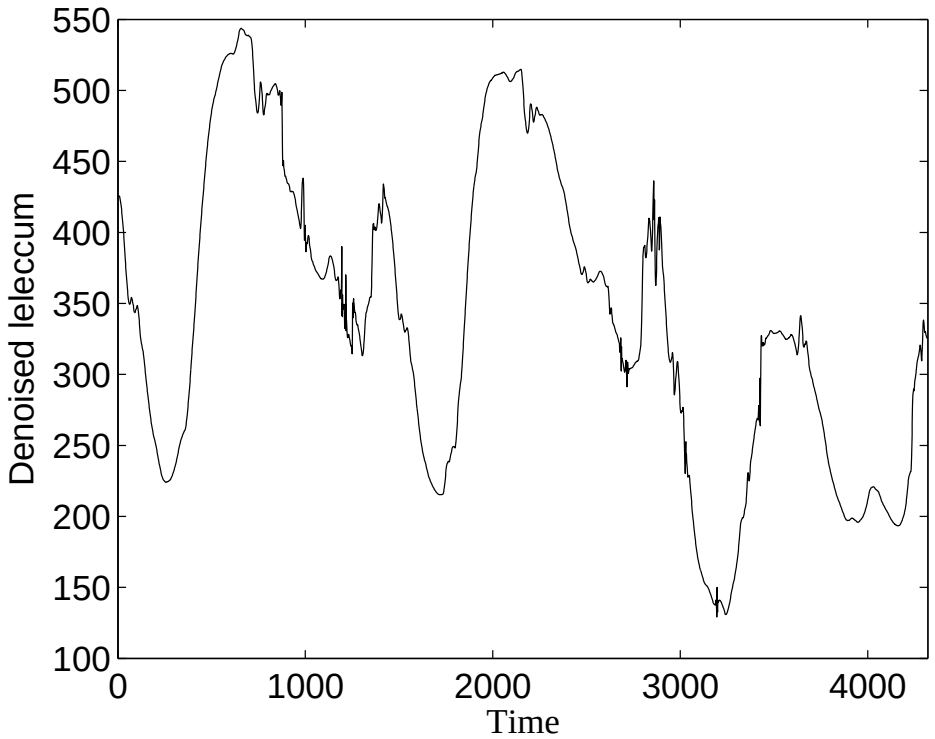

Figure 36: Denoised signal from Experiment 10.2.

Do-it-yourself: Wavelet transforms

- One can see that the wavelet is able to perform effective denoising.
- Note that while the thresholding process sets to zero most noisy coefficients, it can also set to zero some signal coefficients, which may lead to a quality loss in the reconstructed signal.
- Therefore, in wavelet denoising it is an important matter to find a threshold that gives a good trade-off between noise elimination and quality of the reconstructed signal.
- The reader is encouraged to further explore this Experiment by trying out different threshold values, as well as different wavelets.
- In the MATLAB wavelet toolbox there are several signals corrupted with noise. Examples are the signals `cnoislop`, `ex1nfix`, `ex2nfix`, `ex3nfix`, `heavysin`, `mishmash`, `nbumpr1`, `nelec`, `ndoppr1`, `noischir`, `wnoislop`, and `wntrsin`, among others. The reader is also encouraged to experiment with them.